Development for electrochemical modification approaches of carbon and advances towards the surface reaction of anions

Satrio Kuntolaksono

(Doctoral Program in Life Science and Green Chemistry)

Dissertation submitted to the Graduate School of Engineering in partial fulfillment of the requirements for the degree of Doctor of Philosophy in Engineering at Saitama Institute of Technology

January 2021

Acknowledgements

First, the author would like to thank my beloved supervisor, Dr. Hiroaki Matsuura, for his academic guidance and devoted efforts during my doctoral degree in Saitama Institute of Technology, Japan. Pursuing doctoral studies in Japan was like a dream that the author had for several years ago and the author really appreciated and never forget that Dr. Hiroaki Matsuura who believed in me and gave me the amazing opportunity of joining his group which made that dream really come true. Dr. Matsuura is extraordinary, dynamic, energetic, good management planner, and an inspiring example as a scientist and researcher. Those are important for me to be a role model for my future career. While studying in his lab, the author found myself growing in academically, time-managed, and professionally. The author am truly grateful for all the lessons he taught me. Thanks to his guidance the author learns to be a more goal-oriented person and always put the best of myself into every task encountered. In addition, the author would like to thank him for his patience, time, discipline, hard work, and commitment to help me in the whole work during three years of my study.

The author would like to thank all of committee members such as Prof. Masakazu Iwasaki, Prof. Osamu Niwa, Prof. Susumu Sato, and Prof. Masaya Uchida for giving me advice, support, time, and correction for my best dissertation. I would a deep thank you to each committee member as follows: Prof. Niwa and Prof. Iwasaki are the senior professors who gave me judge in doctoral entrance examination around end of February 2018. They also encourage me for hard work and motivation during my study at Saitama Institute of Technology. As the author remember, they always say to me that you're Japanese so excellent, the author really appreciate for that. Prof. Sato and

through the last year my doctoral degree.

Dedication

This dissertation is dedicated to the people who have supported me very close during my three years of education, especially to my mother who already in heaven and my father. With that love, encouragement, prays of day and night make me able to get such success and honor. Thanks for making me see this adventure through to the end.

Declaration

This is to certify that to the best of my knowledge, the content of this dissertation is my own work under controlled with my supervisor. This dissertation has not been submitted for any degree or other purposes.

The author certifies that this dissertation is the product of my own work and that all the assistance received in preparing this dissertation and sources have been acknowledged.

Satrio Kuntolaksono

List of publications

1. **<u>Satrio Kuntolaksono</u>** and Hiroaki Matsuura, "Coulometric Analysis of Nitrite Using Electrochemically Activated Carbon Felt Electrode", *Sensors and Materials*, **31(4)**, 1215-1224 (2019).

2 **<u>Satrio Kuntolaksono</u>**, Chihiro Shimamura, and Hiroaki Matsuura, "Electrochemical Detection for Sulfite Using Glassy Carbon Electrode Modified by Electrodeposition of Platinum Particles on Nitrogen-Containing Functional Groups", *Electrochemistry*, **88(5)**, 441-443 (2020).

3. **<u>Satrio Kuntolaksono</u>**, Chihiro Shimamura, and Hiroaki Matsuura, "Amperometric Sulfite Sensor Using Electrodecorated Pt Particles onto Aminated Glassy Carbon Electrode Prepared by Stepwise Electrolysis", *Analytical Sciences*, **36**, 1547-1550 (2020).

Contents

Chapter 1   General Introduction

Chapter 2 Simple Electrochemical Modification of the Carbon Electrode Surface with Nitrogen Atoms and Platinum Nanoparticles

Chapter 3   Potential-Controlled Coulometric Analysis of Nitrite Using Aminated Carbon Felt Electrode

Chapter 4   Electrochemical Performance of Pt Particles Deposited on N-Containing Functional Groups: Application to Sulfite Detection

Chapter 5   Electrochemical Sensor of Sulfite Using Electrodeposition of Pt Particles Nitrogen-Containing Functional Groups Prepared by Stepwise Electrolysis

List of Figures

List of Tables

Chapter 1   General Introduction

1.1.   Introduction of Carbon Materials

Carbon is an element with symbol C and atomic number 6. It is nonmetallic and tetravalent, such that it forms four bonds to other atoms or can accept four electrons and become stable. Consequently, a new compound can be created by the formation of new bounds with carbon. One of the example is benzene, which is a cyclic hydrocarbon, where each carbon atom is a part of a ring with six members and bonded to only one hydrogen atom. All carbon-carbon bonds in the benzene molecule are identical in length. In addition, according to the molecular orbital theory, benzene involves the formation of three delocalized π – orbitals covering all six-carbon atoms, whereas the valence bond theory describes two stable resonance structures for the ring. One such representation includes the molecular structure of benzene as a superposition of the multiple benzene rings than single benzene ring. This type of structure is called the resonance hybrid of the benzene molecule. Benzene can be combined and connected with multiple benzene rings to form two or three layers, as well as spheres, ovals, or tubes. The various structures of formed with benzene are called carbon allotropes, which consist of fullerenes,[1] carbon nanotube (CNTs),[2] and graphene.[3]

In 1985, Kroto et al. discovered a new allotrope of carbon, called fullerene.[1,4,5] Fullerene has sp^2- and sp^3- hybridized carbon.[6] Fullerene is soccer ball-like molecule with a diameter of ~0.7 nm,[6,7] which consists of 60 carbon atoms (C_{60}), and contains no other elements.[8] Each carbon atom has three bonds that are directed toward other three carbon atoms. Fullerene consists of 20 hexagons and 12 pentagons, implying the presence of two types of bonding such as hexagon-hexagon bonding (6-6 bonding) and

pentagon-hexagon bonding (5-6 bonding).[9,10] The lengths of 6-6 and 5-6 bonding have been calculated as 1.39 and 1.45 Å, respectively. The electrons are more localized on the 6-6 bonding than on 5-6 bonding.[11] The addition of carbon atoms to the C_{60} spherical equator produces oblong molecules with formulas of C_{70}, C_{76}, C_{84}, etc.[12,13] The fullerenes are commonly used as catalysts, lubricants, and biomedical.[14] In 1991, the second family formed by the carbon allotropes included the one-dimensional CNTs.[15] CNTs have attracted significant interest because of their electronic and mechanical properties, as well as interesting physical properties such as metallic or semiconducting characteristics depending on the chirality of the carbon atoms in the tube. There are two types of CNTs. Single-walled CNTs (SWCNTs), consist of a single graphene sheet rolled seamlessly to form a cylinder with a diameter of 1 nm and length of up to centimeters.[15] Multi-walled carbon nanotubes (MWCNTs) consist of an array of such cylinders formed concentrically and separated by 0.35 nm, similar to the basal plane separation in graphite.[16] MWCNTs can have diameters from 2 to 100 nm and lengths of tens of microns.[17] In addition, MWCNTs can occur in various morphologies such as hollow tube, bamboo, and herringbone. The morphologies of the CNTs depend on their mode of preparation.[18] CNTs are prepared either by the arc-discharge method, which is used to prepare C_{60} and C_{70} fullerenes, or by chemical vapor deposition on metal particles.[19] The CNTs have been primarily applied in biosensing, tissue engineering, and drug delivery.[20-22] These are applicable in the plastic industry for composite materials, electronics industry for manufacturing display, conductive transparent film semiconductor industry for transistor channels, and energy industry for batteries and solar cells. In addition, CNTs have been employed in analytical science because of their flexibility, thermal stability, high aspect ratio, conductivity, and reactivity.[23] In 2004,

graphene was discovered as a new two-dimensional carbon allotrope[24] with sp^2 hybridization.[25] Graphene is the thinnest known material and a basic building block for constructing many carbon materials. Graphene can be rolled into one-dimensional CNTs and assembled into graphite structure. If pentagons are added into the graphene structure, it can be wrapped into a spherical fullerene shape. Graphene has received significant attention because its unique properties, including high surface area, electronic conductivity, excellent mechanical, optical, thermal, and electrochemical properties, rendering it as an attractive topic in physics, chemistry, and material science.[26] The excellent mechanical properties include a Young's modulus of 1.0 TPa, stiffness of 130 GPa, and optical transmittance of ~97.7%.[26]

Graphite is a three-dimensional carbon allotrope with sp^2 hybridization. The graphite material family includes two types of materials, carbon fiber and glassy carbon (GC).[15] The carbon fiber is also known as carbon felt (CF) in some cases. The carbon fiber has been utilized in electrochemistry, particularly for applications requiring a small "footprint" such as in vivo monitoring of the living tissue.[15,27,28] In general, these have diameters in the range of 5-50 μm and are prepared from small hydrocarbons/polymers or by catalytic chemical vapor deposition. Carbon fiber occurs in a wide range of structure and crystallite size, which include three general types. Radial fibers have graphene planes radiating out from the center of the fiber, while "onion" fibers consist of concentric cylinders of graphene planes and "random" fibers have a random orientation of graphitic planes. CF is similar to carbon fiber, and is commonly used as an electrode because of its good electronic conduction. It has a high surface area, porosity, and provides abundant redox reaction sites, excellent electrolytic efficiency, and mechanical stability at relatively low cost.[29] CF is the best candidate for comparison

with carbon fiber. As it is similar to carbon fiber, CF is extensively employed in electrochemical, energy, and environmental sector. Another important member of the graphite family is GC. GC is prepared by heat-treating various polymers, often polyacrylonitrile. The polymer is heated under pressure in an inert atmosphere at 1000-3000 °C, the temperature range in which the heteroatoms evaporate until only carbon remains.[15,30] The C-C bonds in the polymer backbone do not break at these temperatures, such that carbon can form graphitic planes of the only limited size with L_a (layer sheet direction) and L_c (interlayer spacing and crystalline size along c-axis) in the range of 30-70 Å.[15] The structure is commonly presented as randomly intertwined ribbons of graphitic planes, and the randomness results in significant uncertainty about the detailed microstructure.[31,32] GC can be prepared from reactive polymeric precursors at ±700 °C,[33] which allows "doping" with various heteroatoms in the polymer, as well as the final product, together with halogens, silicon, and metal catalysts.[34,35] Typically, GC is utilized in electrochemistry and sensors. Fundamentally, CF and GC are carbon materials, which have been extensively used in the fields of electrochemistry and sensors. These two materials can function as electrodes, particularly as working electrodes. The advantages of utilizing CF and GC electrodes include chemical stability in different solutions ranging from acidic to basic solutions, low background current, wide potential window, tolerance for a wide range of temperatures, environmental friendliness, cost-effectiveness, and chemical inertness, in comparison to the metal electrodes.[15,36-39] However, surface reactions and active sites are the most important factors for applications in the fields of electrochemistry and sensors. For example, if the electrodes are used directly, these cannot achieve high activity performances and the active sites do not play a key role. Therefore, the surface modification of the electrodes

4

is necessary before their usage in the sensors. Because of the modification of the electrodes, the surface reaction affords a high activity, improves the surface characteristics, and active sites are introduced on the electrodes. Many techniques and methods are available to modify the surfaces of the CF and GC electrodes. Further details will be described in the next section.

1.2.   Surface Modification of Carbon Materials

Surface modification involves the modification of the surface areas of the carbon electrode materials to afford new surface structures. The main purpose of the surface modification of the carbon electrode material is to introduce specific catalytic centers in typically inactive and electron-conducting materials. This can be beneficial achieving high performances and improving both the selectivity and sensitivity.

According to the fundamental theory, two main approaches are used, chemical modification and physical modification[40] (Figure 1.1). The physical modification method is also known as bottom-up processing. The main principle of this method involves the creation of a new material from the raw material using a physical technique. Many types of physical modification techniques are available, including the gas modification, plasma ion-beam modification, microwave modification, and sputtering. The sputtering method is more commonly used than the other modification techniques. Sputtering is a physical process in which the solid (target) atoms are released and transferred into the gas phase through the impact of high-energy ions (mainly gas ions). Sputtering is commonly understood as the sputter deposition, a high vacuum-based coating technique that belongs to the groups of physical vapor deposition (PVD) processes. Furthermore, the principle of sputtering involves the usage of plasma energy (partially ionized gas) directed on the target surface to attract the atoms of the material one by one and their subsequent deposition on the substrate. According to this principle, a plasma is created by the ionization of a pure gas (typically, argon) with a potential difference or electromagnetic excitation. This plasma is composed of Ar^+ species, which are accelerated by a magnetic field and are confined around the target. When each has enough energy to collide the atoms and direct them to the substrate. The plasma is

generated at high pressure; however, it should start forming from a low pressure before entering argon to avoid contamination by the residual gases. To understand the principle of this method, several types of sputtering techniques have been utilized by the researchers, which include plasma sputtering,[41-44] unbalanced magnetron sputtering,[45-47] electron cyclotron resonance sputtering,[48-53]

Next, the top-down modification/chemical modification method is described. The principle of the top-down modification method involves the utilization of the carbon material whose the surface is modified by chemical process. Three types of modifications, including acidic modification, basic modification, and electrodeposition are employed. One example is the activated carbon material. The acidic modification of the activated carbon surface involves a typical wet oxidation technology using HNO_3, H_2O_2, H_2SO_4, citric acid, and other oxidant.[40] The numbers and types of oxygen-containing functional groups on the activated carbon surface can be changed to improve the ability to remove metal ion from aqueous solution.[40,54] The surface oxygen-containing functional groups can be classified into three classes: acidic, basic, and neutral. Functional groups such as carboxylic acid, carboxylic anhydride, lactone, and phenolic hydroxyl are considered as the sources of surface acidity.[54-56] In contrast, basic surface modification can be associated with resonating π-electrons of the carbon aromatic rings that attract protons and basic surface functionalities (nitrogen-containing groups) that can bind to protons.[57-60] Electrodeposition, sometimes referred to as electroplating, is a method of depositing electric current on a conductive target material that provides precise control for coating the epitaxial species in the form of nanoparticles and nanowires onto a conductive target material.[61] Electrodeposition is one of the most important techniques for depositing nanoparticles on the

7

graphene/carbon material surfaces. Numerous methods for the modification of carbon material surfaces by introducing various functional groups on their surfaces are available. For example, by air oxidation (i.e., heating in air) or treatment with chromium acid solution, the carbon atoms can be modified into oxygen-containing functional groups such as carboxyl groups (-COOH), which can be further converted into amines (R-NH$_2$), esters, and alcohols (R-CH$_2$OH). Heating and refluxing in thionyl choride are used to convert the carboxyl group into highly acid chloride, as shown in Figure 1.2. Notably, the amide bond can be more stably immobilized than the ester bond. The carbon electrodes can be chemically modified by electrolytic oxidation or electrolytic reduction in a solution containing a substance to be immobilized (Figure 1.3). Functional compounds to which this method can be applied include amino compounds, diazonium salts or diazonium compounds, and carboxylic acid, and the radicals generated in the electrolytic reaction react directly with the carbon surface. Physical (bottom-up) and chemical (top-down) modifications of the carbon materials allow their usage in chemical engineering applications in the fields of catalysis and sensor.

1.3.   Application in Chemical Analysis

Chemical analysis is the study of the chemical composition and structure of a substance (physical properties). This involves the identification, characterization, and measurement of the chemical species in a sample. Analytical chemistry includes two types of analysis, qualitative and quantitative analyses. Qualitative analysis is the determination of the elements and compounds present in the sample of an unknown substance. Quantitative analysis is the determination of the amount (by weight) of each element or compound present.

There are two types of methods available in analytical chemistry: classical and instrumental methods.[62] Classical methods are sometimes called wet-chemical methods. These methods are a group of analytical methods that only require the use of chemicals, balance, calibrated glassware, extraction, distillation, boiling or melting points, and gravimetric and titrimetric measurements. In contrast, the instrumental methods include analytical measurements (conductivity, luminescence, spectrophotometry, photometry, calorimetry, electrochemistry, light absorption, spectroscopy, fluorescence, chromatography, and electrochemistry) performed using instrumentation, as summarized in Table 1.1. The advantages of instrumental methods in comparison to the classical methods include higher sensitivity, higher accuracy, and rapid detection. For this reason, the instrumental methods are more popular than the classical methods.

Chemical sensing is a type of instrumentation method. A chemical sensor is a device that measures and detects chemical qualities in an analyte (scientific term for a chemical substance being observed) and converts the sensed chemical data into electronic data. It is a device that provides information about the material, which includes of the quantity as well as substance type and state. A target species is

9

commonly termed as an analyte or determinant. A chemical sensor contains two components, receptor and transducer. As in Figure 1.4, the receptor is in physical contact with the analyte. In many cases, the function of a receptor is fulfilled by a thin layer that interacts with the analyte molecules or participates in a chemical equilibrium together with the analyte. The receptor layer may respond selectively to particular substances or a group of substances. Among the various interactions, the most important ones for a chemical sensor are adsorption, ion exchange, and liquid-liquid extraction. The second component in a chemical sensor is the transducer. The transducer collects the chemical information of the interaction between the receptor and analyte, and converts it into the corresponding electrical information. This information is transferred to a computer or mechanical component. The transducer may increase or decrease the resistance, which is related to the data of the computer signal. Table 1.1 includes the instrumental method parameters, which are related to the measurement principle of chemical analysis. Three types of methods including optical, spectroscopy, and electrochemical methods are summarized. Optical methods include fluorescence, light scattering, and absorbance. Spectroscopy is used to measure the interactions of the molecules with an electromagnetic radiation and includes atomic spectroscopy and nuclear magnetic resonance spectroscopy. Electrochemical analysis methods measure the electrical potential in volts and/or electric current in amperes using an electrochemical cell containing the analyte.[63,64] Electroanalytical methods can be categorized according to the which aspects of the cell are controlled and performed. The four main classes are potentiometry, voltammetry, amperometry, and coulometry.[65] Potentiometry is discussed in Chapter 3, 4, and 5, coulometry is described in Chapter 3, voltammetry is presented in Chapter 4, and amperometry is discussed in Chapter 5.

References

1. R. E. Smalley, *Rev. Mod. Phys.*, **69**, 723 (1997).

2. S. Berber, Y. K. Kwon, and D. Tomanek, *Phys. Rev. Lett.*, **84**, 4613 (2000).

3. A. K. Geim and K. S. Novoselov, *Nat. Mater.*, **6**, 183 (2007).

4. B. S. Kademani, V. L. Kalyane, and V. Kumar, *SRELS J. Info. Mana.*, **39(4)**, 409 (2002).

5. S. Ahmad, *IETE Tech. Rev.*, **16(3-4)**, 297 (1999).

6. H. W. Kroto, J. R. Heath, S. C. O'Brean, R. F. Curl, and R. E. Smalley, *Nature.*, **318**, 162 (1985).

7. H. W. Kroto, A. W. Allaf, and S. P. Balm, *Chem. Rev.*, **91**, 1213 (1991).

8. F. Wudl, *Acc. Chem. Res.,* **25**, 157 (1992).

9. M. Buhl and A. Hirsch, *Chem. Rev.,* **101**, 1153 (2001).

10. E. H. L. Falcao and F. Wudl, *J. Chem. Technol. Biotech.*, **82**, 524 (2007).

11. H. P. Luthi and J. Almlof, *J. Chem. Phys. Lett.*, **135**, 357 (1987).

12. A. Astefanei, O. Nunez, and M. T. Galceran, *Anal. Chim. Acta*, **882**, 1 (2015).

13. M. S. Dresselhaus, G. Dresselhaus, and P. C. Eklund, *Science of Fullerenes and Carbon Nanotubes: Their Properties and Applications*, Academic Press, New York (2017).

14. G. G. Wildgoose, C. E. Banks, H. C. Leventis, and R. G. Compton, *Electrochim. Acta*, **152**, 187 (2006).

15. S. Iijima and T. Ichihasi, *Nature*, **363**, 603 (1993).

16. S. Iijima, *Nature.*, **354**, 56 (1991).

17. J. N. Coleman, U. Khan, W. J. Blau, and Y. K. Gun'ko, *Carbon*, **44**, 1624 (2006).

18. G. Lalwani and B. Sitharaman, *Nano LIFe,* **3(3)**, 1342003 (2013).

19. G. M. Jenkins and K. Kawamura, *Polymeric Carbons, Carbon Fiber, Glass, and Char*; University Press: Cambridge, England, (1976).

20. A. Bianco, K. Kostarelos, and M. Prato, *Curr. Opin. Chem. Biol.,* **9**, 674 (2005).

21. S. Polizu, O. Savadogo, P. Poulin, and L. Yahia, *J. Nanosci. Nanotechnol.,* **6**, 1883 (2006).

22. B. S. Harrison and A. Atala, *Biomaterials,* **28**, 344 (2007).

23. M. Valcarel, S. Cardenas, and B. M. Simonet, *Anal. Chem.*, **79**, 4788 (2007).

24. K. S. Novoselov, A. K. Geim, and S. V. Morozov, *Science,* **306(5696)**, 666 (2004).

25. M. Inagaki and F. Kang, *J. Matr. Chem. A.,* **2(33)**, 17 (2017).

26. H. Marsh, *Introduction to Carbon Science*, Butterworths, London (1989).

27. R. M. Wightman, *Science.,* **311**, 1570 (2006).

28. M. L. A. V. Heien, M. A. Johnson, and R. M. Wightman, *Anal. Chem.,* **76**, 5697 (2004).

29. T. X. H. Le, M. Bechelany, and M. Cretin, *Carbon,* **122**, 564 (2017).

30. G. M. Jenkins and K. Kawamura, *Polymeric Carbons, Carbon Fiber, Glass, and Char*; University Press: Cambridge, England, (1976).

31. M. T. McDermott, C. A. McDermott, and R. L. McCreery, *Anal. Chem.*, **65**, 937 (1993).

32. C. A. McDermott and R. L. McCreery, *Langmuir*, **153(12)**, A2255 (2006).

33. D. T. Fagan, I. Hu, and T. Kuwana, *Anal. Chem.*, **57**, 2759 (1985).

34. M. E. Huston, W. Huang, R. L. McCreery, T. Neenan, and M. Callstrom, *Chem. Mater.,* **5**, 1727 (1993).

35. H. D. Hutton, W. Huang, D. Alsmeyer, J. Kometani, R. L. McCreery, T. Neenan, M. R. Callstrom, *Chem. Mater.,* **5**, 1110 (1993).

36. G. M. Jenkins and K. Kawamura, *Nature,* **231**, 175 (1971).

37. W. E. Van der Linden and J. W. Dieker, *Anal. Chim. Acta*, **119**, 1 (1980).

38. G. N. Kanau, *Anal. Chim. Acta*, **207**, 1 (1988).

39. E. Frackowiak and F. Beguin, *Carbon*, **39**, 937 (2001).

40. M. Liu and C. Xiao, *E3S Web of Conferences*, **38**, 02005 (2018).

41. S. Ohta, S. Shiba, T. Yajima, and O. Niwa, *Electrochemistry*, **88(5)**, 387 (2020).

42. S. Prantontep, S. J. Caroll, C. Xirouchaki, M. Streum, and R. E. Palmer, *Rev. Sci. Instrum.,* **76**, 245103 (2005)

43. P. Braut, A. Caillard, A. L. Thomann, J. Mathias, C. Charles, R. W. Boswell, S. Escribano, J. Durand, and T. Sauvage, *J. Phys. D: Appl. Phys.*, **37(24)**, 3419 (2004).

44. K. Takahashi, T. saito, A. Ando, Y. Yabuta, H. Mizuguchi, N. Yamamoto, R. Kamei, and S. Hara, *Vacuum*., **171**, 109000 (2020).

45. S. Ohta, S. Shiba, T. Yajima, T. Kamata, D. Kato, and O. Niwa, *J. Photopol. Sci. and Tech*., **32(3)**, 523 (2019).

46. T. Kamata, D. Kato, H. Ida, and O. Niwa, *Diam. Relat. Mater.*, **49**, 25 (2014).

47. D. Kato, A. Oda, M. Tanaka, S. Iijima, T. Kamata, M. Todokoro, Y. Yoshimi, and O. Niwa, *Electroanal.*, **26**, 618 (2014).

48. O. Niwa, J. Jia, Y. Sato, D. Kato, R. Kurita, K. Maruyama, K. Suzuki, and S. Hirono, *J. Am. Chem. Soc.*, **128**, 7144 (2006).

49. J. Jia, D. Kato, R. Kurita, Y. Sato, K. Maruyama, K. Suzuki, S. Hirono, T. Ando, and O. Niwa, *Anal. Chem.*, **79**, 98 (2007).

50. D. Kato, N. Sekioka, A. Ueda, R. Kurita, S. Hirono, K. Suzuki, and O. Niwa, *J. Am. Chem. Soc.,* **130**, 3716 (2008).

51. D. Kato, N. Sekioka, A. Ueda, R. Kurita, S. Hirono, K. Suzuki, and O. Niwa, *Angew. Chem. Int. Ed.*, **47**, 6681 (2008).

52. D. Kato, M. Komoriya, N. Nakamoto, R. Kurita, S. Hirono, and O. Niwa, *Anal. Sci.*, **27**, 703 (2011).

53. D. Kato, M. Sumimoto, A. Ueda, S. Hirono, and O. Niwa, *Anal. Chem.*, **84**, 10607 (2012).

54. M. S. Shafeeyan, W. M. A. W. Daud, A. Houshmand, and A. Shamiri, *J. Anal. Appl. Pyrolysis*, **89**, 143 (2010).

55. C. A. Leon y Leon and L. R. Radovic, in: P. A. Thrower (Ed), *Chemistry and Physics of Carbon*, Marcel Dekker, New York, (1994), p. 213-310.

56. H. P. Boehm, *Carbon*, **32**, 759 (1994).

57. A. Rehman, M. Park, and S. J. Park, *Coatings*, **9**, 103 (2019).

58. C. Moreno-Castilla, F. Carrasco-Marin, E. Utrera-Hidalgo, and J. Rivera-Utrilla, *Langmuir*, **9**, 1378 (1993).

59. M. V. Lopez-Raman, F. Stoeckli, C. Moreno-Castilla, and F. Carrasco-Marin, *Carbon*, **37**, 1215 (1999).

60. M. F. R. Pereira, S. F. Soares, J. J. M. Orfao, and J. L. Figuiredo, *Carbon*, **41**, 811 (2003).

61. A. Barhoum and A. S. H. Makhlouf, *Emerging Applications of Nanoparticles and Architecture Nanostructures*, Elsevier, (2018), p. 1-28.

62. D. A. Skoog, H. F. James, and S. R. Crouch, *Principles of Instrumental Analysis*. Belmont, CA: Brooks/Cole, Thomson. p.1. (2007).

63. A. J. Bard and L. R. Faulkner, *Electrochemical Methods: Fundamentals and Applications*. New York: John Willey & Sons, 2nd Edition, 2000

64. D. A. Skoog, D. M. West, and F. J. Holler, *Fundamentals of Analytical Chemistry*. New York: Saunders College Publishing, 5th Edition, 1988.

65. J. Wang, *Analytical Electrochemistry*. New Jersey: John Willey & Sons, 3rd Edition, 2006.

Figures and Tables

```
                    ┌─────────────────────────┐
                    │  Surface Modification of │
                    │     Carbon Materials     │
                    └─────────────────────────┘
           ┌────────────────┘         └────────────────┐
           ▼                                            ▼
┌──────────────────────────┐         ┌──────────────────────────────┐
│  Chemical Modification / │         │ Physical Modification / Bottom-Up │
│  Top-Down Modifications  │         │        Modifications          │
└──────────────────────────┘         └──────────────────────────────┘
```

Chemical Modification / Top-Down Modifications	Physical Modification / Bottom-Up Modifications
1. Acidic Modification	1. Gas Modification
2. Basic Modification	2. Plasma Modification
3. Electrodeposition Modification	3. Sputtering Modification

Figure 1.1. Modification techniques for carbon materials.
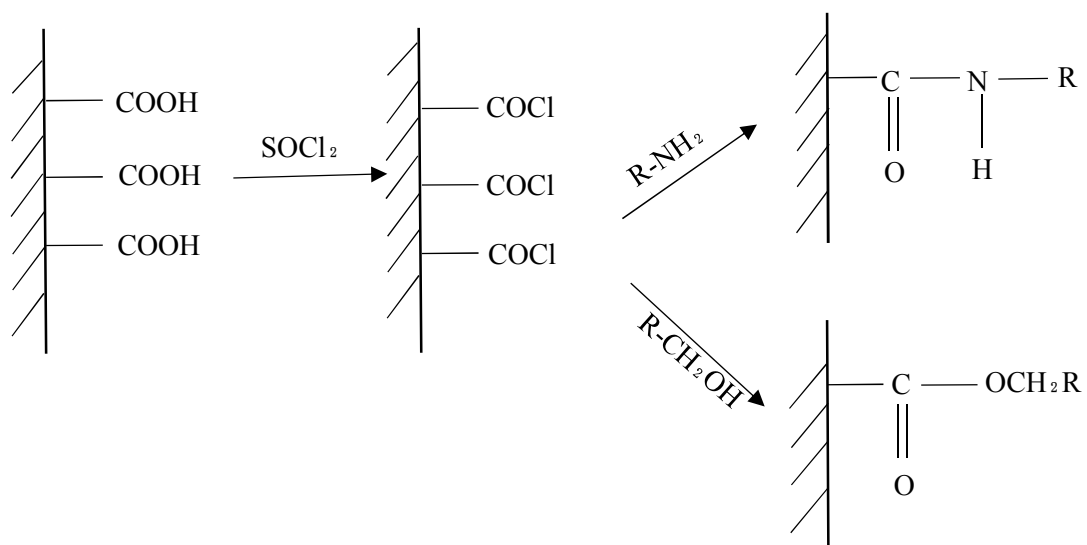
Figure 1.2. Method of modifying carbon electrode surface by covalent bonding.
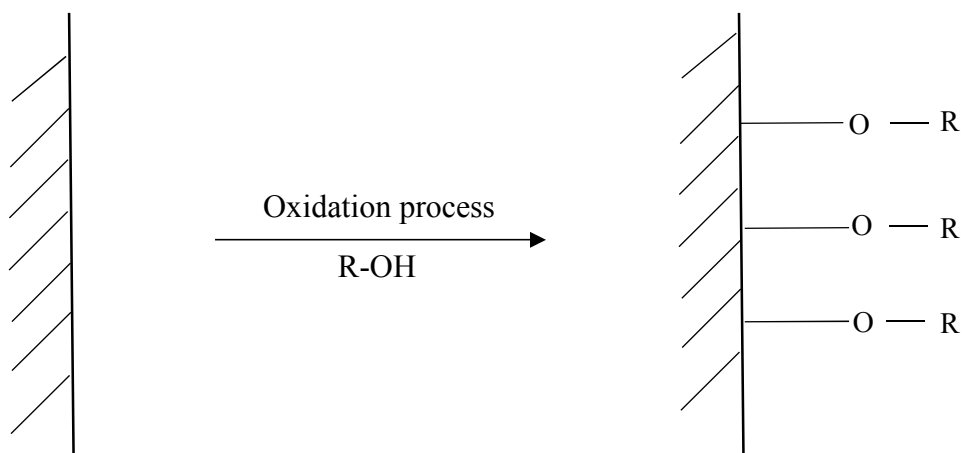
Figure 1.3. Method of modifying carbon electrode surface by electrolysis.
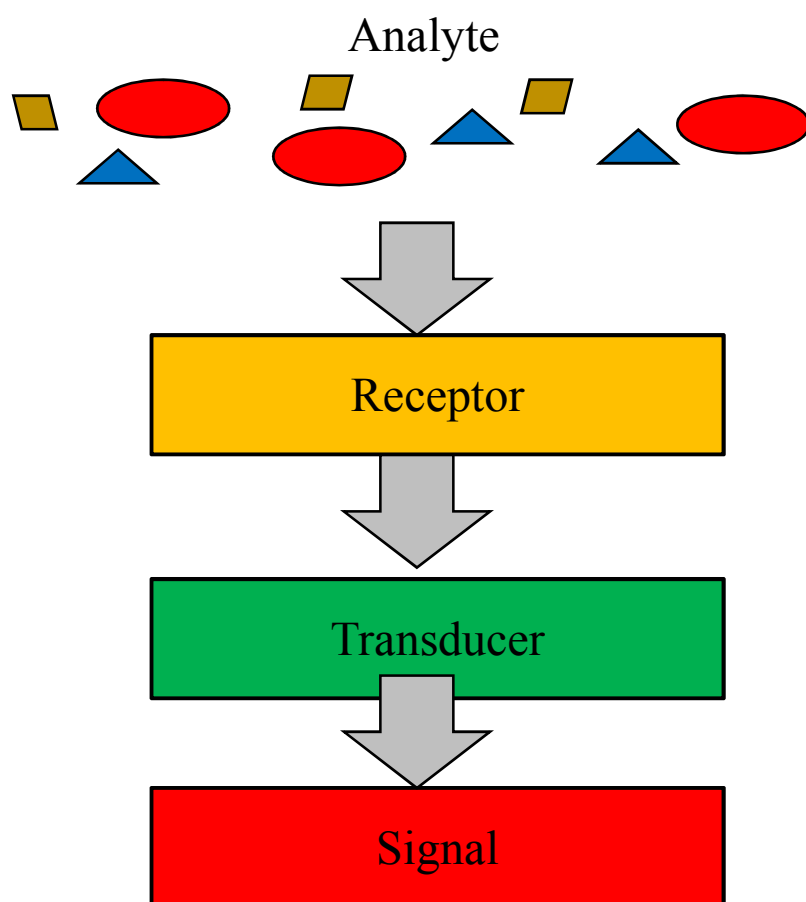
Figure 1.4. The illustration of general schematic system at chemical sensor.

Table 1.1. Instrumentation method based on the chemical analysis.

Instrumental method	Measuring principle
Electrochemical method	Potentiometric sensors
	Voltammetric sensors
	Amperometric sensors
	Coulometric sensor
Spectroscopic methods	Atomic spectroscopy
	Nuclear magnetic resonance spectroscopy
	Fluorescence
Optical methods	Light scattering
	Absorbance

Chapter 2

Simple Electrochemical Modification of the Carbon Electrode Surface with Nitrogen Atoms and Platinum Particles

2.1. Introduction of Nitrogen-Containing Functional Groups on the CF Electrode Surface.

2.1.1. Abstract

For the first time, a CF electrode was employed for the introduction of nitrogen-containing functional groups on its surface via a simple electrochemical modification, which was performed by the electro-oxidation of the carbon electrode. Nitrogen-containing functional groups were successfully formed on the CF electrode by the electro-oxidation process that was carried out for one hour with an applied potential of +1.1 V (vs. Ag/AgCl). These parameters were used to employ ammonium carbamate to modify the CF electrode, and afford the aminated carbon felt (ACF) electrode. In solutions with a wide range of pH, the oxygen reduction wave at the ACF electrode was shifted into the higher potential compared to the bare CF electrode because of the active sites of the nitrogen-containing functional groups attached to the surface of the ACF electrode.

2.1.2. Introduction

Carbon electrode materials for electrochemistry and sensing have been studied extensively in recent years. Two types of carbon electrode materials were used, CF and GC electrodes. The CF and GC electrodes have advantages such as wide potential windows, physical and chemical stabilities, low cost,[1-4] and large surface areas.[5] Before applications in the fields of electrochemistry, electroanalysis, and sensing, the two electrode surfaces must be modified via physical or chemical modification. Chemical modification methods are of significant interest in electroanalytical chemistry, electrochemistry, and electrocatalysis.[6] Electrochemical modification methods are examples of the chemical modification. There are many techniques for introducing a variety of functional groups containing non-metallic elements such as nitrogen,[7-10] oxygen,[11-14] and fluorine-containing functional groups.[15-17] These functional groups have been incorporated onto the carbon electrode surfaces to improve the electrode surface properties, increase the catalytic performances, and expand the potential applications of the resulting electrodes.

Recently, the modification of the carbon surfaces by nitrogen-containing compounds has attracted significant attention of the scientists worldwide. The electrochemical modification of the carbon surfaces by nitrogen-containing compounds has been investigated by several research groups, and the electrochemical introduction of various amines has been successfully carried out.[18,19] The attachment of amines can be accomplished by the covalent bonding of amine radicals formed by one-electron oxidation. The introduction of amino groups to the carbon electrode surface is limited, and only a few studies are been reported because the carbon bonds with nitrogen in the original amine compounds are very strong and difficult to break even after their

introduction to the carbon surfaces. Based on the prior reports, the introduction of amine groups was accomplished using the ammonium carbamate solution via a simple electrochemical treatment,[20] where the GC electrode was used.[20] Nitrogen-containing functional groups such as amines can be easily introduced on the GC electrode surface by the electrochemical oxidation of ammonium carbamate.[21,22] The surface of the GC electrode contains primary amine groups (aromatic amine groups such as aniline), but other nitrogen-containing functional groups such as the secondary amine groups containing pyrrole-type nitrogen and quaternary amine moieties containing graphitic quaternary nitrogen may also be introduced on the carbon electrode surface (GC electrode).[23,24] This modified carbon electrode with amine groups is AGC electrode or ACF electrode.

Furthermore, CF electrodes were investigated. The optimal applied potential and time for the application of the electrochemical oxidation process using an ammonium carbamate aqueous solution were selected. A wide pH range of the solution was employed to analyze the reduction wave of oxygen by comparing the modified and unmodified electrodes.

2.1.3. Experimental Section

Ammonium carbamate ($H_2NCOONH_4$) was purchased from Merck KGaA, Darmstadt, Germany, while dipotassium hydrogen phosphate and potassium dihydrogen phosphate were acquired from Fujifilm Wako Pure Chemical Industries, Ltd., Osaka, Japan. These solutions were used to prepare a phosphate buffer solution (0.1 M; pH 7.0). Sodium hydroxide (NaOH) (0.1M; pH 13.0) and sulfuric acid (0.5 M; pH 0.0) were purchased from Fujifilm Wako Pure Chemical Industries, Ltd., Osaka, Japan. The GF-20-5F CF electrode with 20 mm diameter and 5 mm thickness was obtained from Nippon Carbon Co., Ltd., Japan. All reagents were of analytical grade and used without further purification. The solutions were prepared with deionized water (Millipore Milli-Q System, Japan).

An ultrasonic bath was purchased from Branson Ultrasonic, Emerson Japan, Ltd. A potentiostat/galvanostat (HA-151B, Hokuto Denko Co., Ltd., Japan) was used to perform the controlled potential electrolysis. Electrochemical (cyclic voltammetric (CV)) measurements were carried out using an automated polarization system (HZ-3000, Hokuto Denko Co., Ltd., Japan) with a three electrode cells consisting of a working CF electrode, aqueous Ag/AgCl (3 M NaCl electrolyte) as the reference electrode, and a platinum wire as the counter electrode. A digital recorder (Gr-3500, Keyence Co., Ltd., Japan) was used to record the time during the electrolysis process. A schematic of the potentiostat/galvanostat consisting of three electrodes, a working electrode, counter electrode, and reference electrode connected to at digital recorder, is shown in Figure 2.1.

The CF electrode was prepared as follows. The bare CF electrode was mixed with ethanol and distilled water and treated in an ultrasonic bath for one hour. The

ultrasonic bath is used to remove all traces of contamination that were firmly or merely attached to the CF electrode surface. In the CV measurements, two types of CF electrodes were used. First, the bare CF electrode was used and applied in 0.1 M ammonium carbamate aqueous solution (pH 9.3) as electrolyte solution[20] (Figure 2.4 to 2.6). Next, the CF electrode was fabricated by electrode-oxidation in 0.1 M ammonium carbamate aqueous solution, which correspond to the time based on the result in Figure 2.6. The results obtained using this fabricated electrode (ACF electrode) are shown in Figure 2.7 to 2.9. All experiments were performed at room temperature.

2.1.4. Results and Discussion

Figure 2.2 and 2.3 show the CV data collected using a bare CF electrode. This is the first report describing the utilization of CF electrode for modifying its surface in 0.1 M ammonium carbamate. The potential range was from +0.4 V to +1.2 V, and the numbers of potential cycles were 100. A 0.1 M aqueous solution (pH 9.3) was selected for the experiments. CV was performed using a bare CF electrode in 0.1 M ammonium carbamate aqueous solution (pH 9.3; Figure 2.2). The CV data show that the oxidation current of ammonium carbamate increases with an increase in the number of potential cycle scans. Furthermore, the current window increases and changes significantly with an increase in the number of potential cycle scans. It is assumed that these results are related to the CF electrode with a large surface area.

Figure 2.3 shows the electrochemical behavior of the bare CF electrode at different scan rates (v) of 10-100 mV/s in 0.1 M ammonium carbamate aqueous solution (pH 9.3). The oxidation current of carbamic acid increases significantly when the scan rate is 10-20 mV/s. The oxidation current also increases when the scan rate is increased from 20 mV/s to 100 mV/s. Moreover, the shape of the current window changes and it increases with an increase in the scan rate during the CV measurements. Next, the optimal applied potential in 0.1 M ammonium carbamate aqueous solution (pH 9.3) was determined using a digital recorder. In this experiment, the optimal time for application in further processing, i.e., electro-oxidation, was also determined. During electro-oxidation, the electrode was set on potentiostat/galvanostat and connected to a digital recorder. The CF electrode was used (Figure 2.2 and 2.3), and the data for the three applied potentials using the potentiostat/galvanostat, +1.0 V, +1.1 V, and +1.2 V, were compared. As shown Figure 2.4, when the applied voltage is +1.0 V, the oxidation

current increases slowly to attain the best value, which corresponds to the time determined using the digital recorder. However, the oxidation peak current to reach the peak require more time. When the applied potential is +1.2 V, the peak oxidation current is rapidly attained in comparison to those at the other potential values (+1.0 V and +1.1 V). Interestingly, if the applied potential is +1.2 V, high noise and unstable performance are observed, possibly because the high potential can damage the CF electrode surface, leading to unstable performance during electro-oxidation. Therefore, a potential of +1.1 V was selected. After determining the optimal potential for the best results, the optimal time for applying +1.1 V in the electrode-oxidation process was determined. The time to attain the linear curve is within one hour processing. After one hour of processing, the oxidation peak start to decrease with time. Therefore, a duration of one hour and an applied potential of +1.1 V were selected.

A wide pH range was evaluated using the CF electrode in the CV measurements. The experimental data are shown in Figure 2.5 to 2.7. Two electrodes, a bare CF electrode (red color) and an ACF electrode (black color) were used. Three types of pH electrolyte solutions containing 0.5 M H_2SO_4 (pH 0.0; Figure 2.5), 0.1 M phosphate buffer solution (pH 7.0; Figure 2.6), and 0.1 M NaOH (pH 13.0; Figure 2.7) were used. Two interesting observation are noted in the CV curves. First is, the presence of redox waves (reduction and oxidation wave) and the observation of a reduction wave in solutions with a wide range of pH values. In addition, the reduction waves move toward the positive potential using the ACF electrode in comparison to that with the bare CF electrode. It is believed that the reduction waves at the bare CF and ACF electrodes are the oxygen waves. Additionally, the shift of the reduction wave toward the positive potential indicates the function of the active site originating from the

nitrogen-containing functional groups attached to the surface of the ACF electrode as the modified carbon electrode.

2.1.5. Conclusions

For the first time, the CF electrode has been successfully utilized for the introduction of nitrogen-containing functional groups on the electrode surface via an electrochemical method. The electrochemical modification was performed using an electro-oxidation process. Ammonium carbamate was used as the chemical reagent. When the CF electrode was used as the working electrode, the oxidation activity of ammonium carbamate at the CF electrode increased with an increase in the number of potential cycles scans in ammonium carbamate aqueous solution. The optimal time and applied potential were one hour and +1.1 V, respectively, as determined using the digital recorder. During observations in solutions with a wide pH range using the modified CF (ACF) electrode, an oxygen reduction wave was observed in the CV data, and the applied potential shifted toward the positive direction compared to that with the bare CF electrode.

References

1. W. E. Van der Linden and J. W. Dieker, *Anal. Chim. Acta*, **119**, 1 (1980).

2. G. N. Kanau, *Anal. Chim. Acta*, **207**, 1 (1988).

3. R. L. McCreery, *Carbon Electrodes: Structural Effects on Electron Transfer Kinetics. In Electroanalytical Chemistry: A Series of Advances;* Bard, A. J.; Ed.; Marcel Dekker, Inc.: New York, 1991; Vol. 17, p. 221-374.

4. E. Frackowiak and F. Beguis, *Carbon*, **39**, 937 (2001).

5. N. Kishimoto and N. Matsuda, *Environ. Sci. Technol.,* **43**, 2054 (2009).

6. R. W. Murray, *Chemically Modified Electrodes, in Electroanalytical Chemistry,* Vol. 13; A. J. Bard, Ed.; Marcel Dekker: New York, 1984; p. 192.

7. T. Kamata, D. Kato, and O. Niwa, *Nanoscale*, **11**, 10239 (2019).

8. G. Yang, H. Chen, H. Qin, and Y. Feng, *Appl. Surf. Sci.*, **293**, 299 (2014).

9. S. A. Chernyak, A. S. Ivanov, E. A. Arkhipova, A. V. Shumyantsev, N. E. Strokova, K. I. Maslakov, S. V. Savilov, and V. V. Lunin, *Appl. Surf. Sci.*, **484**, 228 (2019).

10. Y. Yamada, J. Kim, S. Matsuo, and S. Sato, *Carbon*, **70**, 59 (2014).

11. H. Notsu, I. Yagi, T. Tatsuma, D. A. Tryk, and A. Fujishima, *Electrochem. Solid-State Lett.*, **2(10)**, 522 (1999).

12. M-C. Hsiao, S-H. Liao, M-Y. Yen, P-I. Liu, N-W. Pu, C-A. Wang, and C-C. M Ma, *ACS Appl. Mater. Interfaces*, **2(11)**, 3092 (2010).

13. E. Dsimoni, G. I Casella, A. Morone, and A. M. Salvi, *Surf. Inter. Anal.*, **15(10)**, 627 (1990).

14. H. Oda, A. Yamashita, S. Minoura, M. Okamoto, and T. Morimoto, *J. Pow. Sour.*, **158(2)**, 1510 (2006).

15. V. V. Tomina, G. R. Yurchenko, A. K. Matkovsky, Y. L. Zub, A. Kosak, A. Lobnik, *J. Flu. Chem*., **132(12)**, 1146 (2011).

16. T. Liang, C. N. Neumann, and T. Ritter, *Angew. Chem. Int. Ed*., **52(32)**, 8214 (2013).

17. F-L. Jin, H-Y. Kim, and S-J. Park, *J. Flu. Chem*., **128(3)**, 184 (2007).

18. B. Barbier, J. Pinson, G. Desarmot, and J. J. Sanchez, *J. Electrochem. Soc*., **137**, 184 (2007).

19. A. J. Doward, *Electroanalysis*, **12**, 1085 (2000).

20. S. Uchiyama, H. Watanabe, H. Yamazaki, A. Kanazawa, H. Hamana, and Y. Okabe, *J. Electrochem. Soc*., **154(2)**, F31 (2007).

21. H. Watanabe, H. Yamazaki, X. Wang, and S. Uchiyama, *Electrochim. Acta*, **54**, 1362 (2009).

22. Y. Yamawaki, K. Asaka, H. Matsuura, and S. Uchiyama, *Bunseki Kagaku*, **63**, 411 (2014).

23. A. Kanazawa, T. Daisaku, T. Okajima, S. Uchiyama, S. Kawauchi, and T. Ohsaka, *Langmuir*, **30**, 5297 (2014).

24. S. Uchiyama, H. Matsuura, and Y. Yamazaki, *Electrochim. Acta*, **88**, 251 (2013).

Figures and Tables
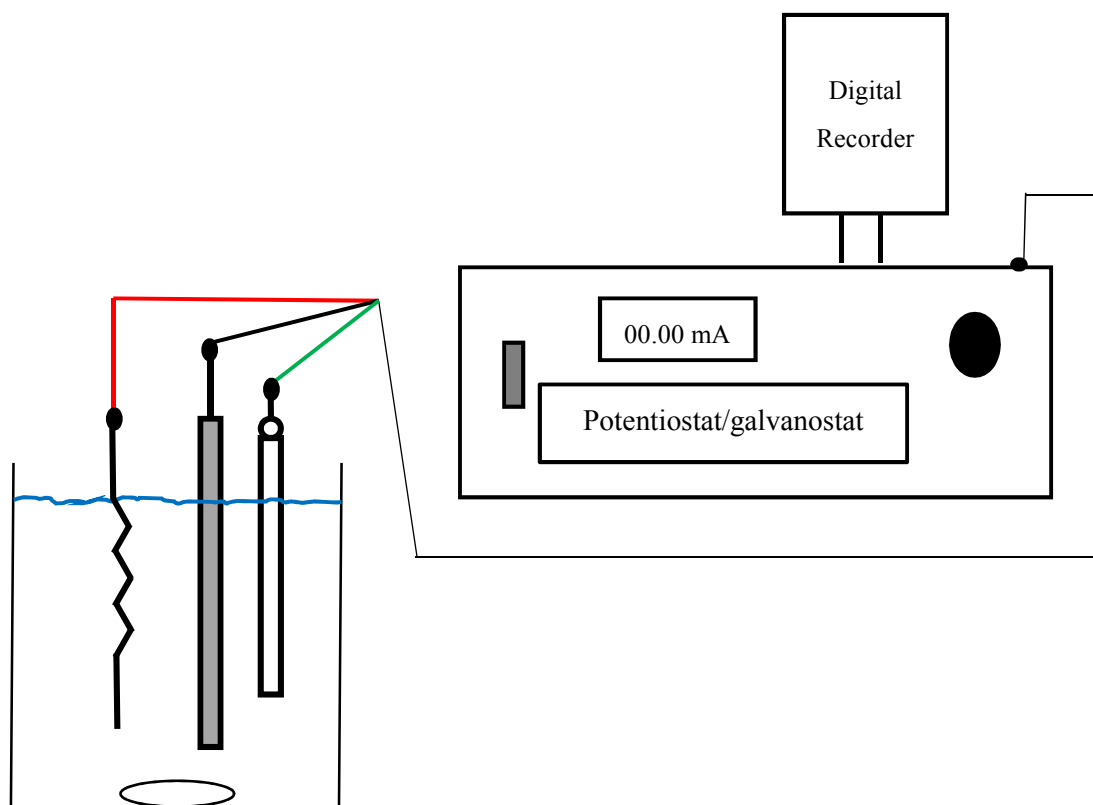
Figure 2.1. Schematic diagram between potentiostat/galvanostat consisting of three electrodes: a working electrode (black line), a counter electrode, (red line), and reference electrode (green line) which is connected with the digital recorder.
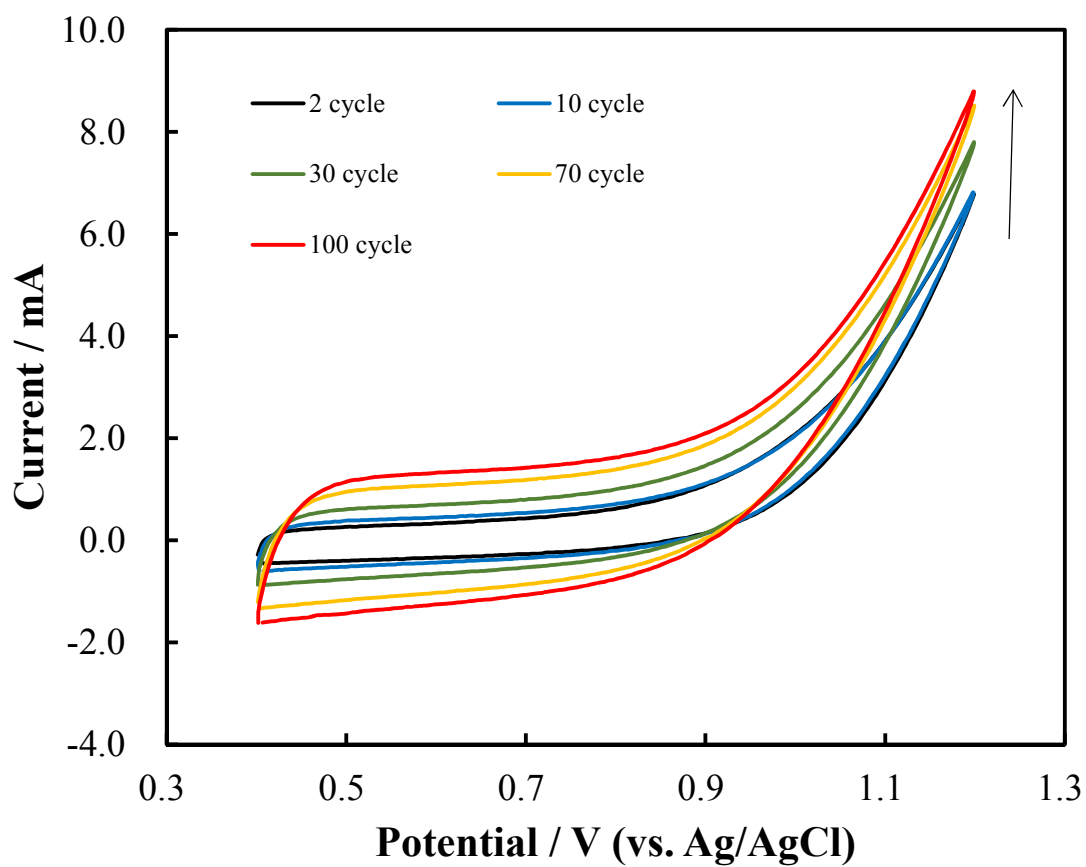
Figure 2.2. Cyclic voltammetry observed by using carbon felt electrode in 0.1 M ammonium carbamate (pH 9.3) aqueous solution at different number of cycles. Applied potential: +0.4 V to +1.2 V. Scan rate: 50 mV/s.
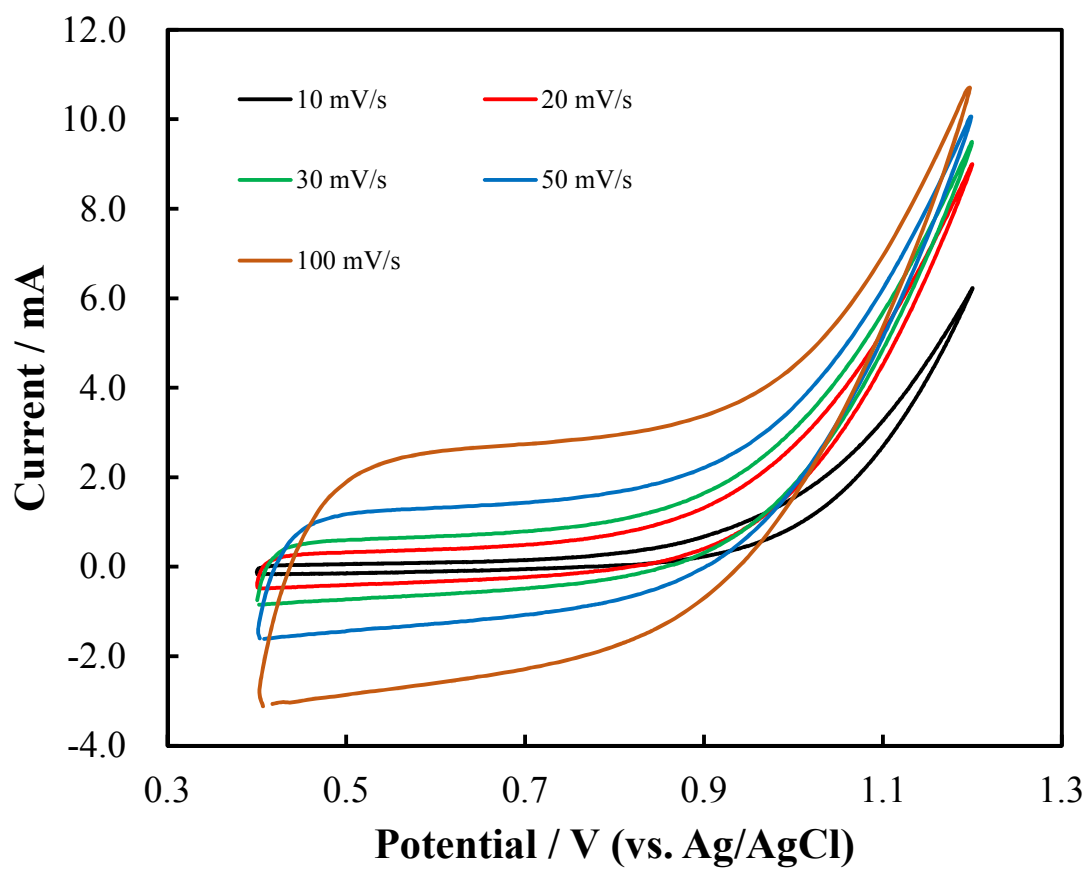
Figure 2.3. Cyclic voltammetry observed by using carbon felt electrode in 0.1 M ammonium carbamate (pH 9.3) aqueous solution at different scan rates.
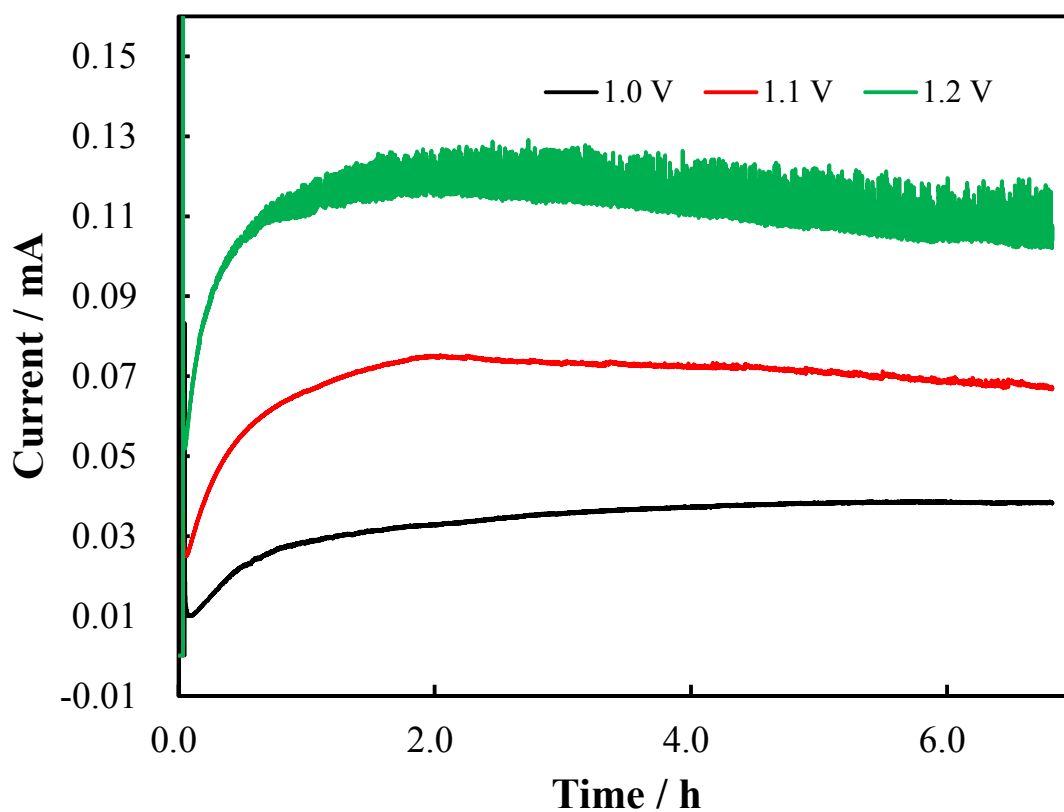
Figure 2.4. Observation best applied potential during electrode oxidation process correspond with time process by using a bare carbon felt electrode and recorded at digital recorder. The electrolyte solution: 0.1 M ammonium carbamate aqueous solution (pH 9.3).
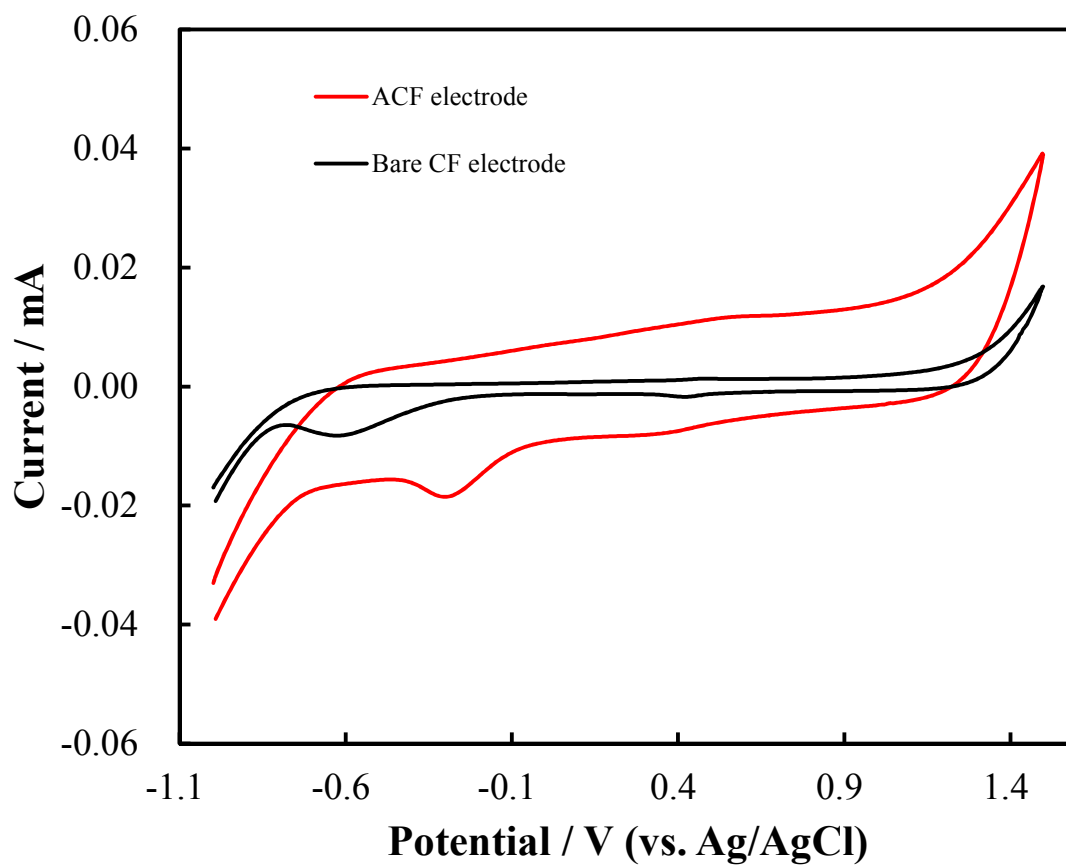
Figure 2.5. Cyclic voltammetry observed by using bare CF electrode (black color) and ACF electrode (red color) in 0.5 M H_2SO_4 solution (pH 0.0). Scan rate: 50 mV/s.
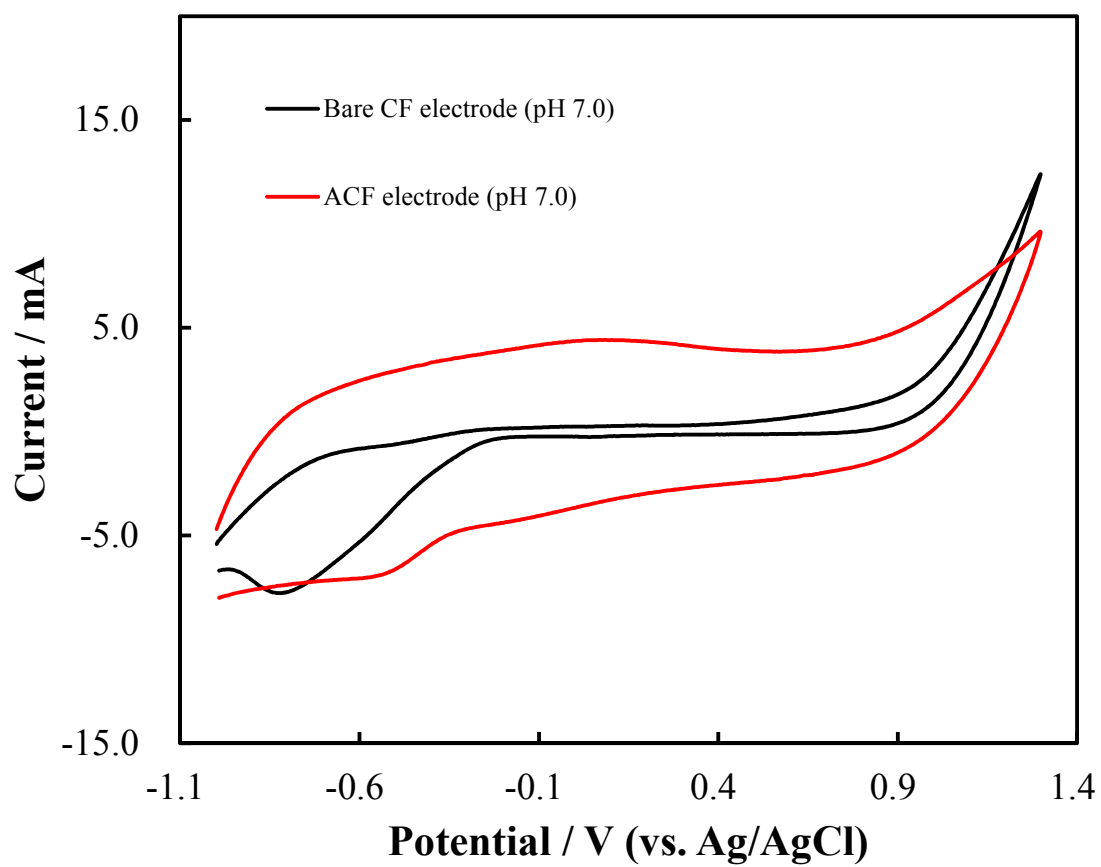
Figure 2.6. Cyclic voltammetry observed by using bare CF electrode (black color) and ACF electrode (red color) in 0.1 M phosphate buffer solution (pH 7.0). Scan rate: 50 mV/s.
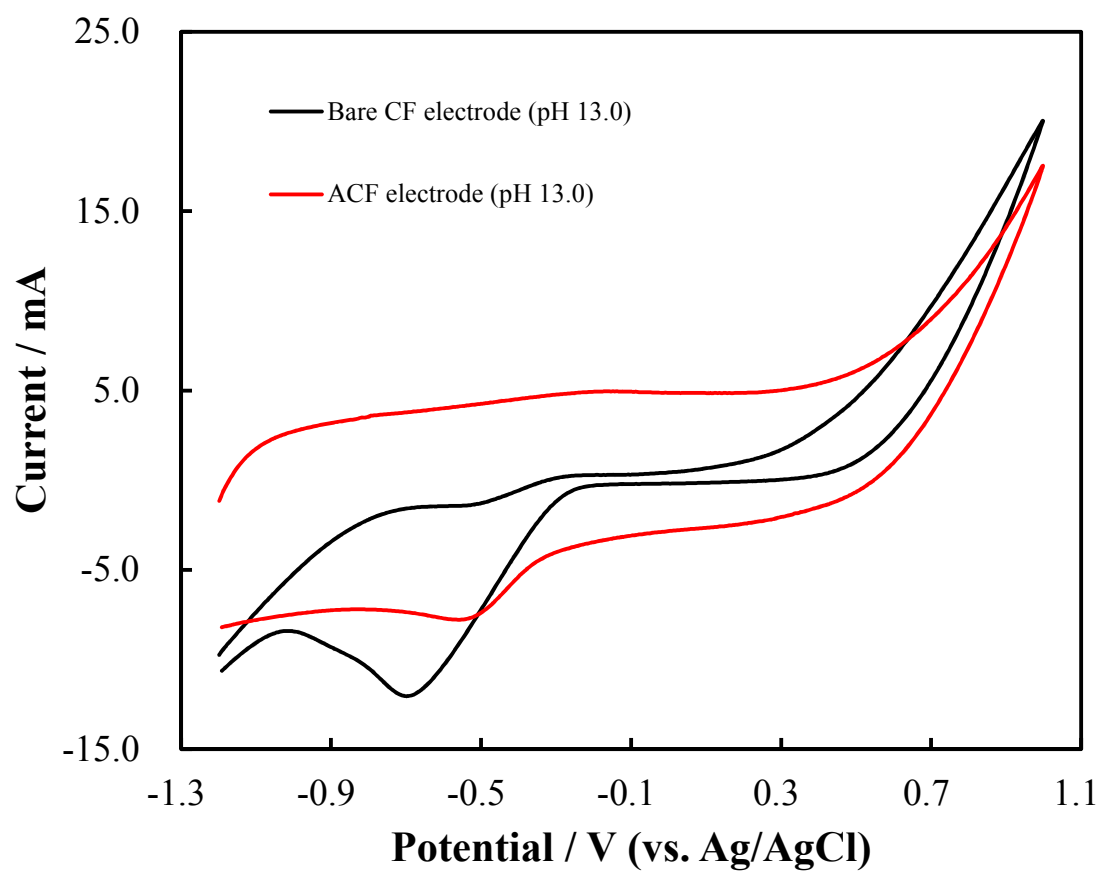
Figure 2.7. Cyclic voltammetry observed by using bare CF electrode (black color) and

ACF electrode (red color) in 0.1 M NaOH solution (pH 13.0). Scan rate: 50 mV/s.

2.2   Electrodeposition of Platinum Particles with Nitrogen-Containing Functional Groups on the Carbon Electrode Surface.

2.2.1.   Abstract

In this chapter, the CF and GC electrodes were used as carbon electrodes. A simple electrodeposition method was used for the deposition of platinum particles attached to the nitrogen-containing functional groups on the carbon surface electrode (Pt-NGC electrode) via electrochemical reduction. The structure, morphology, and composition of the Pt-NCF electrode were investigated using scanning electron microscopy (SEM) and X-ray photoelectron spectroscopy (XPS). A digital recorder was used to determine the optimal duration of electrochemical reduction. The best processing time to achieve stability was 20 h for the Pt-NGC electrodes, which was better than that of the Pt-GC electrode. The size of the platinum nanoparticles were <100 nm. Finally, the Pt-NGC electrode was found to be superior to the conventional electrode (Pt disk electrode) for solutions with a wide range of a pH values.

2.2.2. Introduction

Nanoparticles are characterized by different physical and chemical properties depending on their sizes, shapes, and structural forms.[1,2] Catalysis is one of the most popular applications of transition metals, particularly noble metals, owing to their high catalytic activities in many reactions. Nanoparticles can facilitate electron transfer and may be easily modified using several biomolecules and chemical ligands.[3] Moreover, such characteristics together with the benefit of miniaturization of sensing devices to nanoscale dimensions render the nanoparticles suitable for important applications in sensors (chemical and biochemical sensing). For this reason, studies on nanoscale materials have increased over time, particularly the metallic nanoparticles. Many metal nanoparticles such as palladium, ruthenium, copper, nickel, and iron are available, but silver, gold, and platinum are the most commonly used nanoparticles.

The catalytic activity of platinum is more expensive than gold and silver. Consequently, catalytic activity has achieved by the utilization of platinum nanoparticles.[4] Platinum nanoparticles possess a wide range of properties that can be used for many practical applications.[3] Platinum nanoparticles are particularly useful for the modification of electrodes because the nobility of platinum affords a high catalytic activity for many reactions, as these can be easily modified with various biomolecules and chemical ligands.[2] In addition, platinum nanoparticles have high surface areas and can enhance the mass transport of the electrodes. Various methods are available for the fabrication of platinum nanoparticles including sputtering,[5,6] reverse micelle formation,[7] electron beam lithography,[8] and chemical vapor deposition.[9] These methods are used in applications such as sensors and fuel cells. Furthermore, platinum nanoparticles can be applied via electrochemical deposition for the modification of electrode surfaces.

In recent years, significant advancement of the electrochemical deposition method has been achieved by the researchers. Electrodeposition, a short name of electrolytic deposition.[10] Electrodeposition is a material production technology that employs an applied potential or current flow through an electrolytic solution containing metal ions. These metal ions are eventually reduced to atoms in an electrically conducting substrate, thereby forming metals, alloys, and metal-based compounds.[11] Here, the platinum wire is used for electrodeposition through an electrochemical reduction process for the modification of the electrode carbon material surface. Based on the previous reports, the platinum wire is connected to the counter electrode, and treated with strong sulfuric acid solution during electrochemical reduction. The platinum wire produces platinum ions, which are transferred and absorbed into the carbon surface material. CF and GC electrodes were used in these experiments.

In the present work, a simple electrodeposition method was used for the deposition of platinum nanoparticles on GC (Pt-NGC electrode) and/or CF electrode (Pt-NCF electrode) with nitrogen-containing functional groups via electrochemical reduction. The structure, morphology, and composition of this Pt-NGC electrode were investigated using SEM and XPS. In addition, the optimal duration of electrochemical reduction was determined using a digital recorder. The Pt-NGC electrode was found to be superior to the conventional electrode (Pt disk electrode) for solutions with a wide range of pH values.

2.2.3. Experimental Section

The CF electrode (GF-20-5F) with 20-mm diameter and 5-mm thickness was purchased from Nippon Carbon Co., Ltd., Japan. The GC electrode with an inside diameter (ID) of approximately 3 mm was purchased from BAS Co., Ltd. (Tokyo, Japan). Ammonium carbamate was purchased from Merck KGaA (Darmstadt, Germany), while potassium dihydrogen phosphate (KH_2PO_4), sodium hydroxide, 0.5 M sulfuric acid, and dipotassium hydrogenphosphate (K_2HPO_4) were purchased from Fujifilm Wako Pure Chemical Industries, Ltd. (Osaka, Japan). Two solutions of potassium dihydrogen phosphate and dipotassium hydrogen phosphate were mixed together to prepare 0.1 M phosphate buffer solution (pH 7.0). All reagents were of analytical grade and used without further purification. The solutions were prepared using deionized water (Millipore Milli-Q System, Japan).

An ultrasonic bath was purchased from Branson Ultrasonic, Emerson Japan, Ltd. A potentiostat/galvanostat (HA-151B, Hokuto Denko Co., Ltd., Japan) was used to perform the controlled potential electrolysis. Electrochemical measurements were conducted using an automation polarization system (HZ-3000, Hokuto Denko Co., Ltd., Japan). A potentiostat/galvanostat was used, and CV measurements were performed using a three-electrode-configuration cell containing a working electrode comprising a modified CF or GC electrode, aqueous Ag/AgCl (3 M NaCl electrolyte) as the reference electrode, and platinum wire as the counter electrode. A digital recorder (Gr-3500, Keyence Co, Ltd., Japan) was used to record the time during electrolysis. SEM was used to investigate the morphology, including the size and characteristics of the platinum particles on the CF and/or GC electrode with nitrogen-containing functional groups. The JIB-4500 SEM instrument was used (JEOL, Ltd., Tokyo, Japan). The

acceleration voltage of 10 kV at a magnification of 10000x for Pt-NCF electrode and 30 kV at a magnification of 3300x for the bare CF electrode were used. XPS (Physical Electronics Quantum 200, from ULVAC-PHI, Inc., Kanagawa, Japan) was used to determine the composition of the sample.

2.2.4. Results and Discussion

Figure 2.8 shows the optimal time of electrochemical reduction. Two different electrodes, Pt-GC (red color) and Pt-NGC (black color), were used. The Pt-GC electrode was prepared by directly electrodepositing platinum particles on the surface of a bare GC electrode. In contrast, for the Pt-NGC electrode, the platinum ions that were dissolved from the platinum wire as the counter electrode in strong acid were deposited on the nitrogen-containing functional groups of the GC electrode. This experiment was monitored using a digital recorder with an electrolyte solution of 1.0 M H_2SO_4. The data obtained for the Pt-NGC electrode became gradually stable after 19-h, and after 20 h, the data became very stable. This was inversely proportional to the observation for the Pt-GC electrode, where stabilization started after22 h, and the noise was high. Therefore, the optimal duration of electrochemical reduction was 20-h. This could be the time limit for the platinum ions that dissolved from a platinum wire counter electrode and were electrodeposited on N-containing functional groups at 20-h.

The morphologies of the modified of the CF and bare CF electrode surfaces were investigated by SEM. Figure 2.9 and 2.10 show the SEM data of the bare CF and Pt-NCF electrodes. The bare CF surface shows hollow tube fibers that are bonded and connected to each other (Figure 2.9). In Figure 2.10, small spherical particles represent the platinum particles on the surface of the CF electrode. Recently, the Pt-NGC electrode was investigated using energy dispersive X-ray spectroscopy (EDX), which is an X-ray technique used to identify the elemental compositions of the materials. Based on the EDX data, the nanoparticles size was <100 nm.[13] This indicated that the platinum nanoparticles were successfully deposited on the GC electrode surface. It was also assumed that the platinum nanoparticles of the Pt-NGC electrode had the same sizes as

those of the Pt-NCF electrode. It was confirmed that during the reduction of the N-GC electrode (Nitrogen-containing functional groups were introduced on the bare GC electrode), the platinum ions migrated from the platinum wire (counter electrode) to the electrolyte solution. These platinum ions were then deposited on the N-GC electrode to form platinum nanoparticles.

XPS is a sensitive and powerful tool for monitoring the structural changes in carbon-based materials. Herein, XPS was used to determine the binding energies of the sample (a) Pt-NCF electrode and (b) Pt-CF electrode. The fabrication of the Pt-CF electrode was similar to that of the Pt-GC electrode. These two electrodes were treated in ultrasonic bath with distilled water for 10 min. Table 2.1 include a summary of the percentages of the elements (carbon, nitrogen, oxygen, and platinum) at the Pt-NCF and Pt-CF electrodes. As shown in Figure 2.11, the high-resolution Pt-4f spectrum exhibits two peaks corresponding to the $4f_{7/2}$ and $4f_{5/2}$ doublet at 72.3 eV and 74.4 eV, respectively, for the (a) Pt-NCF electrode, while two peaks corresponding to the $4f_{7/2}$ and $4f_{5/2}$ doublet at 70.6 eV and 73.4 eV for (b) Pt-CF electrode. The two peaks for $4f_{7/2}$ and $4f_{5/2}$ shift toward higher binding energies by approximately 1 eV compared to those of the (b) Pt-CF electrode.[13] The measured charge and the platinum coordination state were found to be different[14] as the platinum nanoparticles were deposited on the nitrogen-containing functional groups to afford the Pt-NCF electrode.[15] The change in the electronic state of platinum is reflected by the interaction of the coordination bonds, corresponding to the complex formation reaction.[16] As expected, the platinum nanoparticles and characteristic reactions were also different. These results are as expected by the author.

A wide pH range was employed to obtain the redox waves between a hydrogen ion (H^+) and a hydrogen molecule (H_2) at Pt-NGC electrode and conventional electrode (Pt disk electrode). Here, 0.5 M H_2SO_4 (pH 0.0), 0.1 M phosphate buffer solution (pH 7.0), and 0.1 M NaOH (pH 13.0) were used. The results are shown in Figure 2.12 to 2.14, based on which, the Pt-NGC electrode is better than the conventional electrode. Furthermore, in three figures, the electrocatalytic redox (reduction-oxidation) waves between hydrogen ion (H^+) and hydrogen molecule (H_2) are observed in wide pH range similar to the observation in the CV measurements.[12] The hydrogen ion (H^+) shows a reduction wave (reduction process) and the hydrogen molecule (H_2) shows an oxidation wave (oxidation process). This is represented by the following reactions:

(1) $2H^+ + 2e^- \longrightarrow H_2$

(2) $H_2 \longrightarrow 2H^+ + 2e^-$
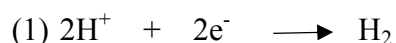
2.2.5. Conclusions

Two types of carbon electrodes, CF and GC electrodes, were used. A simple electrodeposition method was used to deposit the platinum particles that were connected to the nitrogen-containing functional groups on the carbon electrode surface (Pt-NGC electrode) and/or Pt-NCF electrode via electrochemical reduction. The structure, morphology, and composition of the Pt-NCF electrode were investigated using SEM and XPS. A digital recorder was used to determine the optimal duration of electrochemical reduction. The optimal time to achieve stability during electrochemical reduction was 20 h for the Pt-NGC electrode, which was better than that of the Pt-GC electrode. The sizes of the deposited platinum nanoparticles were <100 nm. The Pt-NGC electrode was superior to the conventional electrode (Pt disk electrode) in solutions with a wide range of pH values. Additionally, an electrocatalytic redox wave was observed between hydrogen ion (H^+) and hydrogen molecules (H_2) in solutions a wide range of pH values.

References

1. G. Vinci and M. Rapa, *Bioengineering*, **6**, 10 (2019).

2. S. Hrapovic, Y Liu, K. B. Male, and J. H. T. Luong, *Anal. Chem.*, **76**, 1083 (2004).

3. A. L. Stepanov, A. N. Golubev, S. I. Mikitin, and Y. N. Osin, *Rev. Adv. Mater. Sci.,* **38**, 160 (2014).

4. F. W. Campbell and R. G. Compton, *Anal. Bioanal. Chem.*, **396**, 241 (2010).

5. T. You, O. Niwa, M. Tomita, and S. Hirono, *Anal. Chem.*, **75**, 2080 (2003).

6. T. You, O. Niwa, T. Horiuchi, M. Tomita, Y. Iwasaki, Y. Ueno, and S. Hirono, *Chem. Mater.,* **14**, 4796 (2002).

7. L-B. Lai, D-H. Chen, and T-C. Huang, *Mater. Res. Bull.,* **36**, 1049 (2001).

8. J. Grunes, J. Zhu, E. A. Anderson, and G. A. Somorjai, *J. Phys. Chem. B.,* **106**, 11463 (2002).

9. P. Serp, R. Feurer, Y. Kihn, P. Kalck, J. L. Faria, and J. L. Figuiredo, *J. Mater. Chem.,* **11**, 1980 (2001).

10. S. Glasstone, *The Fundamentals of Eelectrochemistry and Electrodeposition.* Palisade, NJ: Franklin Publishing. (1960).

11. F. A. Lowenheim, *Modern Electroplating.* New York: John Willey & Sons. (1974).

12. H. Matsuura, T. Takahashi, S. Sakamoto, T. Kitamura, and S. Uchiyama, *Anal. Sci.,* **33**, 703 (2017).

13. C. Shimamura, M. Jinnai, S. Kuntolaksono, S. Sato, and H. Matsuura, *J. Surface Finish. Soc. Of Japan,* Accepted. (in Japanese).

14. M. Nagoshi, *J. Surface Anal.,* **78(1)**, 78 (2000). (in Japanese).

15. A. Kanazawa, T. Daisaku, T. Okajima, S. Uchiyama, S. Kawauchi, and T. Ohsaka, *Langmuir, 30,* 5297 (2014).

16. Y. Yoshida, *The Imaging Society of Japan*, **50(5)**, 463 (2011).

Figures and Tables
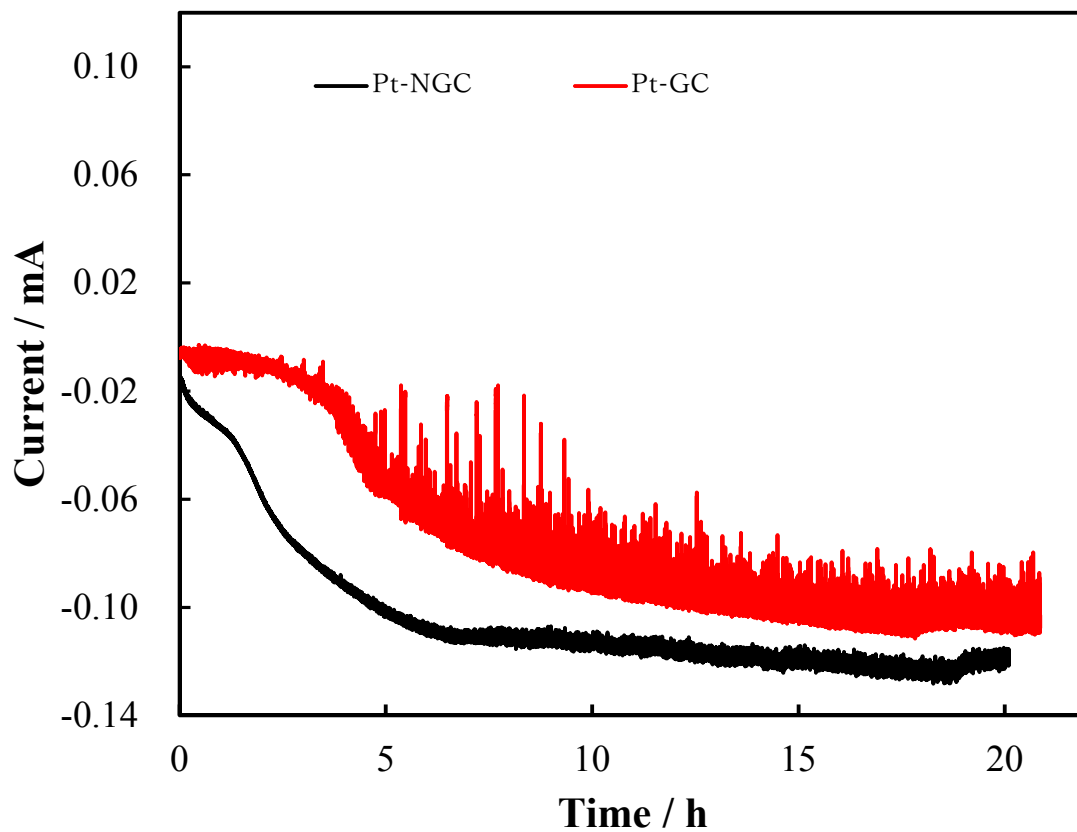
Figure 2.8. Observation at digital recorder to select the best time in the electrode reduction process using different electrode (red color: Pt-GC electrode) and (black color: Pt-NGC electrode). The supporting electrolyte solution: 1.0 M sulfuric acid and the applied potential: -1.1 V.

30.0kV   x3,300   5 μ m
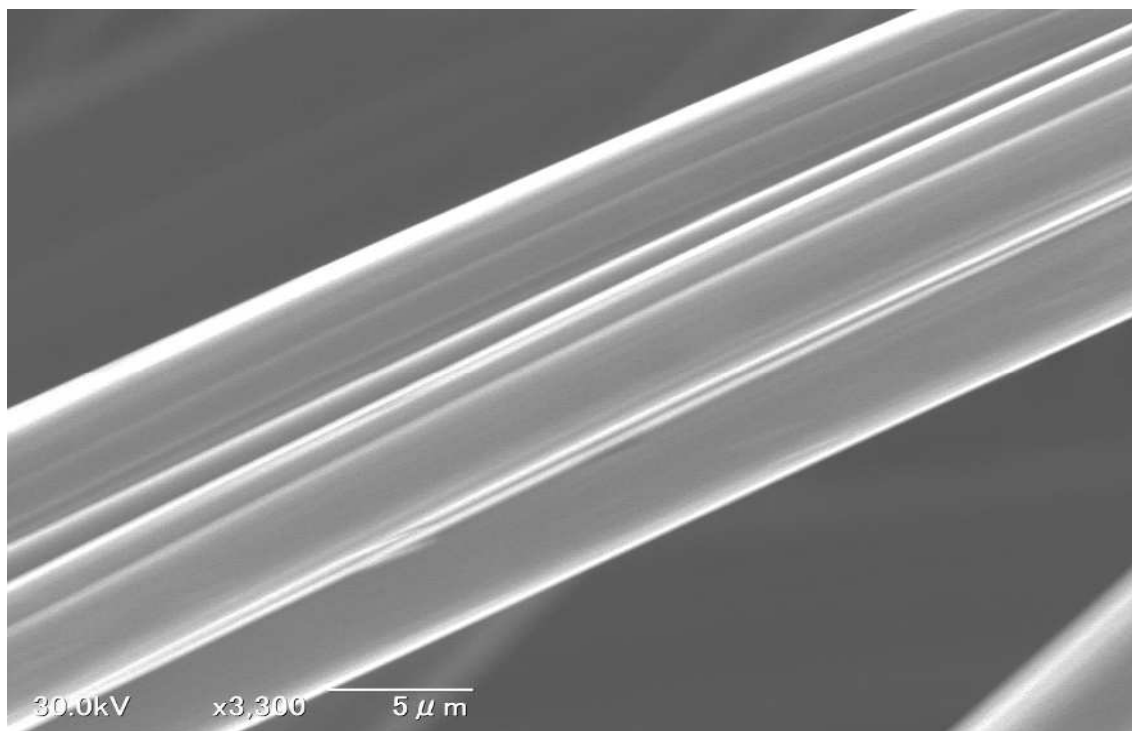
Figure 2.9. Scanning Electron Microscope (SEM) image of a bare CF electrode.
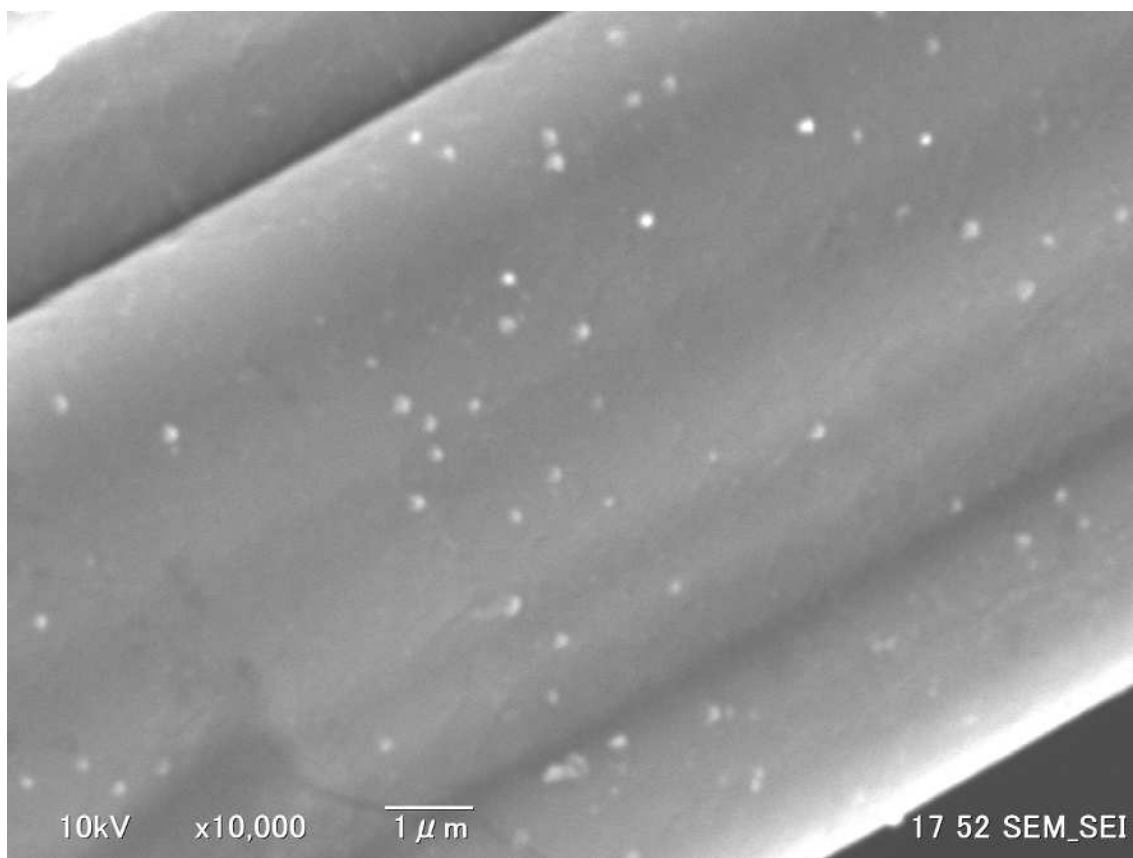
Figure 2.10. Scanning Electron Microscope (SEM) image of Pt-NCF electrode.
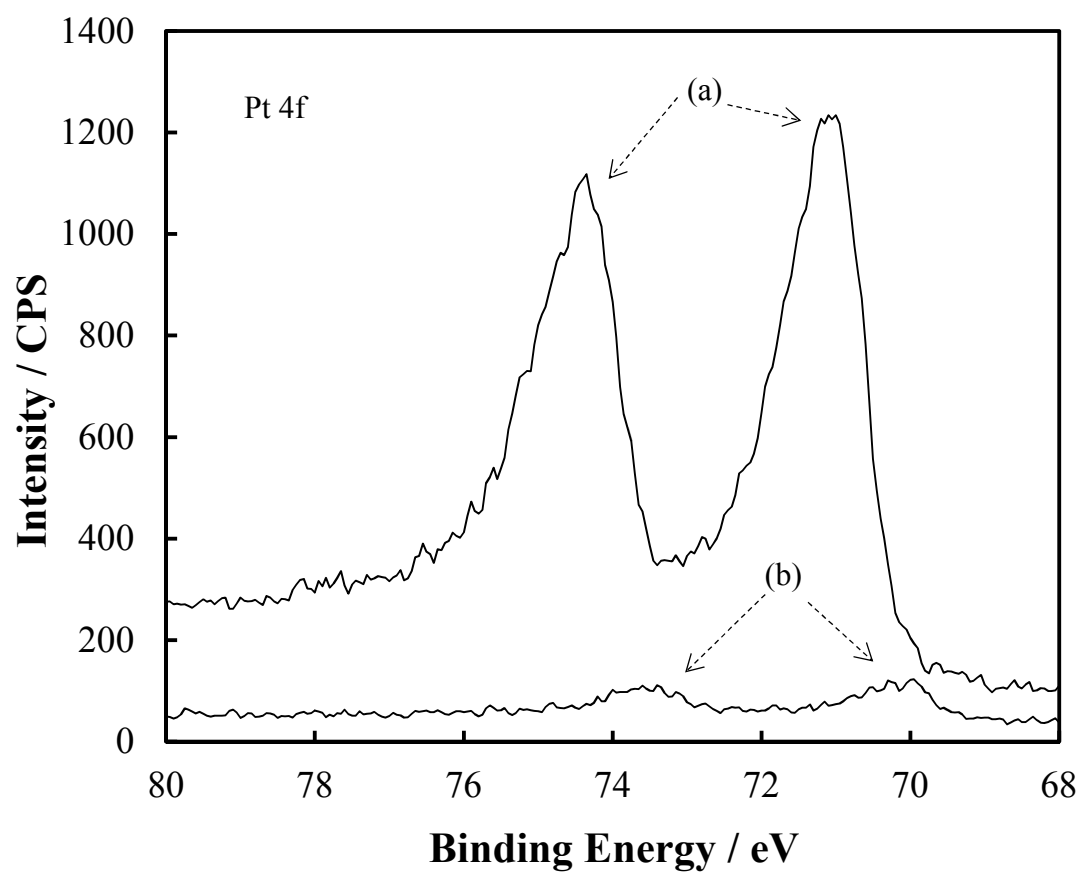
Figure 2.11. XPS spectra of Pt 4f by using (a) Pt-NCF electrode and (b) Pt-CF electrode with 10 minutes of ultrasonic treatment.
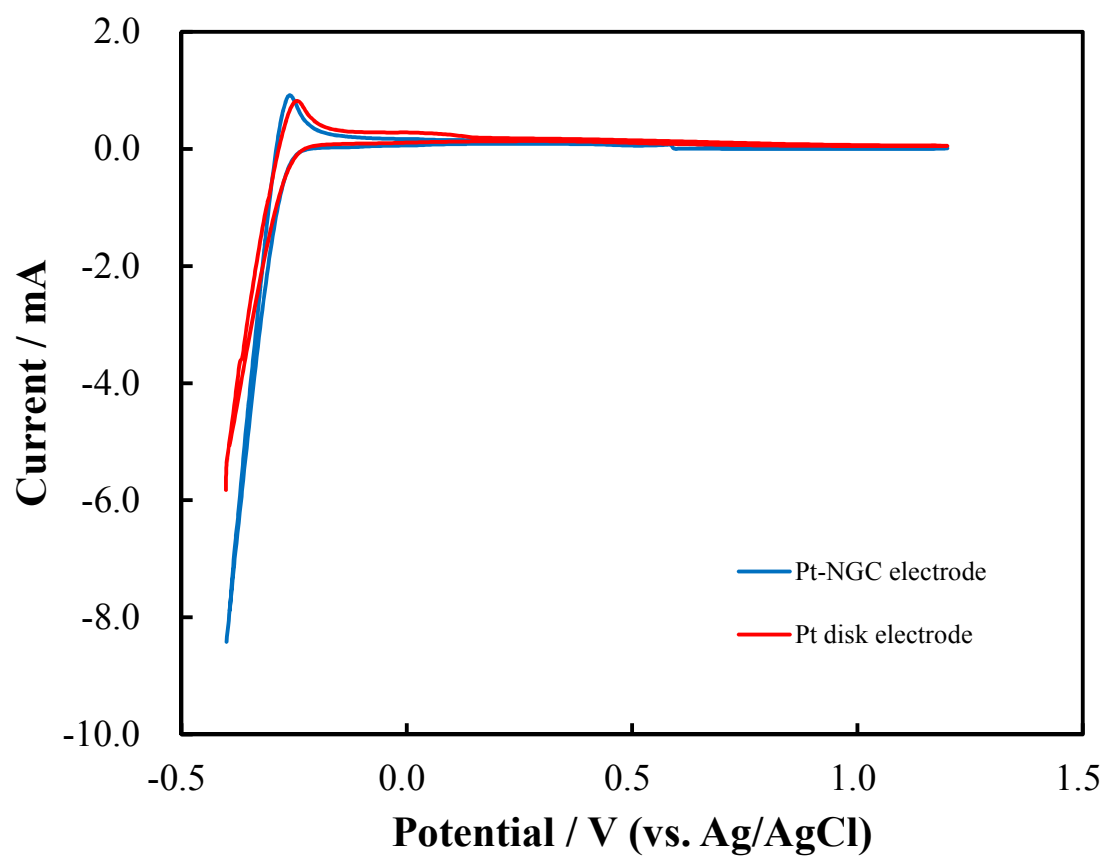
Figure 2.12. Cyclic voltammetry observed by using Pt-NGC electrode (blue line) and Pt disk electrode (red line) in 0.5 M H_2SO_4 (pH 0.0). Scan rate: 50 mV/s.
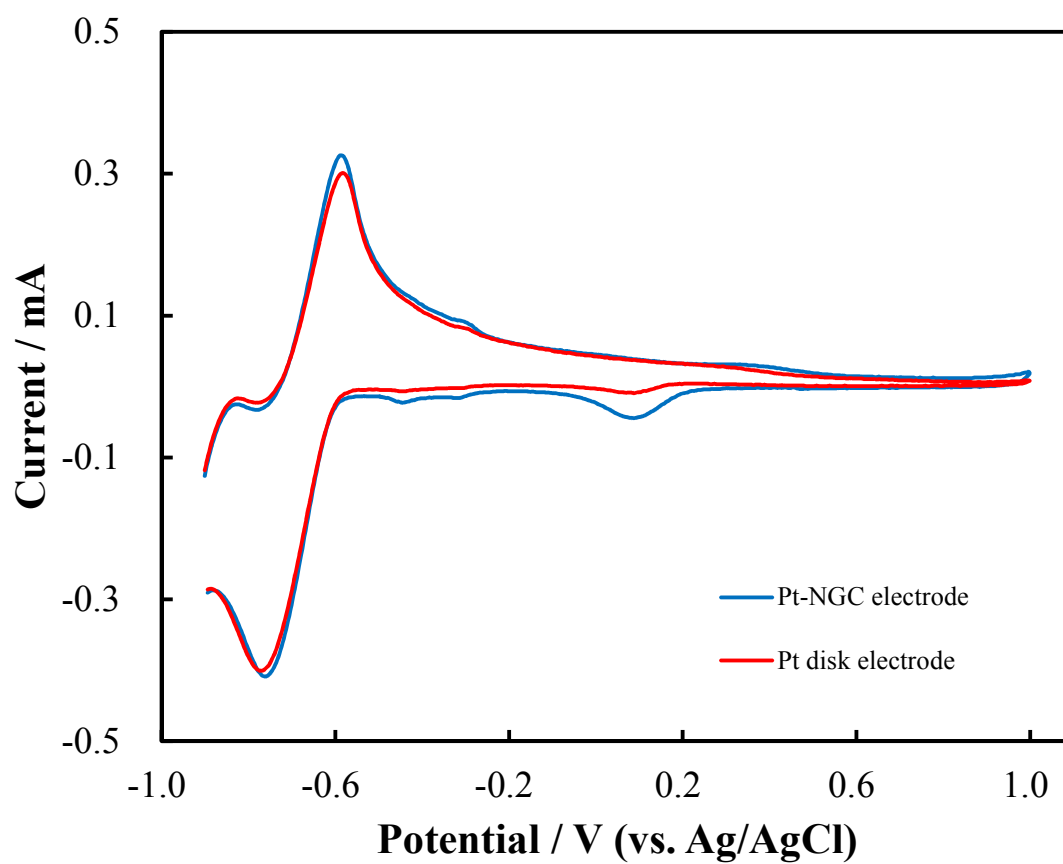
Figure 2.13. Cyclic voltammetry observed by using Pt-NGC electrode (blue line) and Pt disk electrode (red line) in 0.1 M phosphate buffer solution (pH 7.0). Scan rate: 50 mV/s.
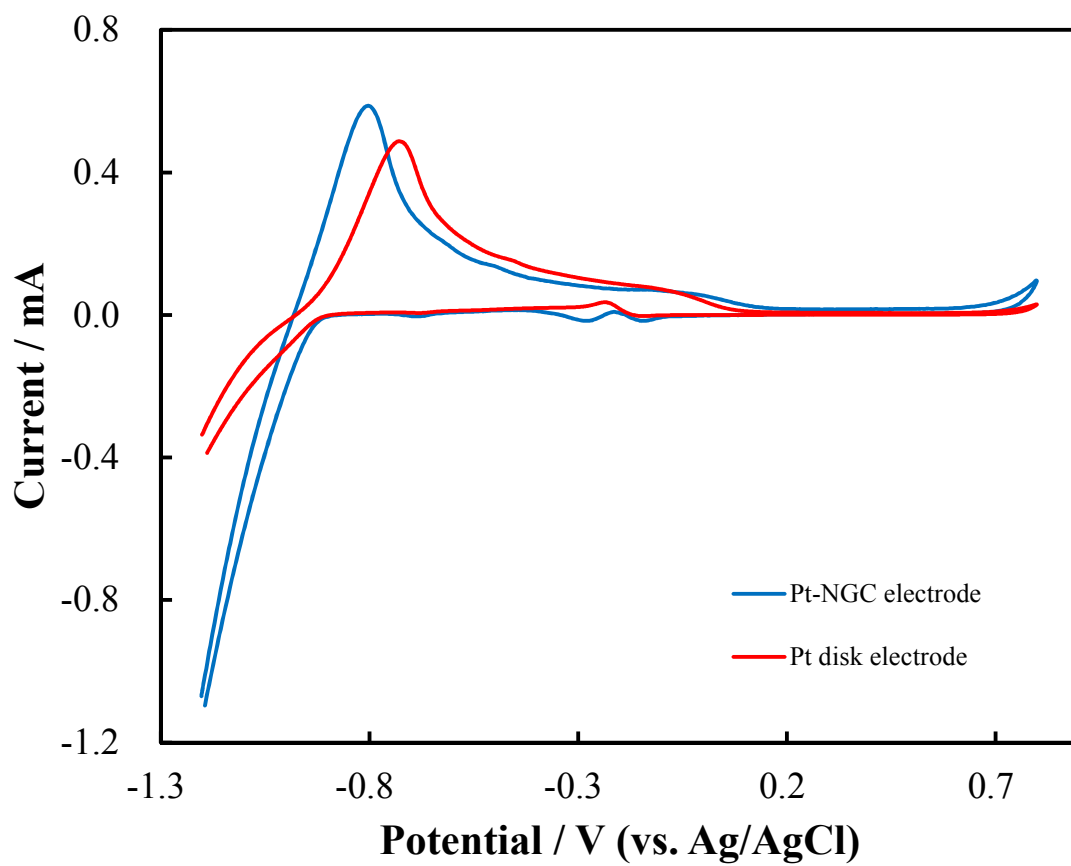
Figure 2.14. Cyclic voltammetry observed by using Pt-NGC electrode (blue line) and Pt disk electrode (red line) in 0.1 M NaOH (pH 13.0). Scan rate: 50 mV/s.

Table 2.1. The atomic ratio for each element which consist on the Pt-NCF electrode and

Pt-CF electrode after 10 minutes ultrasonic treatment.

	Atomic ratio each element		
	C	O	Pt
Pt-NCF electrode	76.4	16.6	7.0
Pt-CF electrode	86.5	13.4	0.1

Chapter 3

Potential-Controlled Coulometric Analysis of Nitrite Using Aminated Carbon felt Electrode

3.1.   Abstract

In this chapter, the author describes the development of an absolute determination method based on potential-controlled coulometry using aminated carbon felt electrode created by the electrode oxidation in ammonium carbamate solution for detection of nitrite. The potential-controlled coulometric cell was assembled using a carbon felt electrode as a working electrode which is made by processing of electrode oxidation at +1.1 V (vs Ag/AgCl) in 0.1 M ammonium carbamate solution. With the optimal applied condition of the sensor was +0.75 V, the nitrite oxidation current was detected immediately by adding 10 µL of 1.0 mM nitrite. Furthermore, the number of electron path processes was two electron paths from the estimation of the electrical charge of nitrite detection. These results indicate that the proposed research method provides an analysis of the absolute quantity amount of nitrite. The relationship between current and time curves was finished completely in a relatively short time (~30 s) for detection of nitrite. The tenth successive measurement of the relative standard deviation (RSD) was 2.2 %. This indicates that our potential-controlled coulometric method can be used for the absolute determination of the nitrite concentration in practical applications.

3.2. Introduction

Nitrite (NO_2^-) is a nitrogen source for green plants,[1] an inorganic compound found in nature,[1] an important component of the nitrogen cycle.[2] Nitrite can be found and used in a wide area, for example in the industrial, environment, agricultural production, as food additives and food preservatives.[3-5] Also, in the food industry, nitrite can able to inhibit the growth of some bacteria and give the meat an attractive color.[6] Discharge of wastewater containing nitrite into the environment is a big source deterioration of lakes, rivers, and water sources, which may cause serious health hazards to humans. Also, it is another example of the use of nitrite as a dye agent, bleach, and corrosion inhibitor in the chemical industry.[7-10]

Despite the application of nitrite in various fields, nitrite has a negative effect on the nitrite itself. The disadvantage of nitrite consists of high toxicity at high concentrations, harmful to human health and the environment.[11-14] As an example, if nitrite has in inside the human body, nitrite may react with amines and probably causes carcinogenic nitrosamines[15,16] as well as oxidizes hemoglobin to methemoglobin which diminishes the oxygen carrying capacity.[17] Furthermore, effect of nitrite in humans may cause hypertension, cancer, spontaneous abortion, birth defects, growth restriction, etc.[18-20] Consequently, the accurate determination of sulfite is very important in food, chemical industries, and environmental monitoring application.

Traditional or conventional method to determining the nitrite concentrations include liquid chromatography (LC)-based techniques.[21-23] Liquid chromatography usually determined the nitrite in meat products. These often involve laborious and time-consuming sample preparation and require highly skilled personnel, making the quest for developing simpler and more cost-effective techniques for rapid monitoring

incessant. Colorimetric techniques have also been applied to determine the amount of nitrite in foods.[23,24] This technique require lab-equipped spectrometers, large sample volumes, and glass consumables to house the reaction.[23] Another example of traditional method for detection nitrite, such as high performance liquid chromatography,[25,26] chemiluminescence,[27,28] flow injection analysis,[29] Raman spectrometry,[30] spectrophotometry,[31,32] and ion chromatography.[33,34] Those technique have disadvantages including complicated pre-treatment of samples that consumes time, expensive,

In contrast, the above problems are overcome by electrochemical techniques that have been widely explored for nitrite quantification and direct detection through accurate, rapid response, low cost, high sensitivity, operational simplicity, and real time quantitative analysis.[35-41] Although nitrite can be determined by either reduction of oxidation, the electrochemical oxidation of nitrite is usually preferred over reduction, in order to avoid major disturbance from oxygen molecules and nitrite.[37,38] Electrochemical techniques for nitrite has mainly been determined using amperometry,[42-44] anodic voltammetry,[45,46] square wave voltammetry,[47,48] differential pulse voltammetry,[49-52] and cyclic voltammetry.[53-55] Those techniques have disadvantages and ineffective for detecting nitrite due to the requires calibration.

To accommodate those problems, the author proposes a new technique and method to detecting nitrite by used electrochemical absolute determination technique. This technique called as the potential-controlled coulometry[57-64] or batch-injection coulometry.[65-67] The positive thing about this technique because the Faraday constant (coulomb/mole) can convert the charges flowing during the complete electrolysis of analytes, allowing the concentration of the analyte to be obtained directly in a single

droplet experiment.[56,57] An alternative reason to be used in the potential-controlled coulometry is a very simple structure of the sensor cell.[57] Then, the sensor does not need calibration during measurement process.[57] However, there is no one paper regarding determine of nitrite by using this analysis technique. Due to the reason, the author was the first reporting paper for employing this technique to detection of nitrite.[67]

Before applying at the sensor, the author must do a preliminary test by using the CF electrode. When a bare CF electrode conducted in the potential-controlled coulometry sensor, the author understands and know that the electrochemical properties of this electrode was poor and low active site function. In order to increase the electrochemical properties and active site of an electrode, a modification of the surface electrode must be attempted. The author proposes to deposit a nitrogen containing functional group on the bare CF electrode. For the steps and modifying method for electrode material are explained in Chapter 2. In addition, the data experiments on the potential-controlled coulometry sensor will be displayed on the results and discussion section of this chapter.

3.3.   Experimental Section

The carbon felt (CF) electrode was acquired from Nippon Carbon Co., Ltd., and the types and size of GF-20-5F, 20 diameters, and 5 mm thickness were used. All chemical reagents were supplied from Merck KGaA., Darmstadt, Germany and Wako Pure Chemical Industries, Ltd., Japan. First, ammonium carbamate ($H_2NCOONH_4$) was purchased from Merck KGaA., Darmstadt, Germany, and used without further purification. Second, the chemical reagents purchased from Wako Pure Chemical Industries, Ltd., Japan, consists of sodium nitrite ($NaNO_2$), potassium hexacyanoferrate ($K_3(Fe(CN)_6)$), acetic acid (CH_3COOH), and sodium acetate (CH_3COONa). The supporting electrolyte was used as an acetic acid buffer solution (pH 4.0)[21] which were prepared of 0.1 M (M = mol/L) sodium acetate and 0.1 M (M = mol/L) acetic acid. The cation exchange membrane used was from Asahi Glass Engineering, Japan. Distilled water produced by a Millipore-Q system (Millipore, Japan) was used to prepare all solutions. All the experiments were conducted at room temperature.

In this paragraph, the author described the equipped measurement which I used in this chapter. An ultrasonic bath was purchased from Branson Ultrasonic, Emerson Japan, Ltd. A potentiostat/galvanostat (HA-151B, Hokuto Denko Co., Ltd., Japan) was used to perform a controlled potential electrolysis. The cyclic voltammetry measurements were carried out using an automation polarization system (HZ-3000, Hokuto Denko Co., Ltd., Japan) with a three-cell consisting of a working carbon felt electrode, an aqueous Ag/AgCl (3 M NaCl electrolyte) as a reference electrode, and a platinum wire as the counter electrode. The potential-controlled coulometry measurement used a digital coulomb meter (Nikko Keisoku Co., Ltd., Japan) and a digital recorder (Gr-3500, Keyence Co., Ltd., Japan).

Next, the author explained the preparation of the aminated carbon felt (ACF) electrode. The CF electrode was mixed with ethanol and distilled water, treated in an ultrasonic bath for 1 h. The aim of using an ultrasonic bath is to remove all traces of contamination that are firmly or merely attached to the surface of the CF electrode. Then, a three-electrode cell consisted of CF working electrode, an Ag/AgCl reference electrode, and a platinum wire counter electrode. CF electrode was electro-oxidized in 0.1 M ammonium carbamate aqueous solution (pH 9.3) at a constant potential of +1.1 V for 1 h (60 minute). All experiments were carried out at room temperature.

During experiment in the cyclic voltammetry, all data were observed under temperature room. The author used two types of CF as working electrode: an ACF electrode and unmodified (bare) CF electrode. An aqueous Ag/AgCl (3 M NaCl electrolyte) reference electrode, a magnetic stirrer, and a platinum wire used as a counter electrode were also employed. The supporting electrolyte solution was 0.1 M acetic acid buffer solution (pH 4.0). The conditions setting in cyclic voltammetry were explained as follows; the potential scan range was +0.4 to +1.1 V, the potential cycle was set on 100, and the potential scan rate was 20 mV/s.

Figure 3.1 illustrates a schematic description of the constructed potential-controlled coulometric cell. The ACF electrode was used as a working electrode. The unmodified (bare) CF electrode without any electrochemical modification treatments was used as a counter carbon felt electrode. The function of using cation exchange membrane is to separate between ACF electrode and the counter carbon felt electrode. The size of platinum wire is 0.5 mm diameter and it was used as a lead wire. A saturated aqueous solution of potassium hexacyanoferrate (III) was used as a counter solution wet in the counter carbon electrode.

Moreover, the author determined the electrical charge (mC) and response time (s) by adding one droplet of 1.0 mM nitrite for three observations (n = 3), and calculated the average value. In order to obtain the best applied potential in the potential-controlled coulometry, the author investigated in the range +0.3 V to +1.0 V. Then, the best applied potential sensor cell was used for all measurements in potential-controlled coulometry. One droplet of 1.0 mM nitrite was added for ten repetitive measurements in the 0.1 M acetic acid buffer solutions, and the sample volume was 10 μL. The numerous added sample volumes were from 0 to 100 μL. The numerous concentrations of 0.1 to 10 mM nitrite were used.

3.4.   Results and Discussion

3.4.1.   Electrochemical Performance of Nitrite

The electrochemical properties of the nitrogen-containing functional groups deposited on CF electrode were investigated by cyclic voltammograms experiments in 0.1 M acetic acid buffer solution (pH 4.0) in with (solid line) and without (dotted line) of 10 mM nitrite. As described in Fig. 3.2, without the addition of nitrite in the ACF electrode, does not have oxidation wave was achieved from nitrite in the potential range from +0.4 to +1.1 V. In contrast, there is an oxidation wave generated when nitrite was added on ACF electrode. Then, the author found that the anodic peak potential was +0.95 V and that the oxidation peak current was 1.44 mA. The author also understands that the induction of the electrocatalytic activity of nitrite has inside in this process. This cyclic voltammogram shows the electro-oxidation product in the electro-inactive species. Then, these results indicate that the nitrite ion will oxidation to the nitrate ion according to Eq. (1).

$$NO_2^- \ + \ H_2O \ \longrightarrow \ NO_3^- \ + 2H^+ \ + \ 2e^- \tag{1}$$
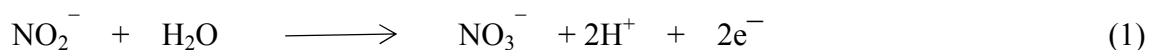
Moreover, the author was the first person who used the CF electrode for the detection of nitrite.[67] During the detection of nitrite, the author has used two kinds of a different electrode material such as CF electrode was modified with nitrogen-containing functional groups (ACF electrode) and unmodified (bare) CF electrode. For comparison purpose, those two kinds electrode as the author mentioned in the previous sentences, was applied for it. Figure 3.3 depicts the cyclic voltammetry of unmodified CF electrode and ACF electrode in 0.1 M acetate acid buffer solution (pH 4.0) having 10 mM nitrite. In the presence of nitrite, ACF electrode exhibits an oxidation peak current in comparison with the bare CF electrode. The oxidation peaks current of the ACF

electrode based sensor in 10 mM of nitrite is approximately 7 times higher than unmodified (bare) CF electrode based sensor. Based on the results reported by Wang et al.,[9] which used to nitrogen-contain functional groups modified on GC electrode, the oxidation peak current at aminated GC electrode was twofold larger than bare GC electrode.[9] The multiple increases in oxidation peak current exhibit the function of active site from a nitrogen atom containing functional groups in the ACF electrode and also aminated GC electrode as a modified carbon electrode. In addition, it is indicating that using carbon felt electrode are better than GC electrode. There are two option reasons it, first, due to the dimensions from the electrode made of carbon material (CF; type of 3 dimensional and GC; type of 2 dimensional), and the second is about the factor of the surface area of electrode material which I used.

As shown in Fig. 3.4, the author initiated measurement of the various concentration of nitrite at ACF electrode in 0.1 M acetic acid buffer solution (pH 4.0). The oxidation peak current was increased with an increase in nitrite concentrations up to 1.0 mM. Furthermore, the relationship between the peak current versus the concentration of nitrite was proportional result. The linear regression coefficient was 0.9937 and the detection limit was determined to be 10 μM. These results illustrated the stability of ACF electrode for electrocatalytic applications in which successive detection of nitrite is performed.

The kinetic characteristic for the nitrite oxidation reaction at ACF electrode was studied by cyclic voltammetry at different scanning rates in 0.1 M acetic acid buffer solution. As described in Fig. 3.5, the peak current increases as the scan rate increases as the scan rate increases from 10 mV/s to 100 mV/s. Furthermore, the oxidation peak current of nitrite is suitable to the scan rates (data not shown). The results indicate that

the electrochemical oxidation of nitrite at ACF electrode surface is a diffusion control process. In addition, I tried to making other data about the correlation between the oxidation peak current and the square root of the scan rate have a good linear relationship; with the linear regression was 0.9865. It is also suggesting that the oxidation of nitrite at ACF electrode is a diffusion control process.

3.4.2. Analytical Performance Using Potential-Controlled Coulometry for Detecting Nitrite

Specifically, Fig. 3.6 will have explained how to decide and how to determine the optimal conditions which will applied to the potential-controlled coulometric sensor in sulfite detection. The author observed the connection between the applied potential and the electrical charge at various applied potential during the potential-controlled coulometric of nitrite. The result between the electrical charge (solid line) and response time (dotted line) are shown in Fig. 3.6. Before enter to the point subject, the author will describe one by one of the meaning of response time and electrical charge.

In this paragraph, the author will explain the response time as follow: response time is the time required to return into the baseline and remain constant when adding a sample to the electrolyte solution in the potential-controlled coulometry. The response time when the applied potential ranges from +0.3 to +0.9 V indicates a rapid measurement. But, when the applied potential was on the +0.9 and +1.0 V, the response was slightly slow. After knowing about the response time at potential-controlled coulometry, let`s move to the electrical charge at potential-controlled coulometry. For this, the author will explain it in the next paragraph.

The amount of substance (mole) of the analyte corresponds to the electrical

charge through the Faraday constant. This means that the number of electrons can be estimated from the electric charge under the measurement to determine the concentration of the analyte. From the electrical charge data in Fig. 3.6, the author knows that the electron number of the electrode reaction was two-electron paths from the estimation of the electrical charge of nitrite detection. The high point of the electrical charge is when the applied potential is +0.5 V. However, in the applied potential range from +0.5 V to +0.8 V, the electrical charge was decreased. On the other hand, the electrical charge decreased significantly when the electrode potential exceeded +0.8 V. These results explain that the catalytic site on the surface of the ACF electrode was destroyed by electrode oxidation. With all the reasons mentioned above, the author decided that the optimal applied potential was +0.75 V.

The results data on the performance of potential-controlled coulometry using the ACF electrode will be explained in Fig. 3.7, 3.8, 3.9, and 3.10. In Fig. 3.7, showed a typical current relationship and time curve obtained by the repetitive measurement of 1.0 mM nitrite. The response time finished in a short time (~30 s) and no detectable residual current fluctuation appeared after the electrolysis had been completed. The tenth successive measurement of the relative standard deviation (RSD) was 2.2 %.

Next, Fig. 3.8 and Fig. 3.9 would describe the advantages of the potential-controlled coulometry for the detection of nitrite (analyte) at ACF electrode. As shown in Fig. 3.8, it explains the relationship between the electrical charge flowing through the electrode oxidation process of nitrite and the volume of sample added. This result indicates good linearity, with the electrical charge corresponding to the added sample volume in the range of 1-100 μL. Moreover, the linear regression was 0.997; it was indicating that the electrolysis efficiency is close to 100% because the

determination is very quickly realized.

Furthermore, Fig. 3.9 described the measurement of the nitrite concentration from high to low concentrations in a 10 μL sample volume. This data shown to us that`s the advantage of utilize potential-controlled coulometry. From this result, the author considers that the calibration curve changes when nitrite was added at various concentrations. It can be described that the high concentration solution (a) has a slow response. In contrast, the low concentration (h) has fast response.

After observed the concentration from high to low, the author tried to determining nitrite concentration from low – high, is shown in Fig. 3.10. And, describe the correlated between the electrical charge and the nitrite concentration. A 10 μL sample was dropped onto the ACF electrode and a nitrite concentration of 0.1 to 10 mM was used. The obtained result indicates that the electrical charge has a correlates with the nitrite concentration in the range from 0.1 to 10 mM with good linearity.

3.5.   Conclusions

The author has prepared nitrogen atoms containing functional groups that can easily be introduced to the surface of a modified carbon felt electrode, called the aminated carbon felt (ACF) electrode. Potential-controlled coulometry can be used for the analysis of nitrite because it does not require calibration, low cost, accurate, and rapid measurement can easily be performed. The author also has succeeded in determining the optimal applied potential of +0.75 V for analytical performance in coulometryc sensor, especially using the electrolyte 1.0 mM nitrite in acetic acid buffer solution (pH 4.0). The advantages of potential-controlled coulometric sensor is that it can determine from high to low sample concentration and simple structure sensor. Thus, the author proposed potential-controlled coulometric sensing as a promising method for nitrite detection.

References

1. R. Sha, A. Gopalakrishnan, K. V. Sreenivasulu, V. V. S. S. Srikanth, and S. Badhulika, *J. Alloys and Compounds*, **794**, 26 (2019).

2. Y. Liu, H. Xue, J. Liu, Q. Wang, and L. Wang, *Microchim. Acta*, **185**, 129 (2018).

3. N. Zhu, Q. Xu, S. Li, and H. Gao, *Electrochem. Commun.,* **11**, 2308 (2009).

4. K. A. Guy, H. Xu, J. C. Yang, C. J. Werth, and J. R. Sharpley, *Int. J. Electrochem. Sci.*, **10**, 1144 (2005).

5. X. Ma, F. Gao, G. Liu, Y. Xie, X. Tu, Y. Li, R. Dai, F. Qu, W. Wang, and L. Lu, *Microchim. Acta*, **186**, 291 (2019).

6. S. Huang, L. Li, L. Mei, J. Zhou, F. Guo, A. Wang, and J. Feng, *Microchim. Acta*, **183**, 791 (2016).

7. M. Ghanei-Motlagh and M. A. Taher, *Biosens. Bioelectron.,* **109**, 279 (2018).

8. A. D. Arulraj, E. Sundaram, V. S. Vasantha, and B. Neppolian, *New. J. Chem.*, **42(5)**, 3445 (2018).

9. X. Wang, T. Cao, Q. Zhuo, S. Wu, S. Uchiyama, and H. Matsuura, *Anal. Methods*, **8**, 3748 (2016).

10. H. Watanabe, H. Yamazaki, X. Wang, and S. Uchiyama, *Electrochim. Acta*, **54**, 1362 (2009).

11. D. M. Zurcher, Y. J. Adhia, J. D. Romero, and A. J. McNeil, *Chem. Commun.*, **50**, 7813 (2014).

12. X. Ma, T. Miao, W. Zhu, X. Gao, C. Wang, C. Wang, C. Zhao, and H. Ma, *RSC Adv.*, **4**, 57842 (2014).

13. P. Poormoghadam, A. Larki, and S. Rastegarzadeh, *Anal. Methods*, **7**, 8655 (2015).

14. L. Lu, C. Chen, D. Zhao, F. Yang, and X. Yang, *Anal. Methods*, **7**, 1543 (2015).

15. International Agency for Research on Cancer (IARC), World Health Organization: IARC Moographs on the Evaluation of Carcinogenic Risk to Humans (2010) 1:116

16. J. Wang, H Zhou, D. Fan, D. Zhao, and C. Xu, *Microchim. Acta*, **182(5)**, 1055 (2015).

17. M. Nasir, M. H. Nawaz, U. Latif, M. Yaqub, A. Hayat, and A. Rahim, *Microchim. Acta*, **184(2)**, 323 (2017).

18. H. Rao, Y. Liu, J. Zhong, Z. Zhang, X. Zhao, X. Liu, and Y. Wang, *ACS Sustain. Chem. Eng.,* **11**, 10926 (2017).

19. Y. Ma, X. Song, X. Ge, H. Zhang, G. Wang, Y. Zhang, and H. Zhao, *J. Mater. Chem. A*, **5(9)**, 4726 (2017).

20. Y. Ma, Y. Wang, D. Xie, Y. Gu, H. Zhang, G. Wang, and P. K. Wong, *ACS Appl. Mater. Interfaces*, **10(7)**, 6541 (2018).

21. L. Chiesa, F. Arioli, R. Ravovic, R. Villa, and S. Panseri, *Food Chem.*, **288**, 361 (2019).

22. M. Iammarino and A. DiTaranto, *Int. J. Food Sci. and Tech.*, **47(9)**, 1852 (2012).

23. E. Trofimchuk, Y. Hu, A. Nilghaz, M. Z. Hua, S. Sun, and X. Lu, *Food Chem.*, **316**, 126396 (2020).

24. T. M. G. Cardoso, P. T. Garcia, and W. K. T. Coltro, *Anal. Methods*, **50**, 7813 (2014).

25. Q. H. Wang, L. J. Yu, Y. Liu, L. Lin, R. G. Lu, J. P. Zhu, L. He, and Z. L. Lu, *Talanta*, **165**, 709 (2017).

26. I. M. Ferreira and S. Silva, *Talanta*, **74(5)**, 1598 (2008).

27. Z. Lin, W. Xue, H. Chen, and J. M. Lin, *Anal. Chem.*, **83(21)**, 8245 (2011).

28. P. Mikuska and Z. Vecera, *Anal. Chim. Acta*, **495**, 225 (2003).

29. L. A. Pradela-Filho, B. C. Oliveira, R. M. Takeuchi, and A. L. Santos, *Electrochim. Acta,* **180**, 939 (2015).

30. X. Liu, L. Tang, R. Niessner, Y. Ying, and C. Haisch, *Anal. Chem*., **87(1)**, 499 (2014).

31. N. Pourreza, M. R. Fat`hi, and A. Hatami, *Microchem. J.,* **104***,* 22 (2012).

32. H. S. Lo, K. W. Lo, C. F. Yeung, and C. Y. Wong, *Anal. Chim. Acta,* **990***,* 135 (2917).

33. J. M. Doyle, M. L. Miller, B. R. McCord, D. A. McCollam, and G. W. Mushrush, *Anal. Chem.,* **72**, 2302 (2000).

34. X. Chen, F. Wang, and Z. Chen, *Anal. Chim. Acta,* **623**, 213 (2008).

35. J. Wang, P. Diao, and Q. Zhang, *Analyst*. **137(1)**, 145 (2012).

36. X. Cao, Y. Xu, and N. Wang, *Electrochim. Acta*. **59**, 81 (2012).

37. V. Mani, A. P. Periasamy, and S. Chen, *Electrochem. Commun.,* **17**, 75 (2012).

38. M. Parsaei, Z. Asadi, and S. Khodadoust, *Sensor Actuator B Chem.,* **220**, 1131 (2015).

39. U. P. Azad and V. Ganesan, *Chem. Commun*., **46**, 6156 (2010).

40. S. Zhang, B. Li, and J. Zheng, *Anal. Methods*, **7**, 8366 (2015).

41. N. Wang, X. Cao, X. Cai, Y. Xu, and L. Guo, *Analyst*, **135**, 2106 (2010).

42. B. He and D. Han, *Food Control*, **103**, 70 (2019).

43. H. Yu, R. Li, and K. Song, *Microchim. Acta*, **186**, 624 (2019).

44. M. Annalakshmi, P. Balasubramanian, S. M. Chen, and T. W. Chen, *Microchim. Acta*, **186**, 8 (2019).

45. W. J. R. Santos, P. R. Lima, A. A. Tanaka,,S. M. C. N. Tanaka, and L. T. Kubota, *Food Chem.*, **113**, 1206 (2009).

46. K. M. Hassan, G. M. Elhaddad, and M. AbdelAzzem, *Microchim. Acta*, **186**, 440 (2019).

47. E. Menart, V. Jovanovski, and S. B. Hocevar, *Electrochem. Commun.,* **52**, 45 (2015).

48. V. Popova, E. Korotkova, J. Barek, M. Stakheyeva, A. Fedorov, M. Patysheva, and O. Cheremisina, *Anal. and Bional. Chem.,* **412**, 5097 (2020).

49. Y. Dai, J. Huang, H. Zhang, and C. C. Liu, *Sensor Actuator B Chem.,* **281**, 746 (2019).

50. C. Lete, M. Chelu, M. Marin, S. Mihau, S. Preda, M. Anastasescu, J. M. Calderon-Moreno, S. Dinulescu, C. Moldovan, and M. Gartner, *Sensor Actuator B Chem.,* **316**, 72 (2020).

51. F. Xiaq, Z. Mo, F. Zhao, and B. Zeng, *Electrochem. Commun.,* **10**, 1740 (2008).

52. T. Navratil and M. Kopanica, *Crit. Rev. Anal. Chem.,* **32**, 153 (2002).

53. R. Demarco, G. Clarke, and B. Pejcic, *Electroanalysis*, **19**, 1987 (2007).

54. F. Manea, A. Remes, C. Radovan, R. Pode, S. Picken, and J. Schoonman, *Talanta*, **83**, 66 (2010).

55. M. Pal and V. Ganesan, *Analyst*, **135**, 2711 (2010).

56. K. S. V. Santhanam and A. J. Bard: *Electroanalytical Chemistry*, A. J. Bard, Ed. (Marcel Dekker, New York, 1970) Vol. 4, p. 215.

57. S. Uchiyama, *Rev. Polarography*, **58**, 6 (2012).

58. A. J. Bard. *Anal. Chem.*, **35(9)**, 1125 (1963).

59. L. Meites and S. A. Moros, *Anal. Chem.*, **31(1)**, 23 (1959).

60. S. Uchiyama, M. Ono, S. Suzuki, and O. Hamamoto, *Anal. Chem*., **60(17)**, 1835 (1988).

61. S. Uchiyama, S. Suzuki, and O. Hamamoto, *Electroanalysis*, **1**, 323 (1989).

62. S. Uchiyama, T. Obokata, S. Suzuki, and O. Hamamoto, *Anal. Chim. Acta*, **225**, 425 (1989).

63. O. Hamamoto, Y. Nakamura, S. Uchiyama, S. Suzuki, and T. Hobo, *Bunseki Kagaku*, **41**, T33 (1992).

64. S. Uchiyama and N. Sekioka, *Electroanalysis*, **17(22)**, 2052 (2005).

65. H. Matsuura, Y. Yamawaki, K. Sasaki, and S. Uchiyama, *J. Environ. Sci*., **25(6)**, 1077 (2013).

66. Y. Yamawaki, K. Asaka, H. Matsuura, and S. Uchiyama, *Bunseki Kagaku*, **63(5)**, 411 (2014).

67. S. Kuntolaksono and H. Matsuura, *Sensors and Materials*, **31(4)**, 1215 (2019).

Figures and Tables
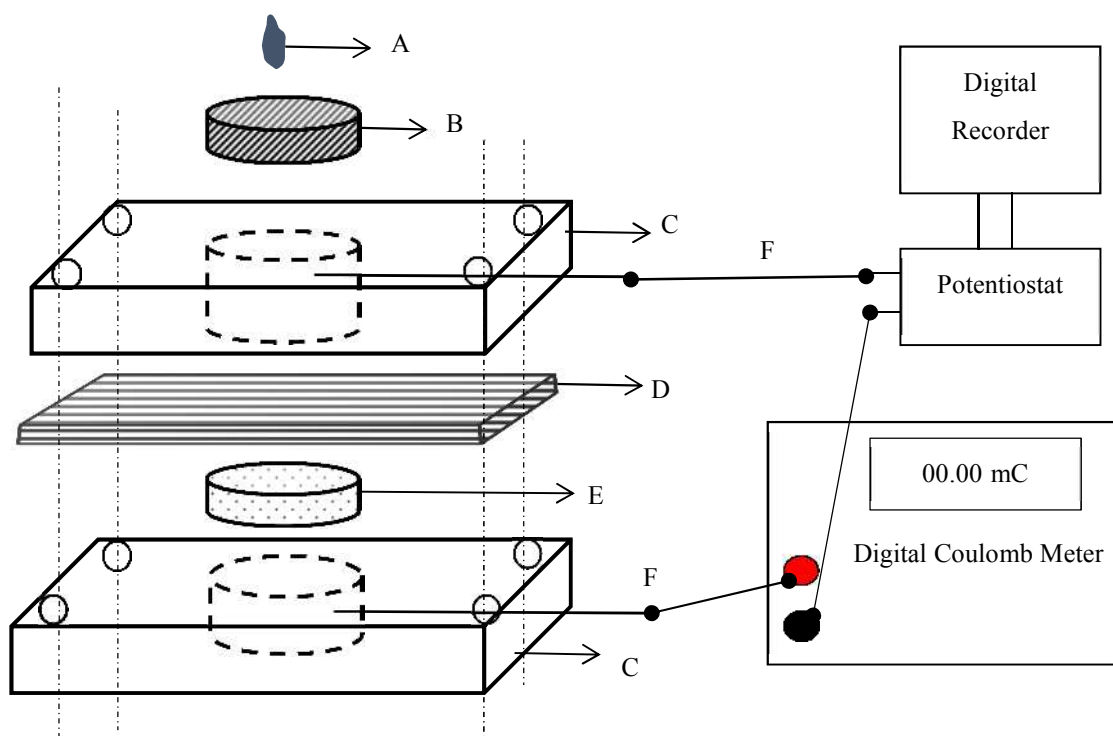
Figure 3.1. Schematic illustration of the potential-controlled coulometric sensor. A: sample addition; B: aminated carbon felt electrode; C: acrylic plate; D: ion exchange membrane; E: carbon felt electrode; F: Pt lead wire.
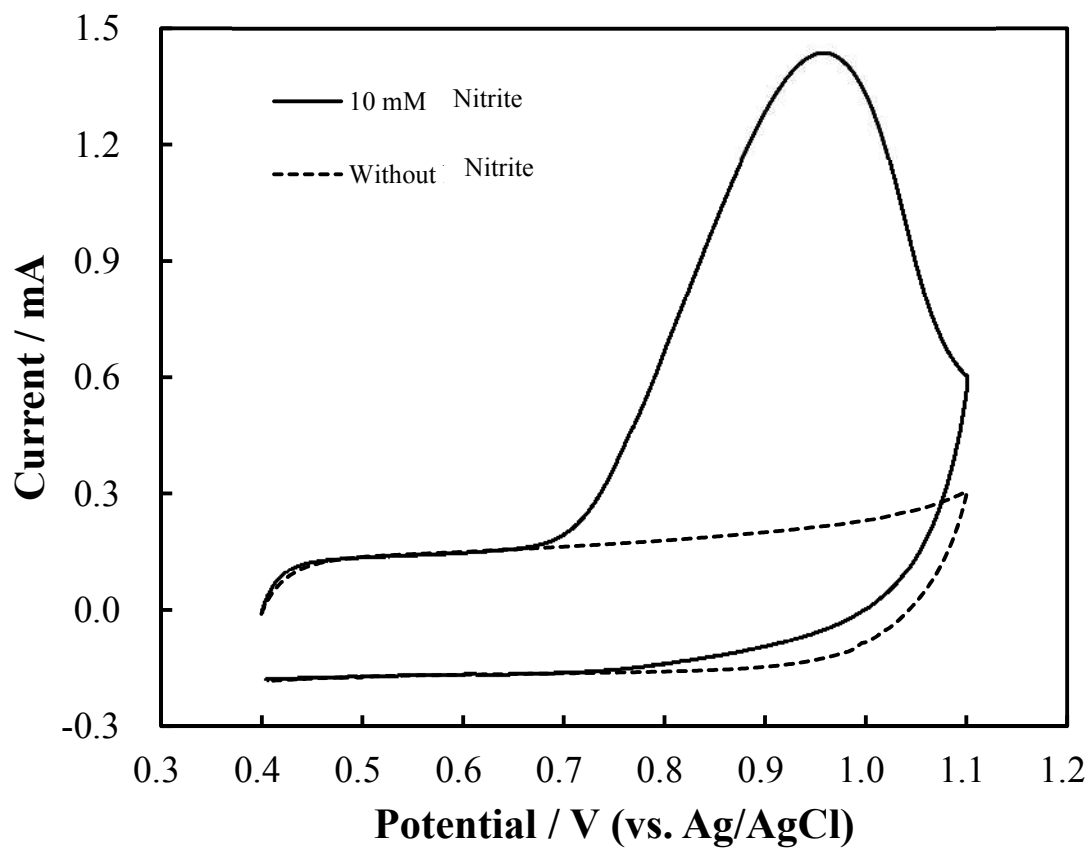
Figure 3.2. Cyclic voltammograms of aminated carbon felt electrode with (solid line) 10 mM of nitrite and without (dotted line) nitrite. Supporting electrolyte: 0.1 M acetic acid buffer solution (pH 4.0), scan rate: 20 mV/s.
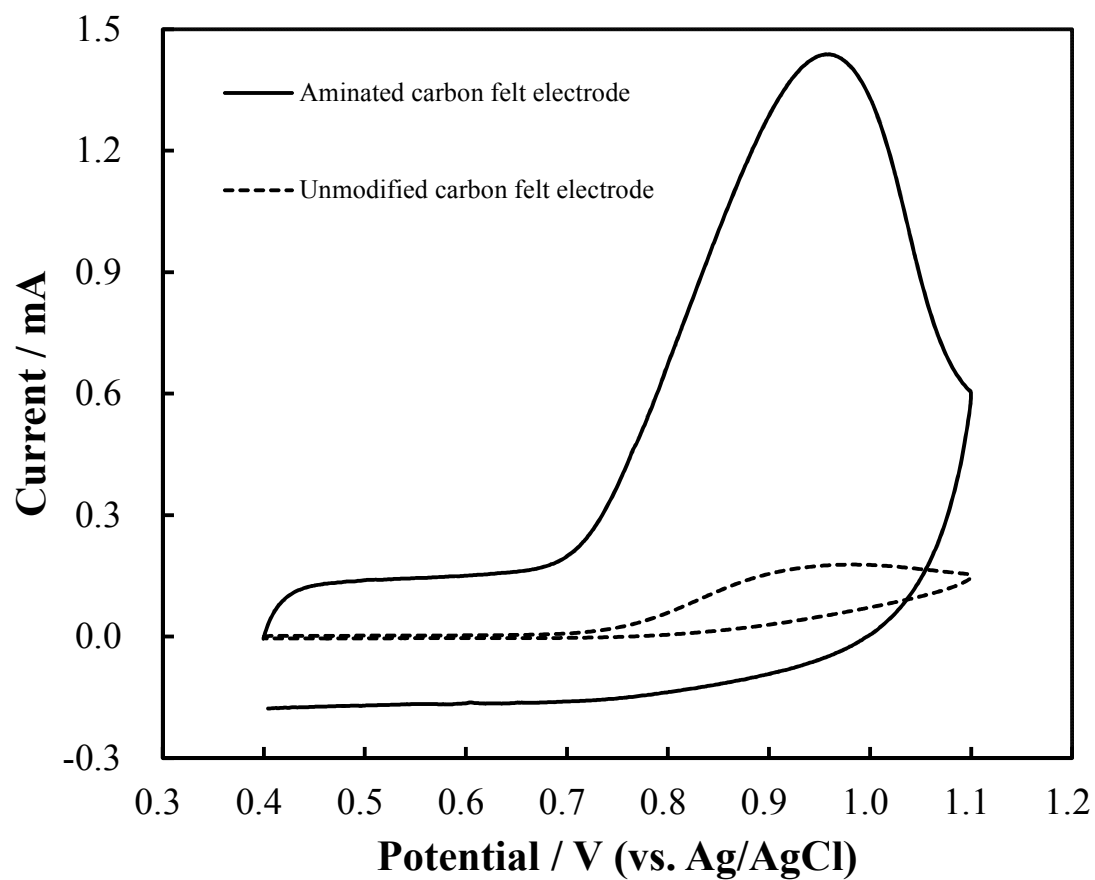
Figure 3.3. Cyclic voltammograms of aminated carbon felt electrode (solid line) and unmodified carbon felt electrode (dotted line) with 10 mM of nitrite. Supporting electrolyte: 0.1 M acetic acid buffer solution (pH 4.0), scan rate: 20 mV/s.
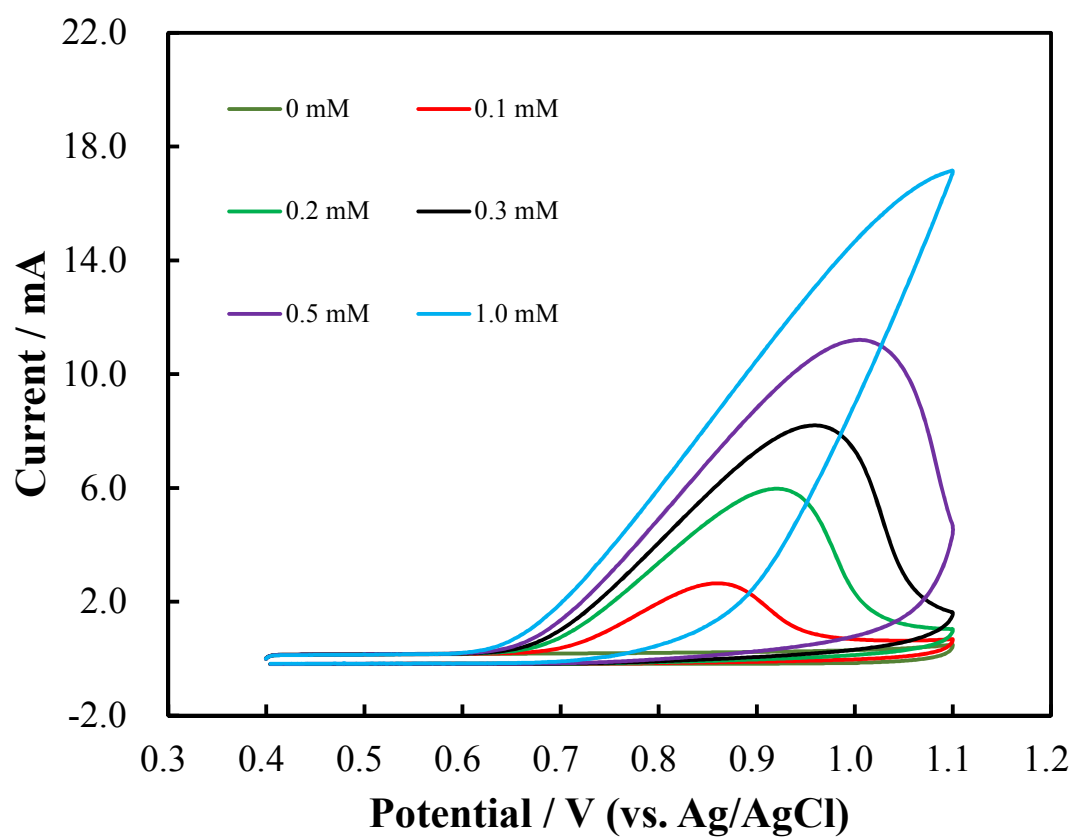
Figure 3.4. Cyclic voltammograms of aminated carbon felt electrode in various concentration of nitrite. Supporting electrolyte: 0.1 M acetic acid buffer solution (pH 4.0), scan rate: 20 mV/s.
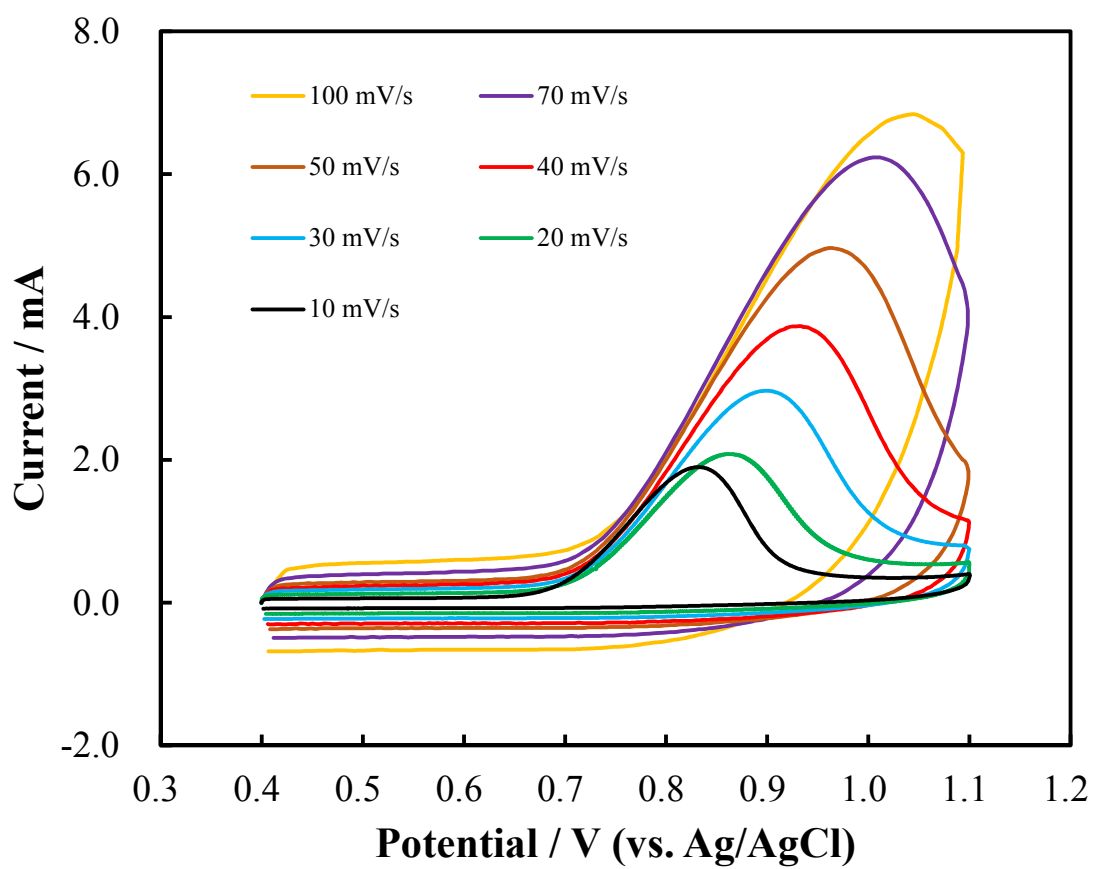
Figure 3.5. Cyclic voltammetry of aminated carbon felt electrode with 0.1 mM of nitrite at different scan rates. Supporting electrolyte: 0.1 M acetic acid buffer solution (pH 4.0), scan rate: 20 mV/s.
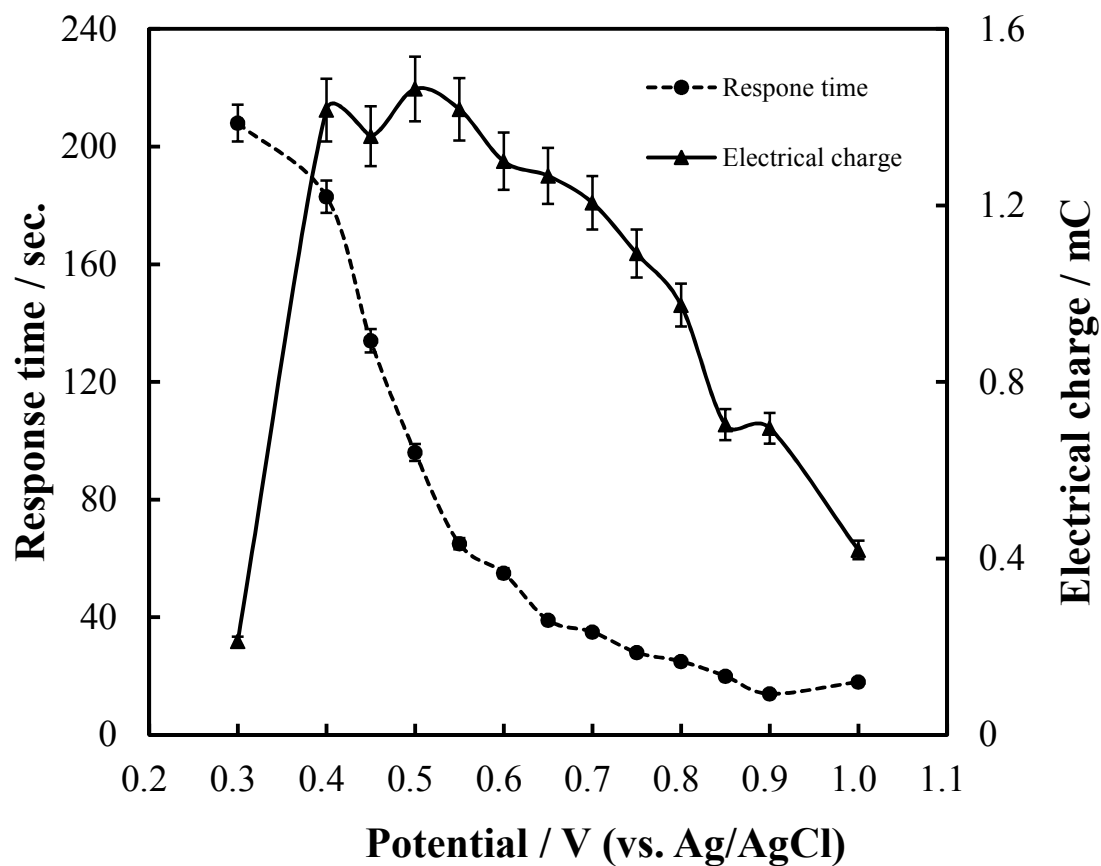
Figure 3.6. Relationship between response time and electrical charge versus applied potential with 1.0 mM of nitrite. Supporting electrolyte: 0.1 M acetic acid buffer solution (pH 4.0), sample volume: 10 μL.
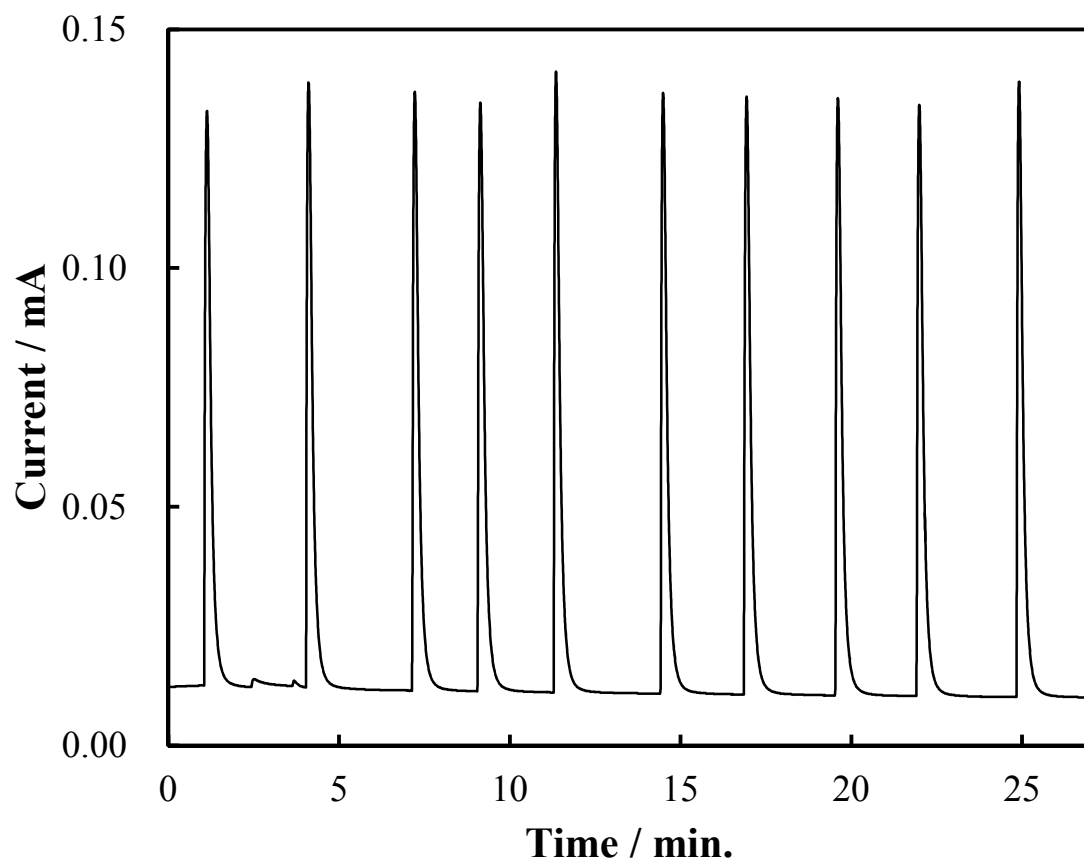
Figure 3.7. Relationship between current responses versus time curve obtained for repetitive measurement of 1.0 mM of nitrite. Supporting electrolyte: 0.1 M acetic acid buffer solution (pH 4.0), working potential: +0.75 V, sample volume: 10 μL.
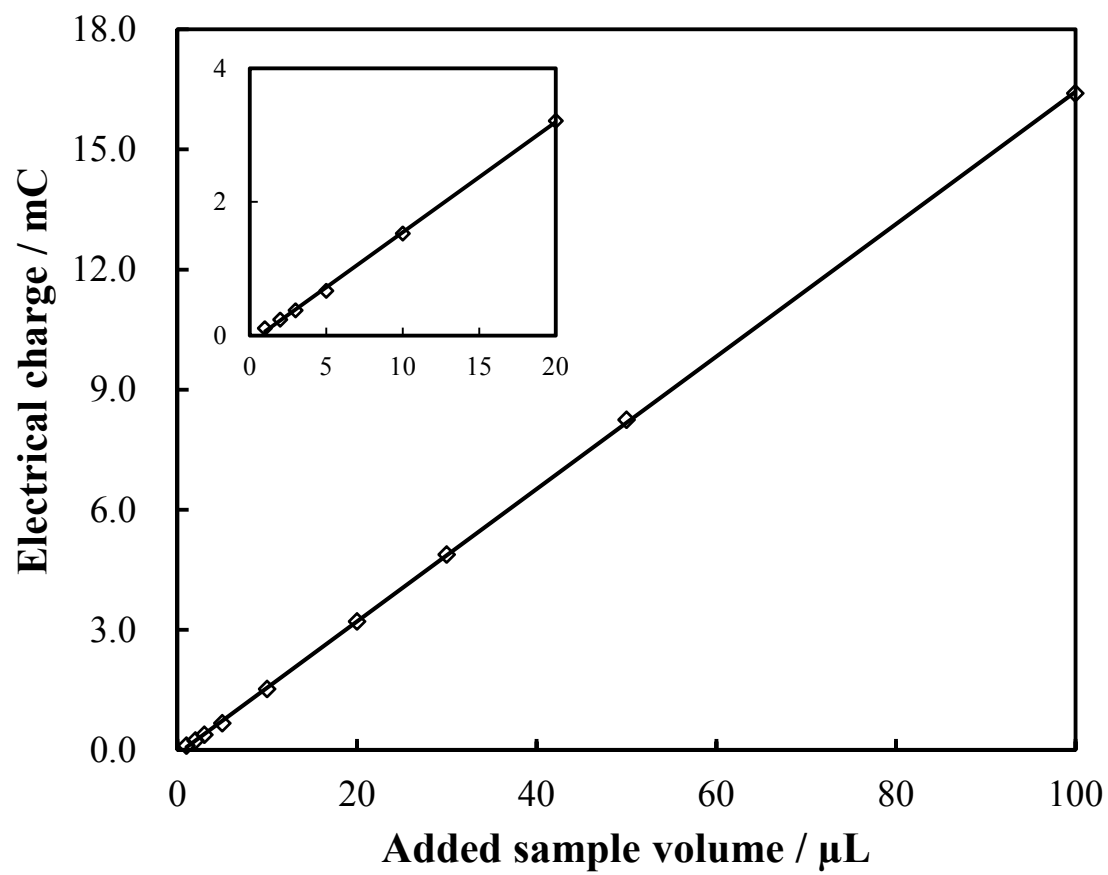
Figure 3.8. Relationship between electrical charge and amount of sample addition.
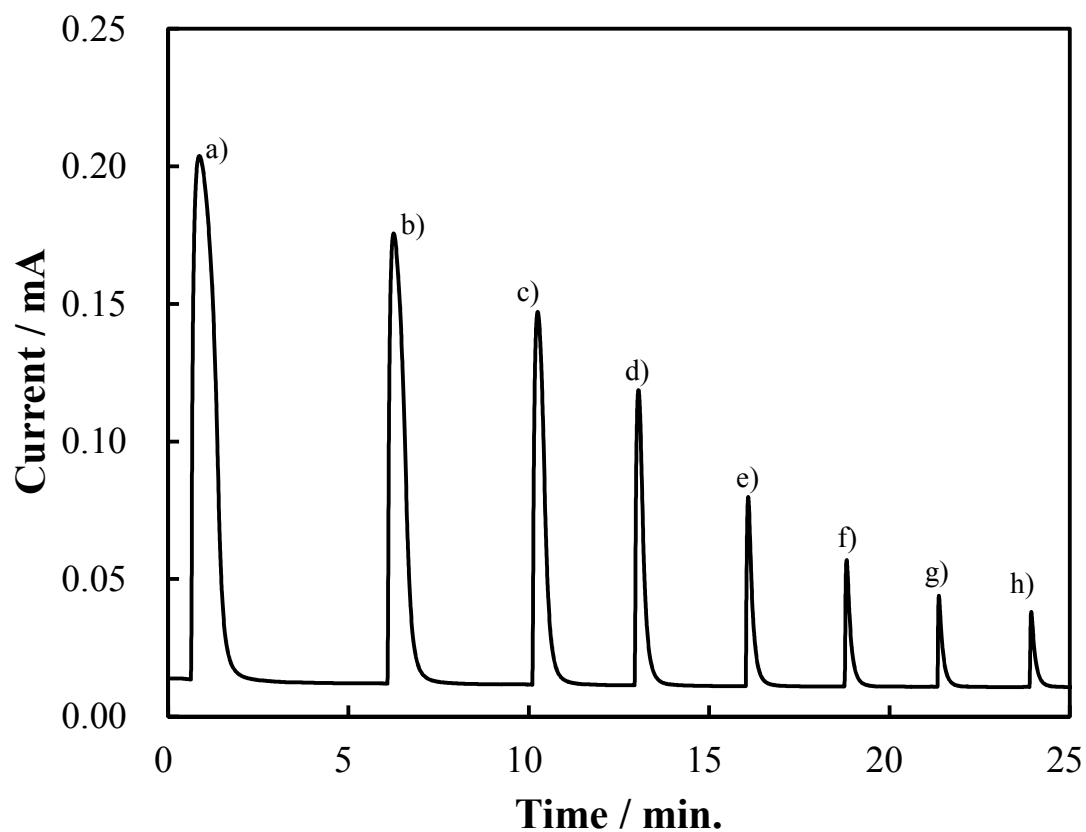
Figure 3.9. Current versus time curve obtained by measurement of nitrite, (a) 5.0 mM; (b) 3.0 mM; (c) 2.0 mM; (d) 1.0 mM; (e) 0.5 mM; (f) 0.3 mM; (g) 0.2 mM; (h) 0.1 mM. Supporting electrolyte: 0.1 M acetic acid buffer solution (pH 4.0), working potential: +0.75 V, sample volume: 10 μL.
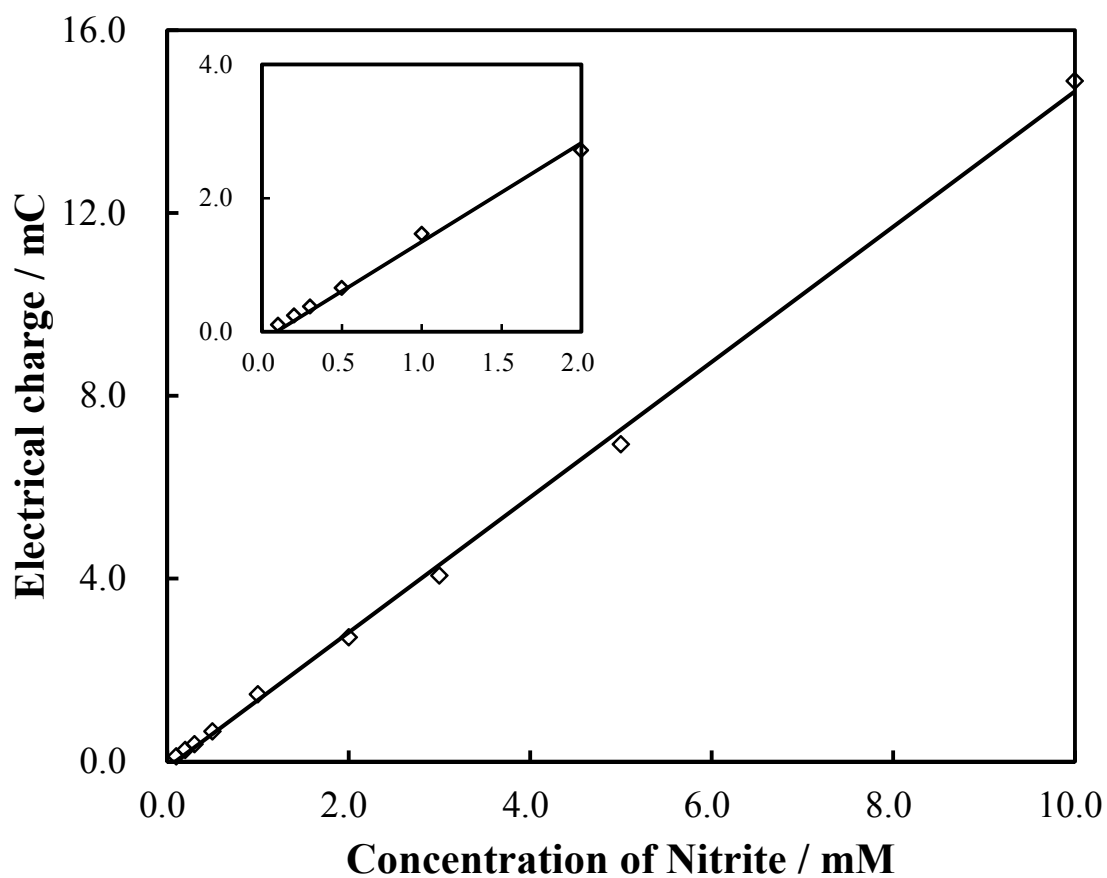
Figure 3.10. Relationship between electrical charge and various concentration of nitrite. Supporting electrolyte: 0.1 M acetic acid buffer solution (pH 4.0), working potential: +0.75 V, sample volume: 10 μL.

Chapter 4

Electrochemical Properties of Pt Particles Deposited on Aminated Glassy Carbon Electrode: Application to Sulfite Detection

4.1.   Abstract

In this chapter, electrochemical detection of sulfite was studied by developing a novel electrochemical sensor based on electro-deposited Pt particles on glassy carbon electrodes modified with nitrogen atoms containing functional groups (Pt-NGC) electrode. The potential range start from 0.0 V to +1.0 V with the electrolyte solution was 0.1 M phosphate buffer solution. The electrochemical properties of Pt-NGC electrode were evaluated by utilization of cyclic voltammograms. This electrode result showed an impressive electrocatalytic activity towards the oxidation of sulfite, which moves the oxidation peak potential to the negative direction of potential unlike Pt disk, a bare glassy carbon electrode, aminated glassy carbon electrode (AGC) electrode, and electro-deposited Pt particles on glassy carbon (Pt-GC) electrode. In addition, the lowest possible detection limit of 100 μM was achieved in the sulfite concentration range up to 10 mM. The Pt-NGC electrode was evaluated on the sample solution for sulfite determination wit impressing recovery of sulfite. Moreover, the proposed Pt-NGC electrode achieved reliable for the determination of sulfite in a sample solution with impressed recovery. Together with that, the possibility mechanism reaction of sulfite is being discussed.

4.2.　Introduction

In the recent years, carbon material based electrode containing glassy carbon (GC; type of 2 dimensional) and carbon felt (CF; type of 3 dimensional) have attracted great attention owing to their accessibility, low cost, electrochemical stability in various solutions (from low acid to base), wide potential window[1] and their large surface area[2] in the fields of electrochemical sensors. Furthermore, the chemical modification of carbon surface has significant to do in numerous fields like electroanalytical chemistry.[3] In actuality, functional groups, commonly include oxygen or nitrogen, and delocalized electrons of graphite structures can arrange the form in which range around acid or base, also characteristic form of carbon surface in which side hydrophilic or hydrophobic.

Start in few years ago, our group leader has developed many methods for electrochemical modification on the GC and CF surfaces. Nitrogen-containing functional groups can be easily to attaching and making bonds on the surface of GC electrodes by the treatment process of electro-oxidation among ammonium carbamate in aqueous medium solution at a constant high positive electrode potential,[4] which called "aminated glassy carbon (AGC)" electrode. Based on these treatment process, our own group found the interesting point that the primary amine group (like aromatic amine groups like aniline), the secondary amine groups (like groups containing pyrrole type nitrogen and quaternary amine-like moieties containing graphitic quaternary nitrogen) can be doped onto a bare GC electrode surface.[5] Furthermore, our group has reported that an electrocatalytic redox waves between a hydrogen ion (H^+) and a hydrogen molecule (H_2) were observed at a highly positive potential range after the long-term electrochemical reduction of AGC electrodes in sulfuric acid. During the electro-reduction of AGC electrode, platinum ions were dissolved from a platinum wire

counter electrode electrodeposited on the AGC electrode.[6] Additionally, our group leader had been reported that the observed hydrogen redox waves are related to mutual redox reactions between hydrazine, diazene, and also diazo groups affiliated to the carbon electrode surface.[7]

Sulfite (SO_3^{2-}) is a kind of food additive substances. It is broadly used in beverages and food[8,9] to inhibit or minimize spoilage due to oxidative processes, to maintain bacterial growth under production and storage of food,[10,11] and also controls enzymatic and non-enzymatic reactions while stabilizing functions and conditions.[12] Sulfite are also employed in production of food packaging materials and as a processing aid to sterilize bottles prior to packaging food and beverages.[13] Sulfite has been reported to cause toxic[14] and damaging to the human body. Due to the negative images, sulfite must be controlled in limited amounts. If not controlled in limited amounts, sulfite may chance to form asthma attacks, swelling, diarrhea, nausea, headaches, stomach irritation, and nettle rash.[15-17]

According to the literature, some scientists have been reported for detection of sulfite. Numerous analytical techniques have been developed for investigation of sulfite, including iodimetric titration,[18] high-performance liquid chromatography,[19] spectrophotometry,[20,21] chemiluminescence,[22] and capillary electrophoresis[23]. There is a drawback to using those methods because of expensive, time-consuming process, and mandatory to take pretreatment of sample. Among these analytical techniques, electrochemical methods are a great option to determination of sulfite because of their simplicity, easy operation, quick detection, and also cheaper. For these reasons, electrochemical methods are chosen and used in practical fields.

In this chapter, Pt-NGC electrode was carried out from the stepwise electrolysis

proses, with the purpose of the possibility detection of sulfite by electrochemical sensing technique. The author studied the phenomena of the electrocatalytic sulfite oxidation process and the opportunity to use Pt-NGC electrode for sulfite determination using voltammetry technique.

4.3.   Experimental Section

In experimental section, the author used so many reagents and was acquired from different companies. It will discuss in this section. Phosphate buffer solution (0.1 M, pH 7.0) was used as supporting electrolyte, and prepared by mixing dipotassium hydrogenphosphate (Fujifilm Wako Pure Chemical Industries, Ltd., Osaka, Japan) and potassium dihydrogen phosphate (Fujifilm Wako Pure Chemical Industries, Ltd., Osaka, Japan). Two other solutions were acquired from Fujifilm Wako Pure Chemical Industries, Ltd., Osaka, Japan) for sodium sulfite ($NaSO_3$) and sulfuric acid (H_2SO_4). Ammonium carbamate was acquired from Merck KGaA (Darmstadt, Germany). Spike recoveries from test solution were used several interferences such as vitamin C, sodium oxalate, potassium chloride, vitamin B6, and citric acid, were acquired from Fujifilm Wako Pure Chemical Industries, Ltd., Osaka, Japan). The GC electrode (diameter of 3 mm) as a working electrode bought from BAS Co., Ltd. (Tokyo, Japan). The polishing diamond and polishing alumina were acquired from BAS Co., Ltd. (Tokyo, Japan). All reagents used in this work were of analytical grade and were used without any further purification. The solutions were prepared with deionized water (Millipore Milli-Q System, Japan).

The author was taking a potentiostat/galvanostat (HA-151B, Hokuto Denko Co., Ltd., Japan) for carried of modified GC electrode by electrolysis process. There are three types of electrode functions: a working electrode was a bare GC electrode, counter electrode was platinum wire, and reference electrode was Ag/AgCl (3 M electrolyte). Before to use, the surface electrode must be polishing above alumina polishing pad. The step process of surface GC modification is described as follows; first, a bare GC electrode was glossing within 1.0 µm polishing diamond, next, 0.05 µm polishing

alumina above alumina polishing pad. After finishing polished the GC electrode, processed at ultrasonic bath treatment (approximately 30-60 seconds), and flushed by deionized water. A polished GC electrode fabricated through the electrode oxidation process in 0.1 M ammonium carbamate with constant potential (+1.1 V) and a 1-hour process. In this context, the name of the electrode is an AGC electrode. After that, the AGC electrode was electro-reduced in 1.0 M sulfuric acid at -1.1 V (vs. Ag/AgCl) for 20 h. During the electrode reduction process of the electro-oxidized GC electrode in strong sulfuric acid electrolyte, platinum ion dissolved from platinum counter electrode is electrodeposited on the surface of nitrogen atoms containing functional groups introduced GC electrode. This modified electrode was namely Pt-NGC electrode. All experiments were performed at room temperature.

Electrochemical properties of the Pt-NGC were evaluated and checked at the voltammetric sensing technique. For determination of sulfite, the author used the Pt-NGC electrode, performed on the automatic polarization system (HZ-3000, Hokuto Denko., Ltd., Japan) with a Pt-NGC as a modified GC electrode, a platinum counter electrode, and an Ag/AgCl (3 M NaCl electrolyte) reference electrode.

4.4.   Results and Discussions

4.4.1.   Electrochemical Behavior of Pt-NGC Electrode

The electrochemical behavior of sulfite at the Pt-NGC electrode has been studied in this chapter. In the present work, 0.1 M phosphate buffer solution with pH 7.0 was selected as the supporting electrolyte for cyclic voltammetry measurement. The applied potential range was chosen from 0.0 V to 1.0 V. Fig. 4.1 shows CV graphs of the Pt-NGC electrode absence sulfite (red line) and presence 5.0 mM sulfite (black line) in 0.1 M phosphate buffer solution (pH 7.0). As shown in Fig. 4.1 (red line), small and broad oxidation waves with a dominant peak at approximately +0.80 V (vs. Ag/AgCl) were observed. The small oxidation waves when the absence of sulfite was correlated to the oxidation formation effect of Pt particles in the Pt-NGC electrode. On the opposite, the presence of 5.0 mM sulfite (Fig. 4.1 (black line)) has an existing oxidation peak current when the author observed in 0.1 M phosphate buffer solution as a supporting electrolyte. It can conclude that the electrochemical performance while achieved with the Pt-NGC electrode and assumed as electrochemical oxidation from sulfite when tested in solution. Moreover, the active sites of Pt-NGC electrode have been introduced onto the bare GC electrode surface thoroughly two stepwise electrolysis processes function as active sites of the electron transfer for the electrocatalytic oxidation of sulfite.

The author performed CV experiment to study the catalytic capability of Pt-NGC electrode. The author selected a 0.1 M phosphate buffer solution as the supporting electrolyte and scan rate was 50 mV/s. Fig. 4.2 exhibit cyclic voltammetry with different electrodes in which containing 3.0 mM of sulfite. The several different materials are a bare GC electrode (blue line), Pt-GC electrode means that

Pt-electrodeposited glassy carbon electrode (red line), AGC electrode (green line), Pt disk electrode (purple line), and Pt-NGC electrode (black line). Peak potential of sulfite oxidation for each electrode material is explained as follows: Pt-NGC electrode, Pt disk electrode, AGC electrode, Pt-GC electrode, and a bare GC electrode were +0.55 V, +0.64 V, +0.68 V, +0.76 V, and +0.99 V, respectively. The nitrogen-containing functional groups, with the AGC electrode, introduced by electrode oxidation in ammonium carbamate aqueous solution function as electron-transfer mediators for sulfite oxidation, which indicates that the AGC electrode had electrocatalytic activity and the oxidation peak potential moved to the negative direction of potential comparing with the Pt-GC electrode and bare GC electrode. Moreover, the oxidation peak potential at Pt-NGC electrode shifted to the increasingly negative direction of potential comparing with two other electrode including Pt disk electrode and AGC electrode. Interestingly, the best oxidation peak current of sulfite was obtained at Pt-NGC electrode not at Pt disk electrode. Those results indicate that the Pt-NGC electrode has high electrocatalytic activity for the oxidation of sulfite. Consequently, the Pt-NGC electrode easily promotes the electrode oxidation of sulfite. On the other hand, the above probably exhibits that the electro-deposited Pt in collaboration with the nitrogen-containing functional groups (such as the primary amine group and other N-containing functional groups) introduced by stepwise electrolysis in ammonium carbamate solution and sulfuric acid act as active sites of the specific electrocatalytic current for sulfite. In previously report explained that electrocatalytic activity of the Pt-NGC electrode for the electrode oxidation of hydrogen molecule did not decrease after ultrasonication performed for 5 min, which indicates that platinum particles on nitrogen-containing functional groups are securely adsorbed onto the GC surface.[6]

Finally, it is indicating that the Pt-NGC electrode is amazing result if compared with the other electrodes in terms of sulfite oxidation.

4.4.2. Effect of Concentration of Sulfite and Scan Rate

Fig. 4.3 and Fig. 4.4 shows the CV of sulfite at Pt-NGC electrode in the concentration range up to 10.0 mM in the pH of 7.0 phosphate buffer solution. To be clearly the cyclic voltammetry results, the author decided to separate into two figures; lower concentration and high concentration. Figure 4.3 explained about the lower concentration of sulfite from 0.0 mM to 0.5 mM. On the opposite part, the high concentration of sulfite was fitted in Fig. 4.4. Those figures showed the resulting phenomenon that the oxidation peak current (Ip) increases with the increasing of sulfite concentration. The limit of detection is the lowest concentration an analyte in sulfite can be detected under stated conditions of the test. The limit of detection was found to be 100.0 μM. The linearity trend between the concentrations of sulfite and currents will describe in Fig. 4.5. The linear regression coefficient was 0.9976. These results demonstrate stability of a Pt-NGC electrode for electrocatalytic applications where a continuous detection of analytes is performed.

Three figures consist of Fig. 4.6, Fig. 4.7, and Fig. 4.8 are explained about the parameter of scan rate which is related with the oxidation peak current and the oxidation peak potential while determination of sulfite. The applied potential was setting around 0.0 V to +1.0 V. To clarify the oxidation mechanism of sulfite, the effect of scan rate (v) ranging from 10 mV/s to 500 mV/s on the Pt-NGC electrode response was investigated and the results are summarized in Fig. 4.6. Increasing the scan rate increases the peak intensities and shifts the peak positively, which reveals the irreversibility of the electrode process. The linear relationship between peak current and the square root of

the scan rate indicates that sulfite oxidation follows a diffusion-controlled process, shown in Fig. 4.7. The calibration curve between peak potential (Ep) versus log(v) was suitable linearity (Fig. 4.8). Then, it can be understanding that the oxidation peak potential was fit with the log(v). According to Laviron`s equation theory[24] was utilized for the calculation of the electron transfer numbers (n). The n was calculated as 1.91, means that the electrochemical oxidation of sulfite will expected a two-electron transfer process. These results make the author infer and believed that the electrochemical oxidation reaction was two electron transfer process at Pt-NGC electrode as Eq. 1:

$$SO_3^{2-} \; + \; 2H_2O \quad \longrightarrow \quad SO_4^{2-} \; + 2H^+ \; + \; 2e^- \tag{1}$$
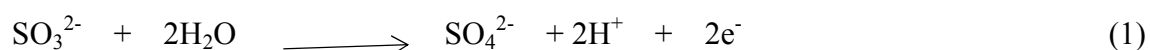
4.4.3. Study of Spike Recovery

To evaluation the electrode good stability, good reproducibility, and selectivity, the author must observe the spike recovery of the sulfite at Pt-NGC electrode. For evaluation of spike recovery, all measurement was obtained by voltammetric sensor. As shown in Table 4.1, the author attempted a spike recovery of 5.0 mM sulfite to determine the reaction selectivity at the Pt-NGC electrode. The potential interfering substances were selected to evaluate for the recovery of sulfite. Regarding what the concentration of sulfite should be, the author determined the concentration of each interfering substance to be 0.2 mM. The allowable tolerance limit for the maximum value of foreign substance concentration is ± 5% from the relative error in measurement. These results indicate that the Pt-NGC electrode is a promising candidate for sulfite detection with excellent reproducibility, good selectivity, and acceptable stability.

4.5. Conclusions

The combination between Pt particles deposited on the nitrogen-containing functional groups for new type modified electrode has been prepared by stepwise electrolysis. This modified electrode (Pt-NGC electrode) employed for detection of sulfite in aqueous solution. The characteristic of the Pt-NGC electrode showed a good electrocatalytic activity and has the lowest peak potential compared with other electrodes (Pt disk electrode, AGC electrode, Pt-GC electrode, and bare GC electrode). The sulfite oxidation peak current (Ip) was proportional to the square root of the scan rate. Additionally, the relationship between the oxidation peak potential and the log (v) showed a suitable linearity. The oxidation peak current (Ip) of sulfite showed a favorable linearity with the concentration of sulfite. These results show that the Pt-NGC electrode has been proved to be highly suitable for detecting sulfite.

References

1. E. Frackowiak and F. Beguin, *Carbon*, **39**, 937 (2001).

2. Kishimoto and N. Matsuda, *Environ. Sci. Technol.*, **43**, 2054 (2009).

3. R. W. Murray, "*Electroanalytical Chemistry and Interfacial Electrochemistry*", ed. A. J. Bard, **1984**, Vol. 13, Marcel Dekker, New York, 191

4. S. Uchiyama, H. Watanabe, H. Yamazaki, A. Kanazawa, H. Hamana, and Y. Okabe, *J. Electrochem. Soc.*, **154**, F31 (2007).

5. A. Kanazawa, T. Daisaku, T. Okajima, S. Uchiyama, A. Kawauchi, and T. Osaka, *Langmuir*, **30**, 5297 (2014).

6. H. Matsuura, T. Takahashi, S. Sakamoto, and S. Uchiyama, *Anal. Sci.*, **33**, 703 (2017).

7. H. Matsuura, S. Akabe, T. Kitamura, T. Takahashi, and S. Uchiyama, *Anal. Sci.*, **31**, 733 (2015).

8. S. Uchiyama, H. Matsuura, and Y. Yamawaki, *Electrochim. Acta*, **88**, 251 (2013).

9. A. F. Gunnison, *Food Cosmet. Toxicol.*, **19**, 667 (1999).

10. S. Satienperakul, P. Phongdong, and S. Liawruangrarth, *Food Chem.*, **121**, 893 (2010).

11. L. Pizzoferrato, G. Di Lullo, and E. Quattrucci, *Food Chem.*, **63(2)**, 275 (1998).

12. T. Fazio and C. R. Warner, *Food Addit. Contam.,* **7**, 433 (1990).

13. R. Walker, *Food Addit. Contam.,* **2**, 5 (1985).

14. K. W. Lien, D. P. H. Hsieh, H. Y. Huang, C. H. Wu, S. P. Ni, M. P. Ling, *Tox. Rep.,* **3**, 544 (2016).

15. L. S. T. Alamo, T. Tangkuaram, and S. Satienperakul, *Talanta,* **81**, 1793 (2010).

16. H. J. Suh, Y. H. Cho, M. S. Chung, and B. H. Kim, *J. Food Compos Anal.,* **20**, 212 (2010).

17. S. S. M. Hassan, M. S. A. Hamza, and A. H. K. Mohamed, *Anal. Chim. Acta*, **570**, 232 (2006).

18. D. H. Allen, *Food Technol.*, **73**, 506 (1985).

19. G. Monnier and S. Williams, *Analyst*, **95**, 119 (1972).

20. S. Theisen, R. Hansch, L. Kothe, U. Leist, R. Galensa, *Biosens. Bioelectron.*, **26**, 175 (2010).

21. L. J. Wang, Y. H. Tang, Y. H. Liu, *J. Pharm. Anal.*, **1**, 51 (2010)**.**

22. P. D. Tzanavaras, E. Thiakouli, and D. G. Themelis, *Talanta,* **77**, 1614 (2009).

23. R. Rawal and C. S. Pundir, *Int. J. Biol. Macromol.*, **51**, 449 (2012).

24. G. Jankovskiene, Z. Daunoravicius, and A. Padaraukas, *J. Chromatogr. A*, **934**, 67 (2001).

Figures and Tables
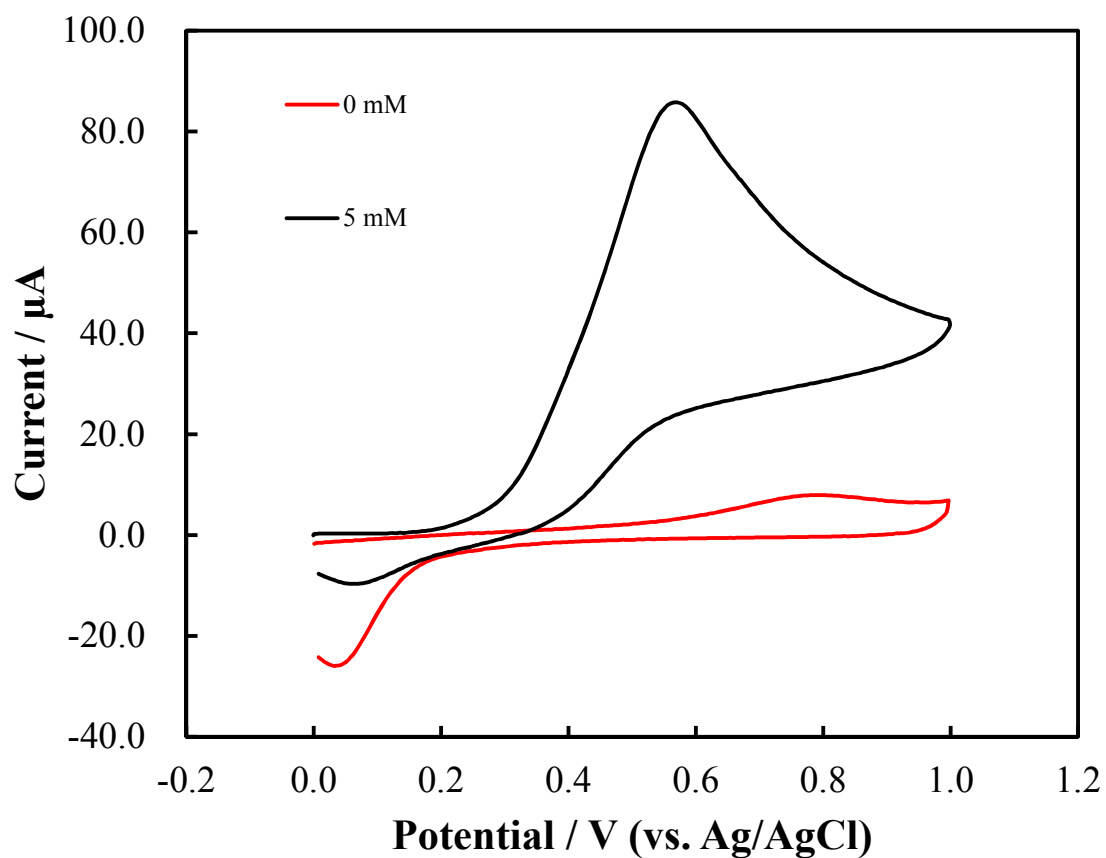
Figure 4.1. Cyclic voltammograms of Pt-NGC electrode; (red color) absence and (black color) presence of 5.0 mM of sulfite. Supporting electrolyte: 0.1 M phosphate buffer solution (pH 7.0), scan rate: 50 mV/s.
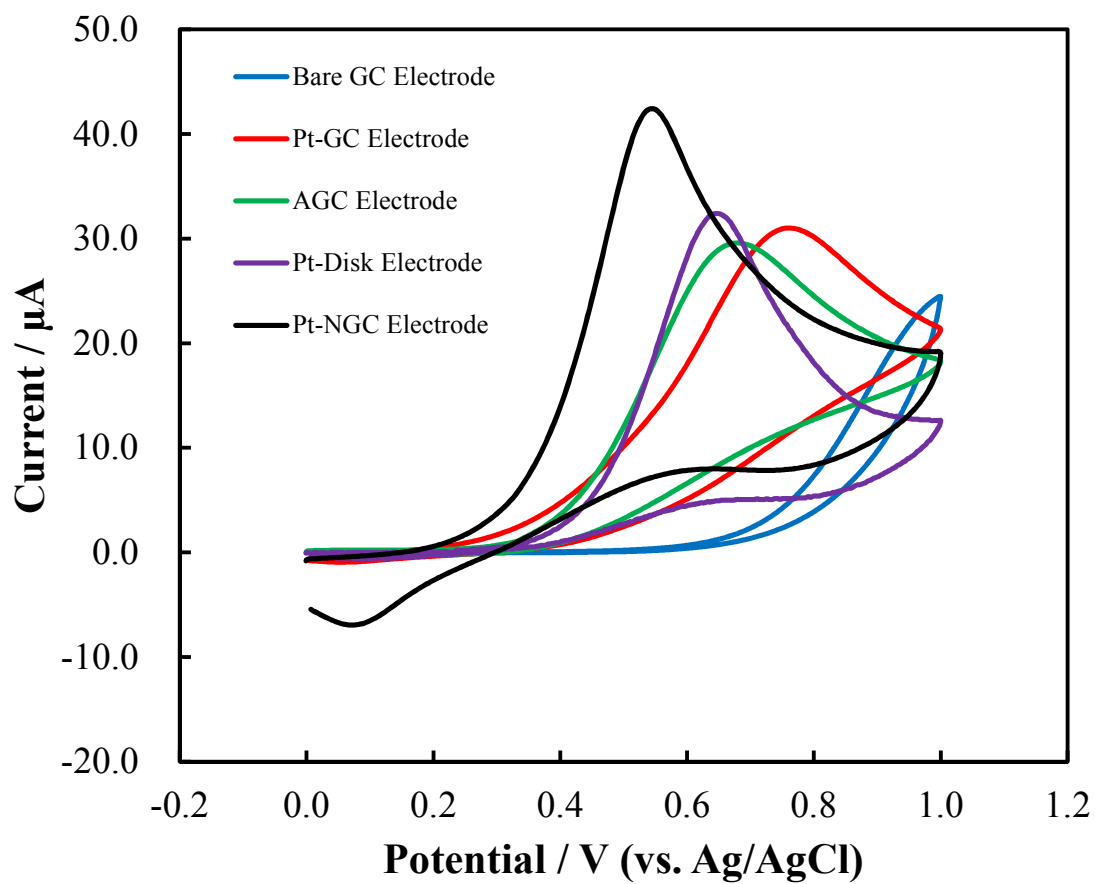
Figure 4.2. Cyclic voltammograms of different electrode materials in the presence of 3.0 mM of sulfite. Supporting electrolyte: 0.1 M phosphate buffer solution (pH 7.0), scan rate: 50 mV/s.
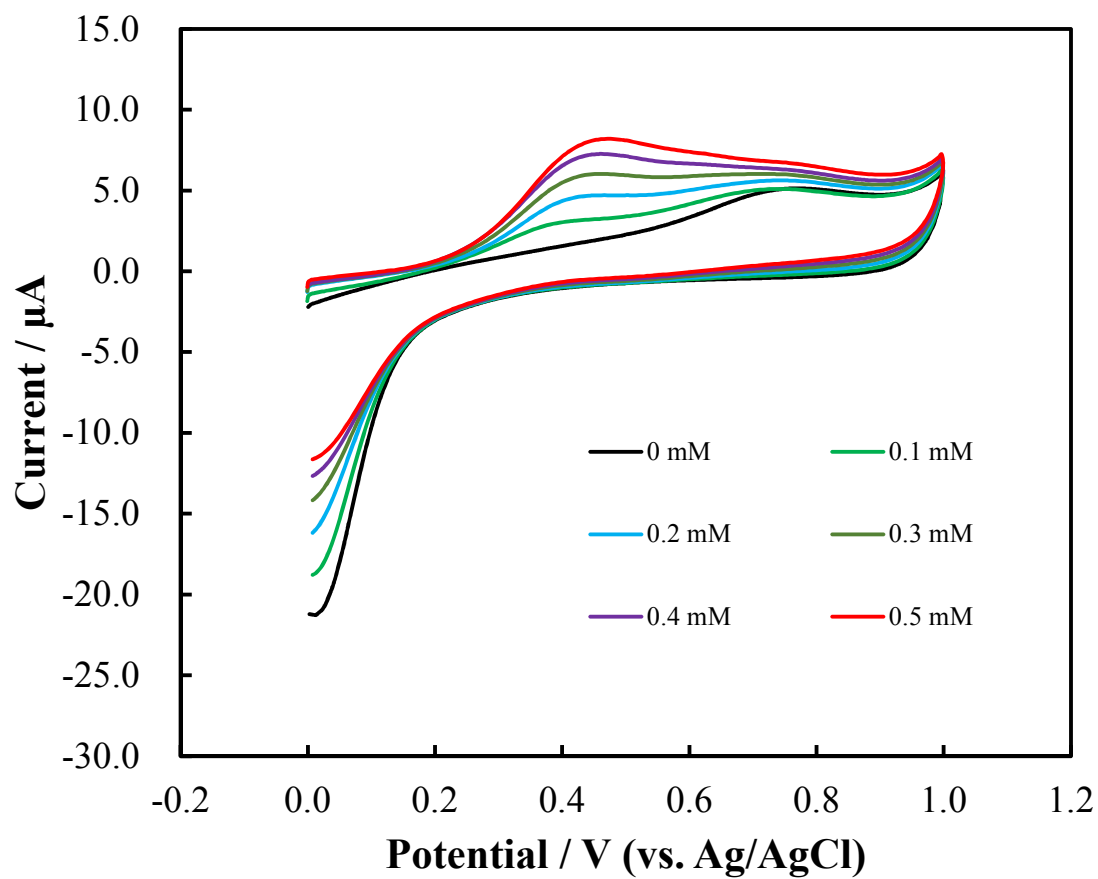
Figure 4.3. Cyclic voltammograms with various concentration of sulfite at Pt-NGC electrode. Supporting electrolyte: 0.1 M phosphate buffer solution (pH 7.0), scan rate: 50 mV/s.
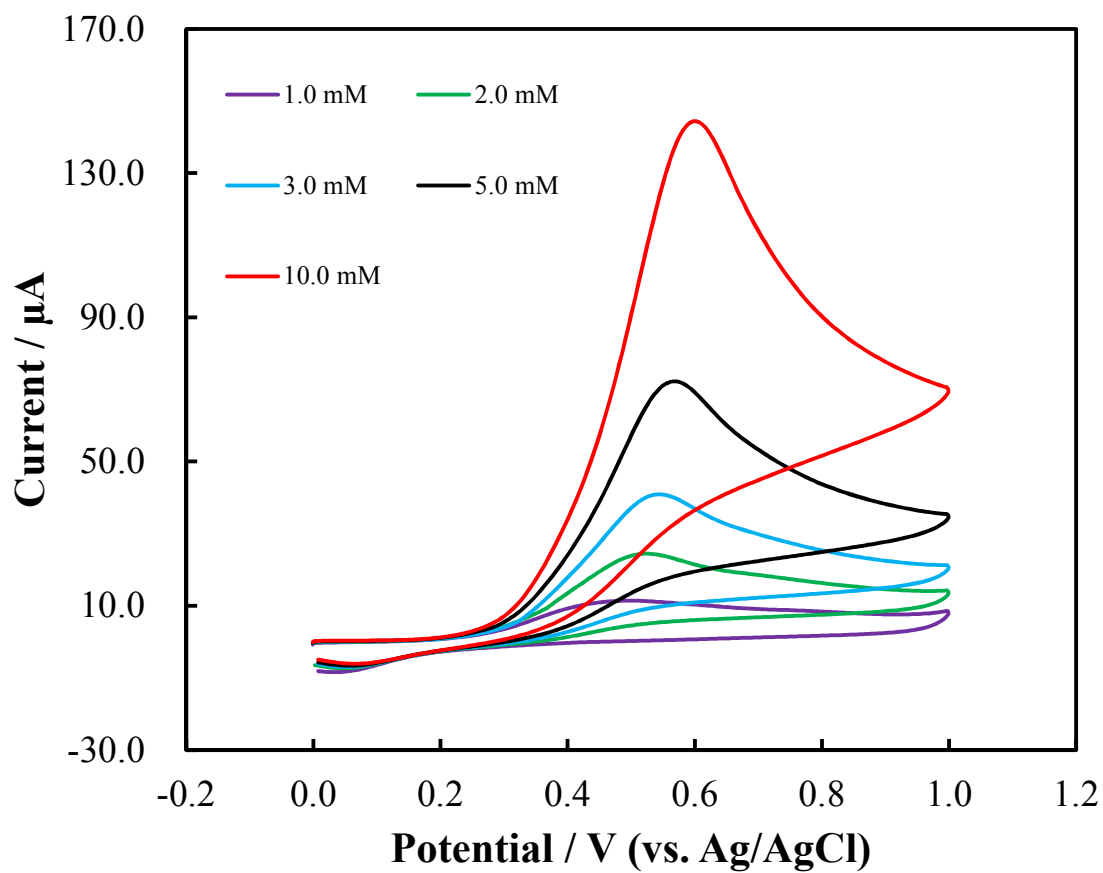
Figure 4.4. Cyclic voltammograms with various concentration of sulfite at Pt-NGC electrode. Supporting electrolyte: 0.1 M phosphate buffer solution (pH 7.0), scan rate: 50 mV/s.
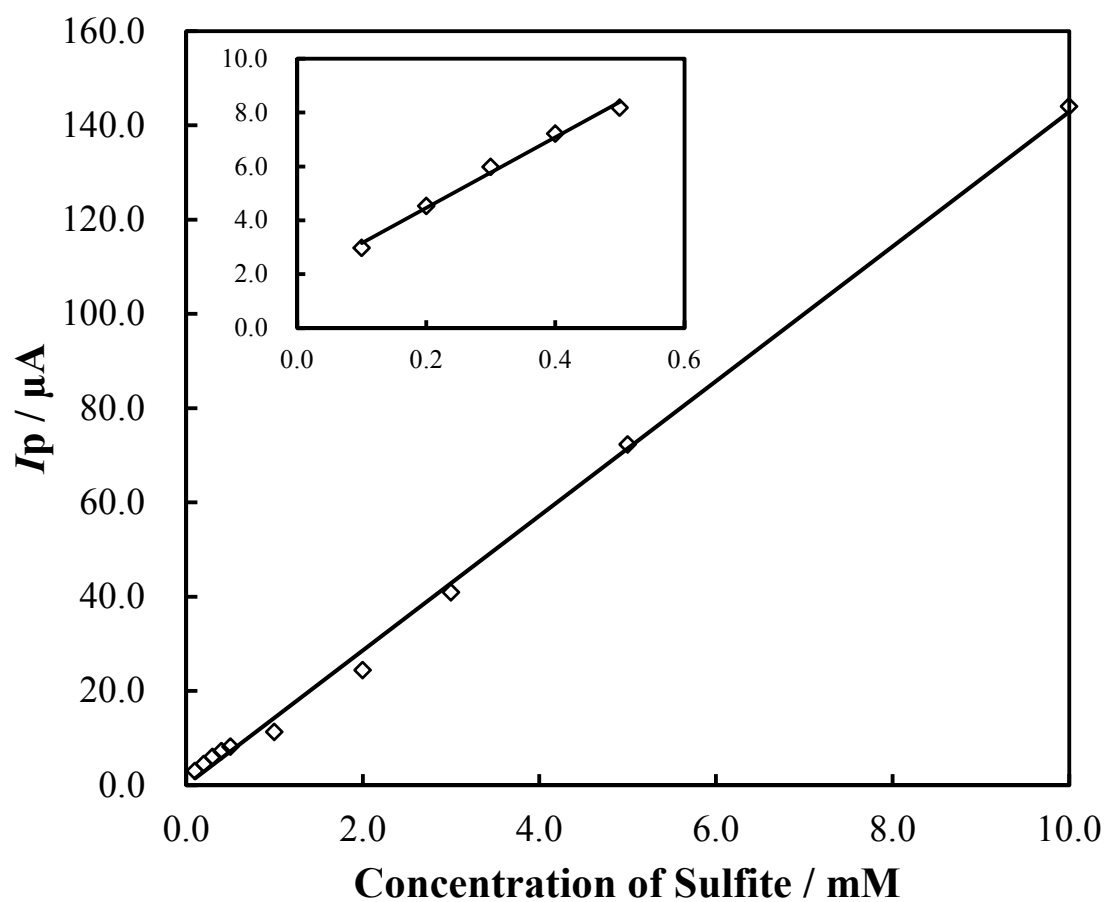
Figure 4.5. The relationship between the concentration of sulfite and the oxidation peak current at Pt-NGC electrode. Supporting electrolyte: 0.1 M phosphate buffer solution (pH 7.0), scan rate: 50 mV/s.
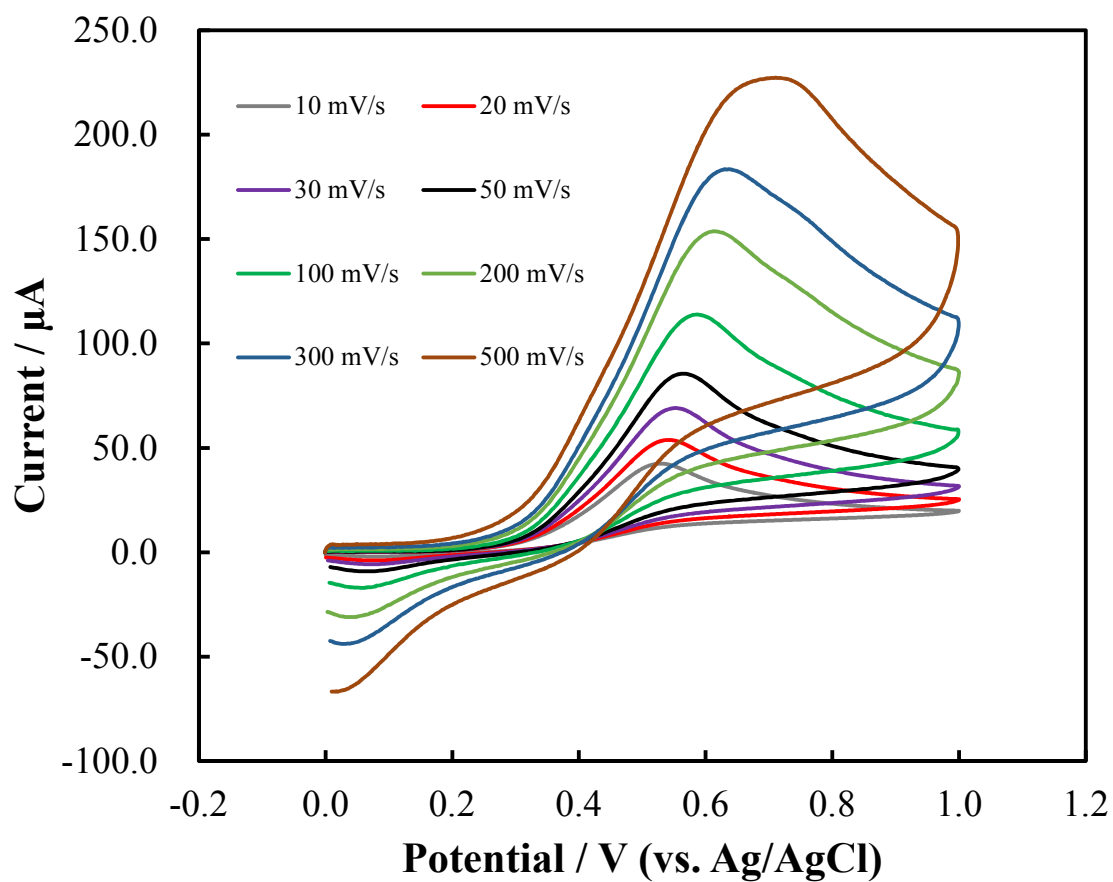
Figure 4.6. Cyclic voltammograms containing of 5.0 mM of sulfite with varying scan rates at Pt-NGC electrode. Supporting electrolyte: 0.1 M phosphate buffer solution (pH 7.0).
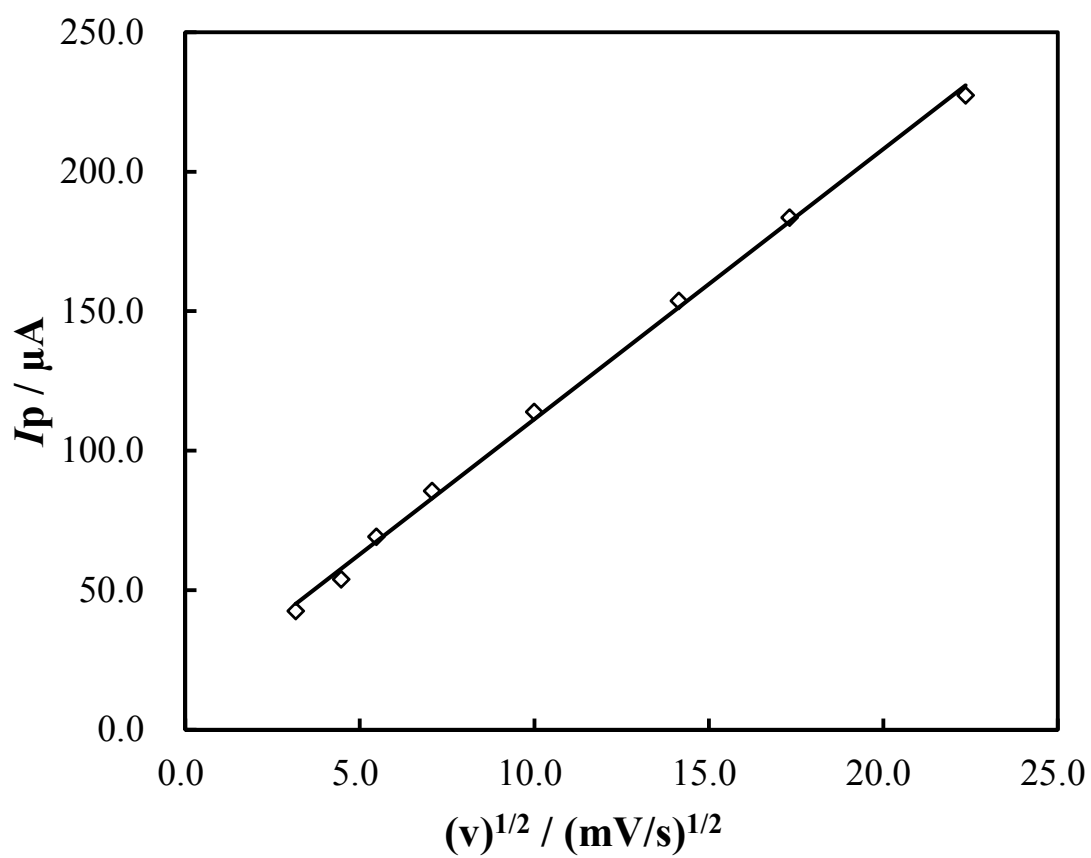
Figure 4.7. The influence of $(v)^{1/2}$ on the peak current (Ip) of 5.0 mM of sulfite at Pt-NGC electrode. Supporting electrolyte: 0.1 M phosphate buffer solution (pH 7.0).
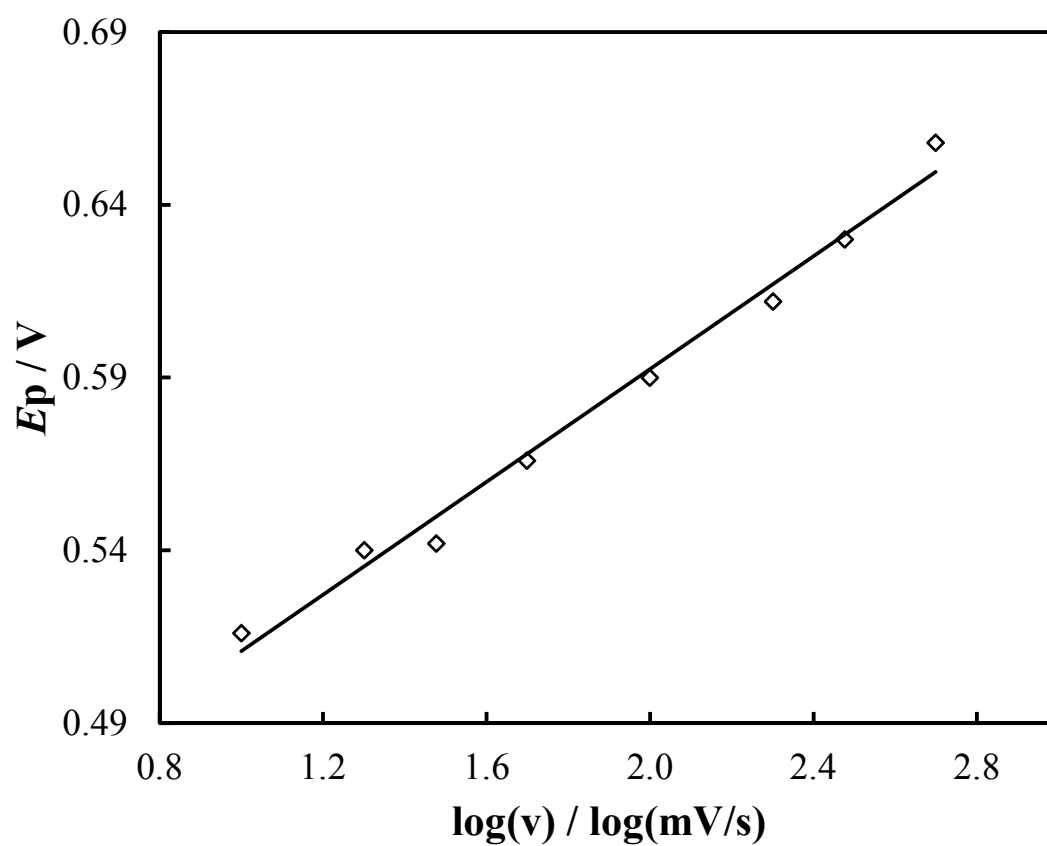
Figure 4.8. The influence of log(*v*) on the peak potential (*E*p) of 5.0 mM sulfite at Pt-NGC electrode. Supporting electrolyte: 0.1 M phosphate buffer solution (pH 7.0).

Table 4.1. Analytical results of sulfite oxidation peak current and spike recovery of 5.0 mM of sulfite from test solution with different kinds of interference at Pt-NGC electrode.

Interference	Concentration / mM	Observed peak current / x 10^2 µA	Certified peak current / x 10^2 µA	Spike recovery / %
Cl^-	0.2	1.059	1.067	99.3
CH_3COO^-	0.2	1.050	1.059	99.2
PO_4^{3-}	0.2	1.067	1.077	99.1
HCO_3^-	0.2	1.077	1.080	99.7
Vitamin B6	0.2	1.047	1.069	98.0
Vitamin C	0.2	1.067	1.093	97.6
Vitamin C	1.0	1.061	1.029	103.1
Oxalate	0.2	1.000	1.010	99.0
Citric acid	0.2	0.978	1.000	97.8
Ammonia	0.2	0.955	0.979	97.5

Chapter 5

Electrochemical Sensor of Sulfite Using Electrodeposition of Pt Particles Nitrogen-Containing Functional Groups Prepared by Stepwise Electrolysis

5.1.   Abstract

This chapter focused on the amperometric sensor performance and interference study (standard interference and real sample interference). A new type of modified electrode sensor for sulfite has been prepared by simple electrolysis based on platinum decorated and nitrogen-containing functional groups on the surface of glassy carbon electrodes. Pt-NGC electrode has been applied to an amperometric sulfite sensor. Before applied on the sensor, the optimal working potential from +0.4 V to +0.9 V was investigated firstly, being selected at +0.6 V. Under optimal condition, a favorable linear relationship between the current response (ΔI) and the sulfite concentration up to 500 μM was exhibited. A low detection limit (based S/N = 3) of 3 μM was also achieved. The sensor can achieve 95% steady state current within 30 s and present well stability, wide linear range of applications, and anti-interference performance during sulfite detection. In regards to the reproducibility, the RSD (n= 10) was 8.9% for 80 μM sulfite. At the end, the new type of electrode was successfully carried out for the determination of sulfite in red wine with good results.

5.2. Introduction

One of the examples from additive is sulfite. Sulfite is widely used in pharmaceutical products, beverages, and food so as to prevent oxidation, inhibit bacterial growth, and control enzymatic reaction during production and storage.[1,2] Apart from these useful advantages, sulfite must be applied in extremely limited quantities due to their potential toxicity and harmful effects on the human bodies. Without tightly control, sulfite can cause nausea, swelling, stomach irritation, headaches, diarrhea, nettle rash, and asthma attacks.[3-6] Therefore, the food industry necessary and require accurate methods for determining sulfite which is crucial for guaranteeing the quality product. Currently, several analytical methods including iodimetric titration,[7] high-performance liquid chromatography,[8] fluorescence,[9] chemiluminescence,[10] capillary electrophoresis,[11] and electrochemical detection[12,13] have been published for determination of sulfite. In contrast to these methods, electrochemical detection techniques realize offers good selectivity, high sensitivity, reliability, rapid detection, simplicity, and also inexpensive.

Up to now, scientists often use the glassy carbon (GC; a form of 2-dimensional shapes) and carbon felt (CF; a form of 3-dimensional shapes) electrodes. Both electrodes can be applied in the electrochemical sensing field as a result of a higher over potential for oxygen reduction,[14,15] chemical stabilities, accessibility, inexpensive, wide potential window,[16] and large surface area[17] in comparison to metal electrodes, such as platinum and gold. The development of new surface structure on the electrodes (GC and CF) by chemical modification process has attracted attention in several areas, especially in electroanalytical chemistry.[18-22] Electrochemical sulfite detection may be based on direct sulfite reduction on glassy carbon[23] or after electrode modification.[24] In different

ways, direct sulfite oxidation is obtained with platinum,[25] gold,[26] glassy carbon,[27] and platinum-modified glassy carbon.[28] In fact, there are still challenges including problems with fouling of the electrode and a high positive potential for oxidation of the sulfite.[25-27] As a consequence, a number of substances may interfere with the detection and measurement of the analyte.

My own group particularly focuses on the development of electrochemical modifications on the carbon surface (GC electrode and CF electrode) for solving those problems which was explained it on the above. The nitrogen-containing functional groups can form chains on the surface of the GC electrode by the electrode oxidation treatment process make use of ammonium carbamate in an aqueous medium solution at a high positive electrode potential;[29] namely as an aminated glassy carbon (AGC) electrode. In particular, it has been revealed by us that nitrogen atoms containing functional groups such as aromatic amine groups like aniline can easily be introduced to the surfaces of the GC and CF electrodes by the electrode oxidation of ammonium carbamate;[30] the electron transfer rates of many inorganic and organic compounds are accelerated to be able to measure excellent redox waves.[31,32] On the past study by my own group, redox waves between hydrogen ions and hydrogen molecules (H_2) at a highly positive potential range after a long-term electro-reduction of the AGC electrode in a sulfuric acid electrolyte solution. During electrode reduction of the AGC electrode in sulfuric acid, platinum ion dissolved from a platinum wire counter electrode was electrodeposited onto the surface of nitrogen-containing functional groups to which a GC electrode was introduced. This electrode was named Pt-NGC electrode. In this electrode, Pt particles are electrodeposited onto the GC electrode modified which was forming with nitrogen-containing functional groups.[33]

In this study, type of electrode (Pt-NGC electrode) which is environmentally friendly and simple process by stepwise electrolysis processes was used for an amperometric sulfite sensor. The author focused on the sulfite sensor performance in amperometric sensor. The Pt-NGC electrode was also used for detection of sulfite in amperometry under optimized conditions. Eventually, the Pt-NGC electrode was studied for the detection limit of sulfite, reproducibility, and the interference substance in an amperometric sulfite sensor. Lastly, the author also tried to observation of red wine by using Pt-NGC electrode.

5.3.   Experiment Section

Ammonium carbamate was from Merck KGaA (Darmstadt, Germany). Sodium sulfite (Na_2SO_3), sulfuric acid (H_2SO_4), dipotassium hydrogen phosphate (K_2HPO_4), and potassium dihydrogen phosphate (KH_2PO_4) were obtained from Fujifilm Wako Pure Chemical Industries, Ltd. (Osaka, Japan). The GC electrode with an inside diameter (ID) around 3 mm was bought from BAS Co., Ltd. (Tokyo, Japan). All of other reagents were of analytical grade and used All other chemicals were of analytical reagent grades and used as received. Deionized water produced by a Milli-Q system (Millipore, Japan) was used for preparation of all the solutions.

Before to use, the GC electrode must be polished on an alumina polishing pad with 1.0 μm polishing diamond and 0.05 μm polishing alumina, carried out with ultrasonic bath (± one minute), then rinsed with deionized water. To perform a potential controlled electrolysis, the author used a potentiostat/galvanostat (HA-151B, Hokuto Denko Co., Ltd., Japan). The platinum spiral function as the counter electrode with the specific size as follows: diameter is 0.5 mm and length of size is 70 mm. An Ag/AgCl (3 M NaCl electrolyte) was used as a reference electrode. For fabrication of the Pt-NGC electrode will explain follows: First, the GC electrode was processed in an electrode oxidation process with a 0.1 M ammonium carbamate aqueous solution at a constant potential of +1.1 V for 60 minutes. After that, the electro-oxidized GC electrode was electro-reduced in 1.0 M sulfuric acid at -1.1 V (vs. Ag/AgCl) for 20 hours. During electrode reduction process by using a electrode oxidation GC electrode in sulfuric acid, the platinum ion dissolved from platinum wire counter electrode was deposited onto the surface of nitrogen-containing functional groups to which a bare GC electrode was introduced. All detection was performed under room temperature.

During the amperometric sensor measurements, an automatic polarization system (HZ-3000, Hokuto Denko., Ltd., Japan) with a three-electrode cell consisting of a working electrode as Pt-NGC electrode, a counter electrode as platinum wire, and an Ag/AgCl (3 M NaCl electrolyte) as the reference electrode is used to determination sulfite on the voltammetric and amperometric sensor. N_2 gas was flowed into the electrolyte during amperometric measurement. The function of N_2 gas is intended to block oxygen molecules so that the sulfite is not oxidizing to become sulfate. Furthermore, the author used the dialysis membrane to covering around the surface of the Pt-NGC electrode, which aims for reducing the diffusion of sulfite from bulk to the Pt-NGC electrode surface. By using the dialysis membrane, it has significant different results. It means that the background noise current is additionally reduced during amperometric measurements of sulfite due to reducing of the electrolyte diffusion. At the end, 0.1 M phosphate buffer solution with pH 7.0 is a type of the supporting electrolyte which the author uses in voltammetric and amperometric measurements.

5.4   Results and Discussions

5.4.1.   Sulfite Sensor Performance

The amperometric sensor has a much current sensitivity than the cyclic voltammetry sensor. Commonly, an amperometric sensor is used to estimate the lower detection limit of an analyte, in this context of sulfite. The working potential greatly affects the amperometric current response of a sensor. In the first step, the author must be investigated and checked the effect of working electrode potential around +0.3 to +1.0 V. Amperometric responses of Pt-NGC electrode under numerous working potential have been applicable in 0.1 M phosphate buffer solutions containing 500 μM sulfite (Fig. 5.1). The results show that +0.6 V was the best current response and it is based on the stability of the signal to ratio. This result is correlated with the results of cyclic voltammetry, which shows the peak potential of sulfite was located at +0.6 V. Due to that explanation, +0.6 V are selected as the optimal working potential.

Fig. 5.2 shows the comparison of the amperometric response of bare GC electrode (black color), Pt-GC electrode (purple color), AGC electrode (green color), and Pt-NGC electrode (red color) with the same continuous addition of 100 μM sulfite at optimal working potential. The current response at the Pt-NGC electrode is fourfold greater as that observed from the bare GC, Pt-GC electrode, and AGC electrodes. The response time required to reach 95% of the maximum steady-state current around 20 seconds. It is indicating rapid current response for sulfite sensing at Pt-NGC electrode. The favorable catalytic sensitivity and rapid response of the Pt-NGC electrode further demonstrates that the Pt-NGC electrode facilitates more effective electron transfer.

Figure 5.3 explained the connection between the current response (ΔI) and the sulfite concentration. The oxidation current increased sharply up to 5000 μM in sulfite

concentration, and achieved 95% of the maximum steady-state current within ca. 30 seconds. A favorable linear relationship (R^2=0.9979) was provided between the ΔI and the sulfite concentration up to 500 µM in Fig. 5.4. In n the linear range, the sensor has a sensitivity of 1.40 µA/mM. The detection limit was estimated to be 3 µM based on the criterion of signal-to-noise (S/N) ratio of 3 under optimized conditions. The amperometric response of Pt-NGC electrode considered a wide linear range of sulfite concentration, good sensitivity, and detection limit. On the other hand, based on the reproducibility of the 10 successive measurements with 80 µM of sulfite, the relative standard deviation (RSD) was calculated 8.9%, shown in Fig. 5.5. All these results demonstrated that the current response was suitable with the increase of sulfite concentration. Table 5.1 shows the comparison of sulfite detection between traditional electrodes and proposed Pt-NGC electrode. The performance of Pt-NGC electrode had in the present work towards sulfite detection is better or comparable with other reported when observed in the amperometric sensor and listed in Table 5.1.

5.4.2.   Interference Study

Part of the interference study will divide into two categories, based on the standard interference and the real sample interference. Based on the standard interference study will explained it. The selectivity of the Pt-NGC electrode has been investigated in amperometry. Fig 5.6 shows a typical amperometric response by addition of 100 µM sulfite and 100 µM of numerous interfering species, including glucose, fructose, oxalate, sucrose, and citric acid. The results show that those interfering species did not interfere with the determination of sulfite. As the same like Fig. 5.6, in Fig. 5.7 the author tried to compare three electrodes are AGC electrode,

Pt-GC, and Pt-NGC electrode for evaluation possible interfering species. Here, the author used other common metal cations and anions for example Na^+, K^+, Cl^-, NO_3^-, HCO_3^-, $H_2PO_4^-$, and HPO_4^{2-} combined with focusing on determination of sulfite. The results show that those cations and anions did not interfere for both of electrodes with the determination of sulfite. In reality according to Fig. 5.7, the Pt-NGC electrode selectivity had superior to AGC electrode and Pt-GC electrode. This is indicating that Pt-NGC electrode has an excellent selectivity.

After the standard interference study, the real sample (red wine) was used to evaluate the Pt-NGC electrode. The sensor is applied to measure sulfite in red wines. The selectivity of the Pt-NGC electrode has been investigated by recovery tests of sulfite. The recovery test results of sulfite from red wine with variation concentration of sulfite (50 μM and 200 μM) are shown in Table 5.2. On the other hand, Figure 5.8 is a result of an amperometric response with the sulfite concentration of 200 μM. It was prepared for two different sample solutions, first, a test solution (0.1 M phosphate buffer) (a) and the second is a red wine sample (b). The sulfite was added into each sample solutions. As shown in Fig. 5.8, the author also evaluated and tested by recovery test of sulfite in red wine with the total sample of 10 (n = 10). The results show that the favorable recovery of sulfite using each possible interfering substance in a real sample was obtained. Moreover, the author proposed amperometric sulfite sensor based on the Pt-NGC electrode is an advantageous analytical technique, as it allows simple and rapid determinations of the sulfite concentration to be applied so easily.

116

5.5. Conclusions

A new-type modified glassy carbon electrode has been developed on the basis of Pt-electrodecorated on the nitrogen-containing functional groups by stepwise electrolysis. The Pt-NGC electrode exhibited a favorable electrocatalytic activity towards sulfite oxidation compared with the bare GC electrode and the AGC electrode. The electrocatalytic activity of sulfite oxidation has been applied to the amperometric sensor of sulfite under the optimized conditions. The linear range for the determination of sulfite concentration up to 500 μM (r^2 = 0.9979) with the detection limit of sulfite was 3 μM (*S/N* = 3). The reproducibility for the determination of 80 μM sulfite is 8.9% (RSD with n= 10). In addition, the Pt-NGC electrode showed high selectivity towards sulfite in the presence of common metal ions and other interfering substance. The author conducted the sulfite recovery test using red wine with the results of good and successful performed.

References

1. A. Isaac, J. Davis, C. Livingstone, A. J. Wain, and R. G. Compton, *TrAC, Trends Anal. Chem*., **25**, 589 (2006).

2. T. Garcia, E. Casero, E. Lorenzo, and F. Pariente, *Sens. Actuators, B*., **106**, 803 (2005).

3. H. Yu, X. Feng, X. Chen, S. Wang, and J. Jin, *J. Electroanal. Chem.,* **801**, 488 (2017).

4. H. J. Suh, Y. H. Cho, M. S. Chung, and B. H. Kim, *J. Food Compos Anal.,* **20**, 212 (2010).

5. S. S. M. Hassan, M. S. A. Hamza, and A. H. K. Mohamed, *Anal. Chim. Acta.,* **570**, 232 (2006).

6. D. H. Allen, *Food Technol*., **73**, 506 (1985).

7. G. Monnier and S. Williams, *Analyst*, **95**, 119 (1972).

8. S. Theisen, R. Hansch, L. Kothe, U. Leist, and R. Galensa, *Biosens. Bioelectron,* **26**, 175 (2010).

9. L.J. Zhang, Z.Y. Wang, X.J. Cao, J.T. Liu, and B.X. Zhao, *Sens. Actuators B*., **236**, 741 (2016).

10. R. Rawal and C. S. Pundir, *Int. J. Biol. Macromol*., **51**, 449 (2012).

11. G. Jankovskiene, Z. Daunoravicius, and A. Padaraukas, *J. Chromatogr. A*, **934**, 67 (2001).

12. L. S. T. Alamo, T. Tangkuaram, and S. Satienperakul, *Talanta*, **81**, 1793 (2010).

13. S. Preecharueangrit, P. Thavarungkul, P. Kanatharana, and A. Numnuam, *J. Electroanal. Chem.,* **808**, 150 (2018).

14. O. Niwa, J. Jia, Y. Sato, D. kato, R. Kurita, K. Maruyama, K. Suzuki, and S. Hirono, *JACS*, **128**, 7144 (2006).

15. A. Negishi, H. Kaneko, and K. Nozaki, *DENKI KAGAKU*, **61(12)**, 1442 (1993).

16. E. Frackowiak and F. Begun, *Carbon*, **39**, 937 (2001).

17. N. Kishimoto and N. Matsuda, *Environ. Sci. Technol.*, **43**, 2054 (2009).

18. R. W. Murray, *Electroanalytical Chemistry and Interfacial Electrochemistry*, ed. A. J. Bard, **1984**, Vol. 13, Marcel Dekker, New York, 191.

19. M. G. Heinemann, B. L. Goncalves, J. R. M. Vicenti, and D. Dias, *Anal. Sci.*, **35**, 1255 (2019).

20. J. Dang, H. Cui, X. Li, and J. Zhang, *Anal. Sci.*, **35**, 979 (2019).

21. R. Zhao, Y. Wang, Z. Zhang, Y. Hasebe, and D. Tao, *Anal. Sci.*, **35**, 733 (2019).

22. T. L. Nguyen, V. H. Cao, T. H. Y. Pham, and T. G. Le, *Electroanalysis*, **31**, 2538 (2019).

23. A. Issac, A. J. Wain, R. G. Compton, C. Livingstone, and J. Davis, *Analyst*, **130**, 1343 (2005).

24. R. H. O. Montes, E. M. Richter, and R. A. A. Munoz, *Electrochem. Commun.*, **21**, 26 (2012).

25. E. Gasana, P. Westbroek, E. Temmerman, H. P. Thun, and P. Kiekens, *Anal. Chim. Acta*, **486**, 73 (2003).

26. H. Y. Li and K. Yang, *Nucl. Power Eng.*, **23**, 18 (2002).

27. T. Balduf, G. Valentin, and F. Lapicque, *Can. J. Chem. Eng.*, **76**, 790 (1998).

28. I. G. Casella and R. Marchese, *Anal. Chim. Acta*, **311**, 199 (1995).

29. S. Uchiyama, H. Watanabe, H. Yamazaki, A. Kanazawa, H. Hamana, and Y. Okabe, *J. Electrochem. Soc.*, **154**, F31 (2007).

30. A. Kanazawa, T. Daisaku, T. Okajima, S. Uchiyama, A. Kawauchi, and T. Osaka, *Langmuir*, **30**, 5297 (2014).

31. X. Wang, T. Cao, Q Zuo, S. Wu, S. Uchiyama, and H. Matsuura, *Analytical Methods*, **8**, 3445 (2016).

32. X. Wang, M. Xi, M. Guo, F. Sheng, G. Xiao, S. Wu, S. Uchiyama, and H. Matsuura, *Analyst*, **141**, 1077 (2016).

33. H. Matsuura, T. Takahashi, S. Sakamoto, and S. Uchiyama, *Anal. Sci.*, **33**, 703 (2017).

34. T. R. L. Dadamos and M. F. S. Teixeira, *Electrochim. Acta*, **54**, 4552 (2009).

35. M. Amatatongchai, W. Sroysee, S. Chairama, and D. Nacapricha, *Talanta*, **133**, 134 (2015).

36. H. Zhou, W. W. Yang, and C. Q. Sun, *Talanta*, **77**, 366 (2008).

37. V. Sudha, S. M. Senthil Kumar, and R. Thangamuthu, *J. Alloys Compd.,* **744**, 621 (2018).
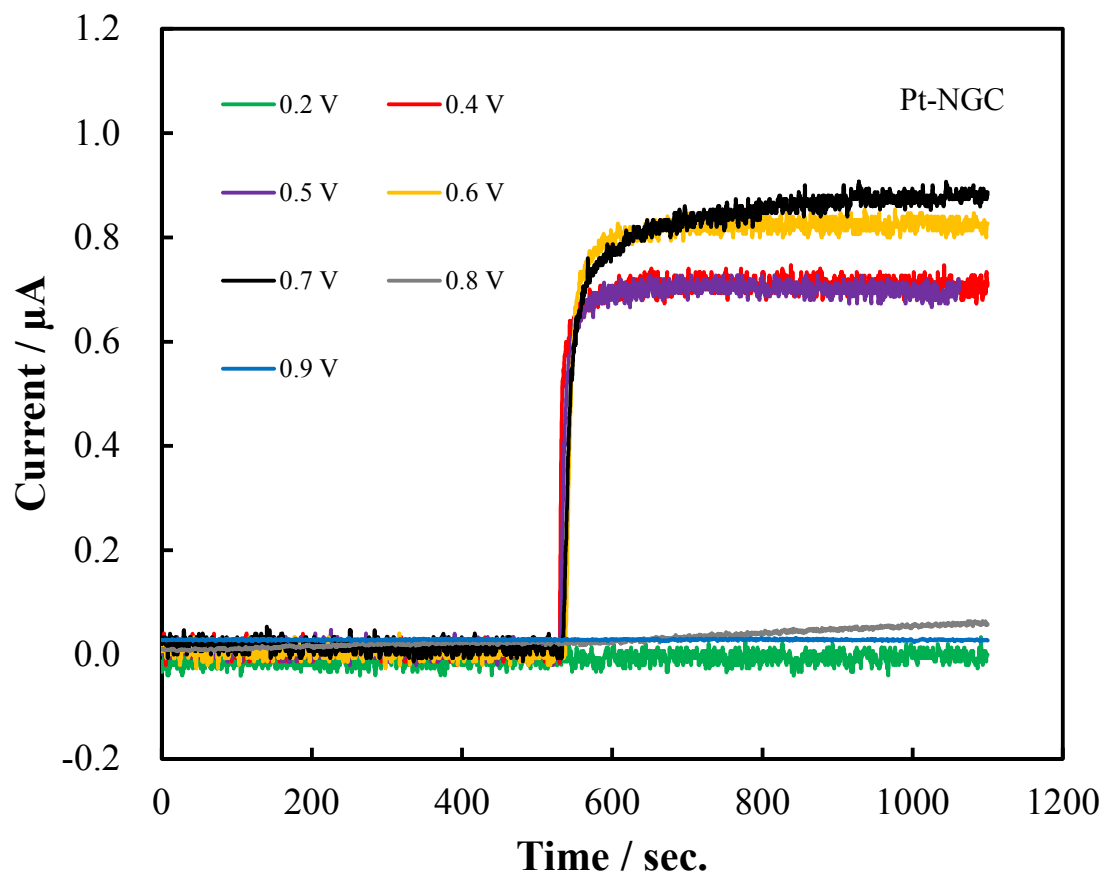
Figure 5.1. Selection of the best-working potential in amperometric sensor containing 500 µM of sulfite at Pt-NGC electrode. Supporting electrolyte: 0.1 M phosphate buffer solution (pH 7.0), rotating speed: 550 ± 50 rpm.
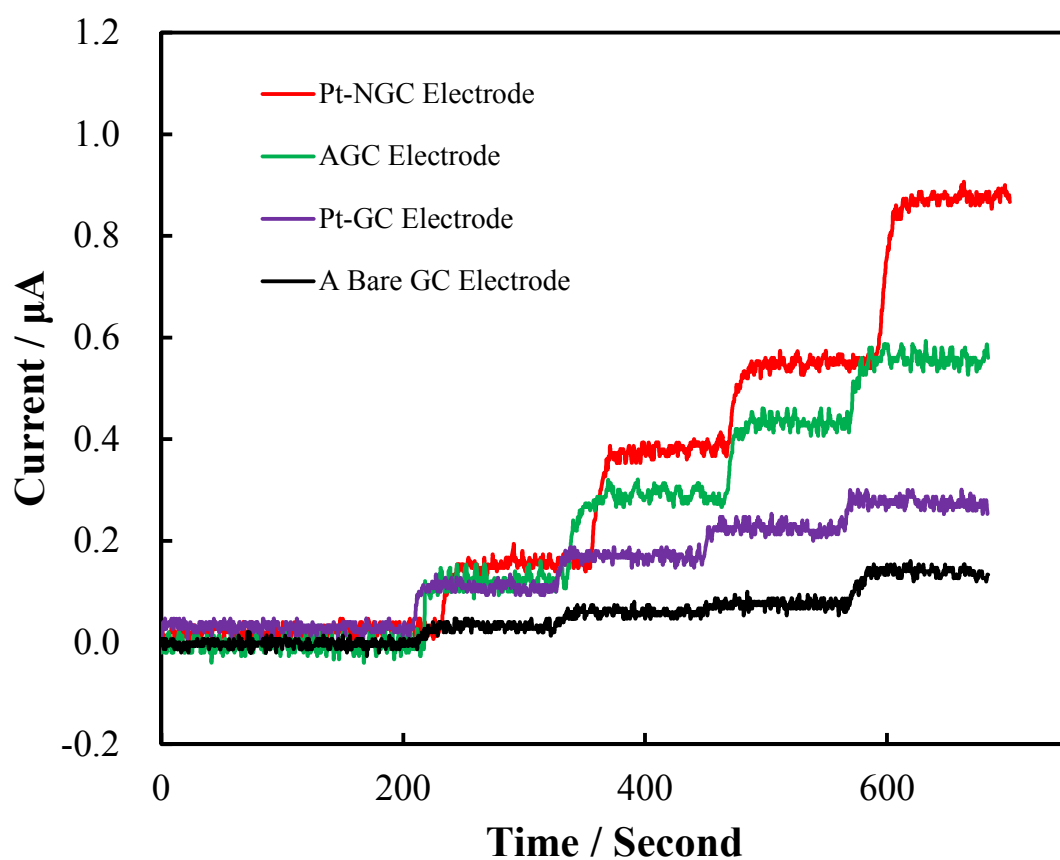
Figure 5.2. Comparison of the amperometric response with the successive addition of 100 µM of sulfite at various electrodes. Supporting electrolyte: 0.1 M phosphate buffer solution (pH 7.0), working potential: +0.6 V, rotating speed: 550 ± 50 rpm.
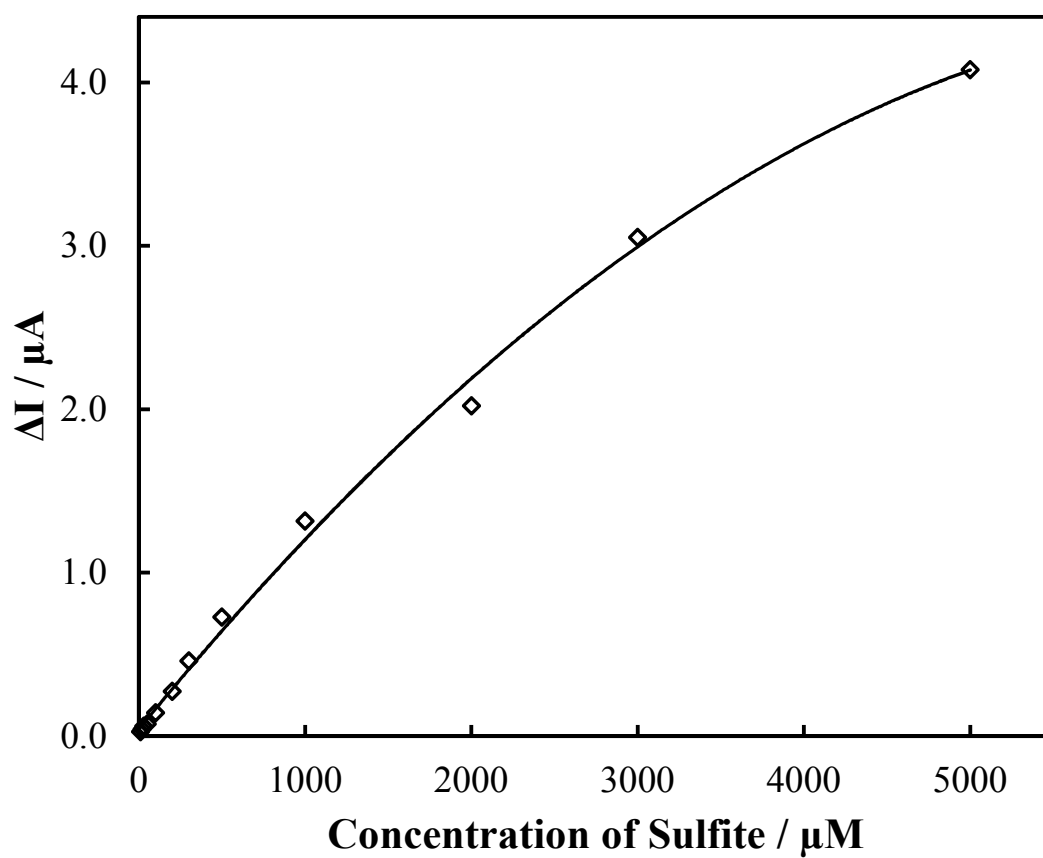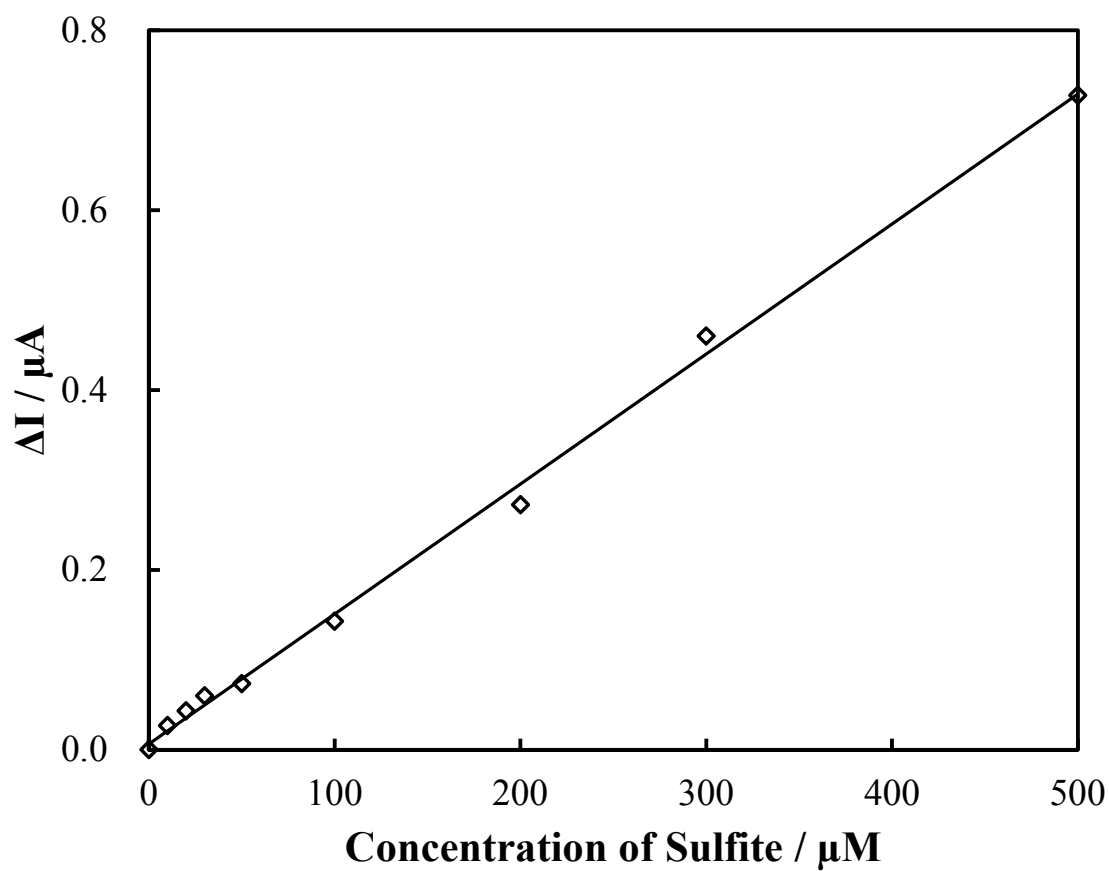
Figure 5.3. Calibration curve of the current response (ΔI) with different concentrations of sulfite at Pt-NGC electrode. Supporting electrolyte: 0.1 M phosphate buffer solution (pH 7.0), working potential: +0.6 V, rotating speed: 550 ± 50 rpm.
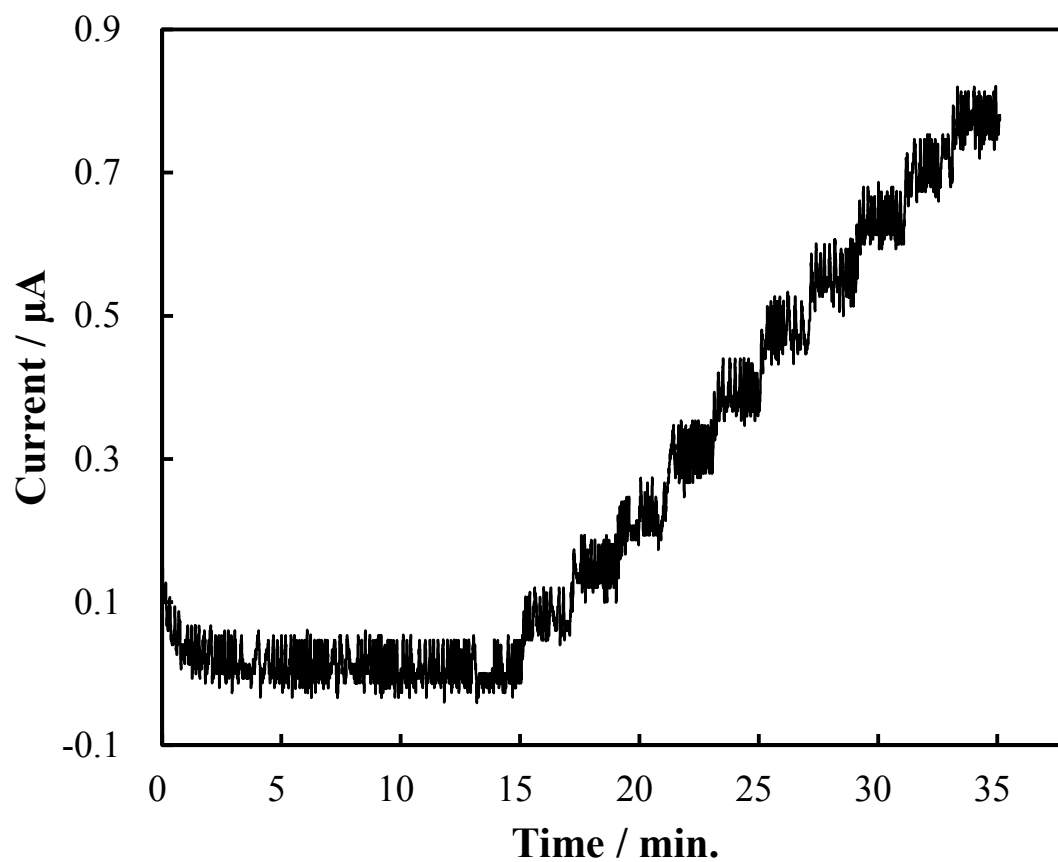
Figure 5.4. The linear relationship between current response (ΔI) and concentrations of sulfite at Pt-NGC electrode. Supporting electrolyte: 0.1 M phosphate buffer solution (pH 7.0), working potential: +0.6 V, rotating speed: 550 ± 50 rpm.

Figure 5.5. Amperometric response for 10 successive measurements of 80 μM of sulfite at Pt-NGC electrode. Supporting electrolyte: 0.1 M phosphate buffer solution (pH 7.0), working potential: +0.6 V, rotating speed: 550 ± 50 rpm.
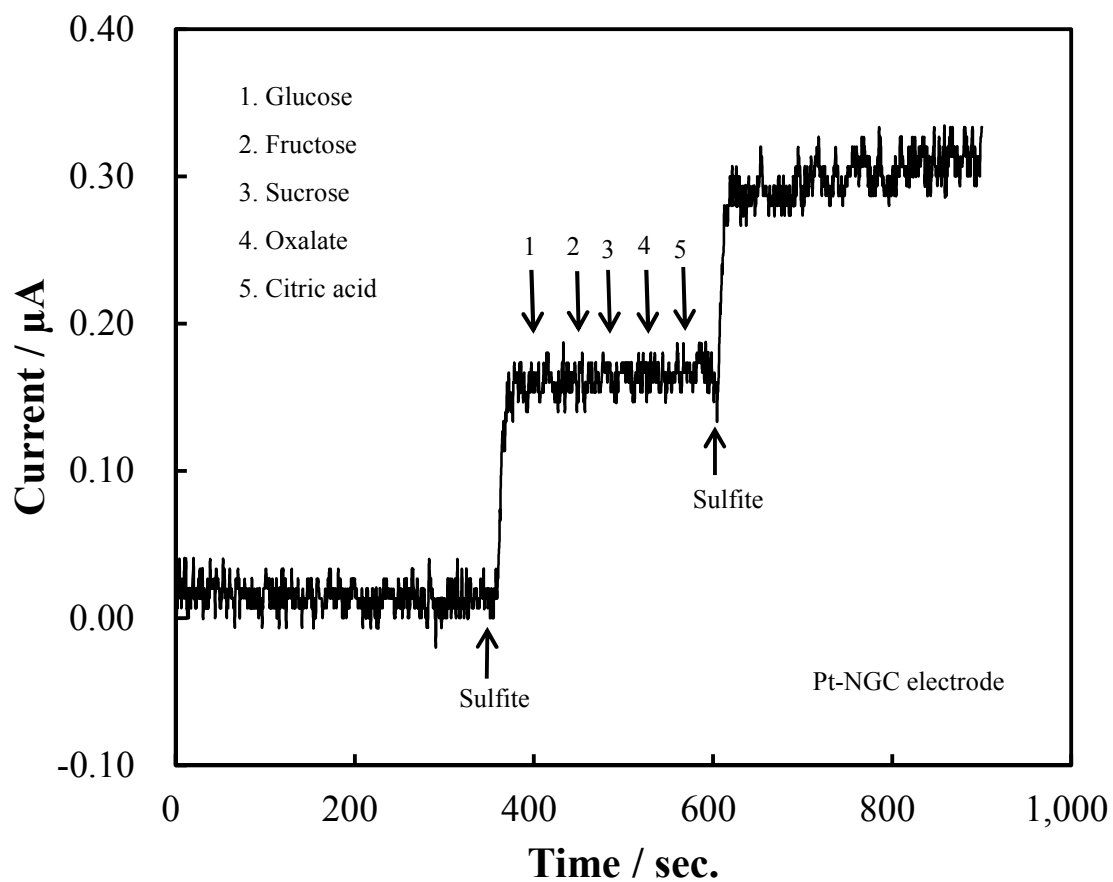
Figure 5.6. Amperometric measurement containing 100 μM concentrations for various interference substances at Pt-NGC electrode. Supporting electrolyte: 0.1 M phosphate buffer solution (pH 7.0), working potential: +0.6 V, rotating speed: 550 ± 50 rpm.
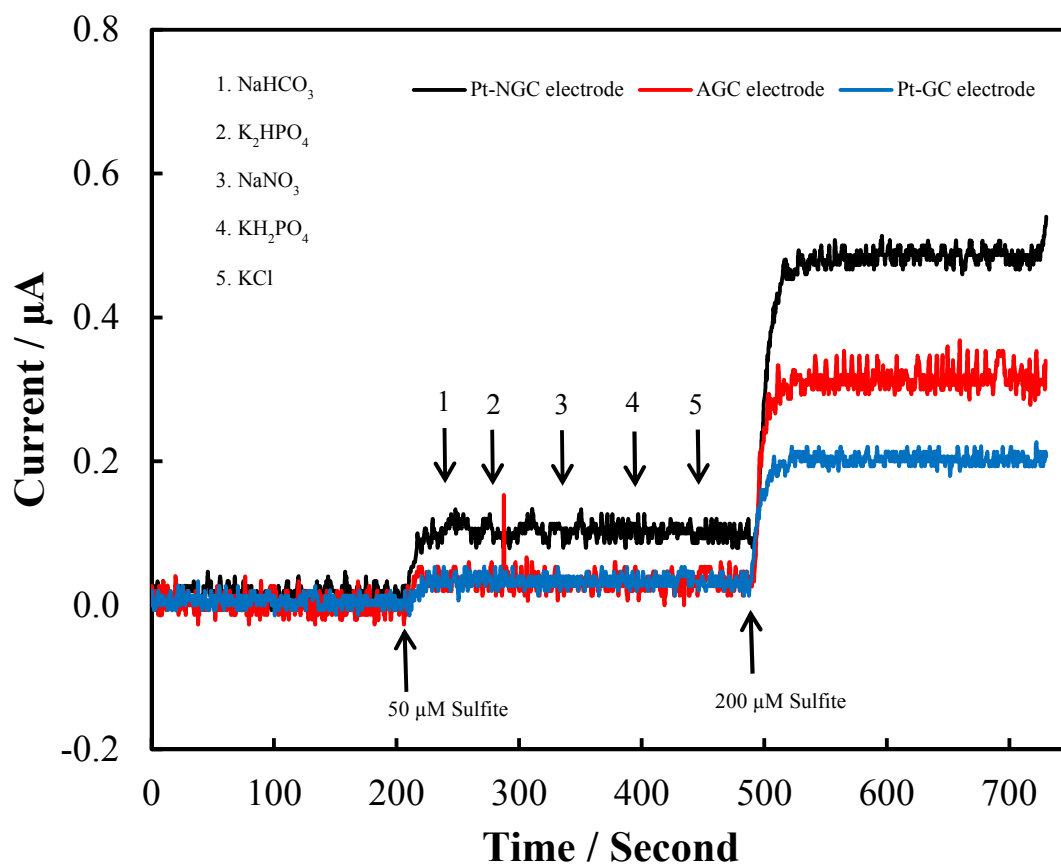
Figure 5.7. Amperometric response of two different sulfite concentrations with 100 μM various of interfering substances at different electrodes. Supporting electrolyte: 0.1 M phosphate buffer solution (pH 7.0), working potential: +0.6 V, rotating speed: 550 rpm.
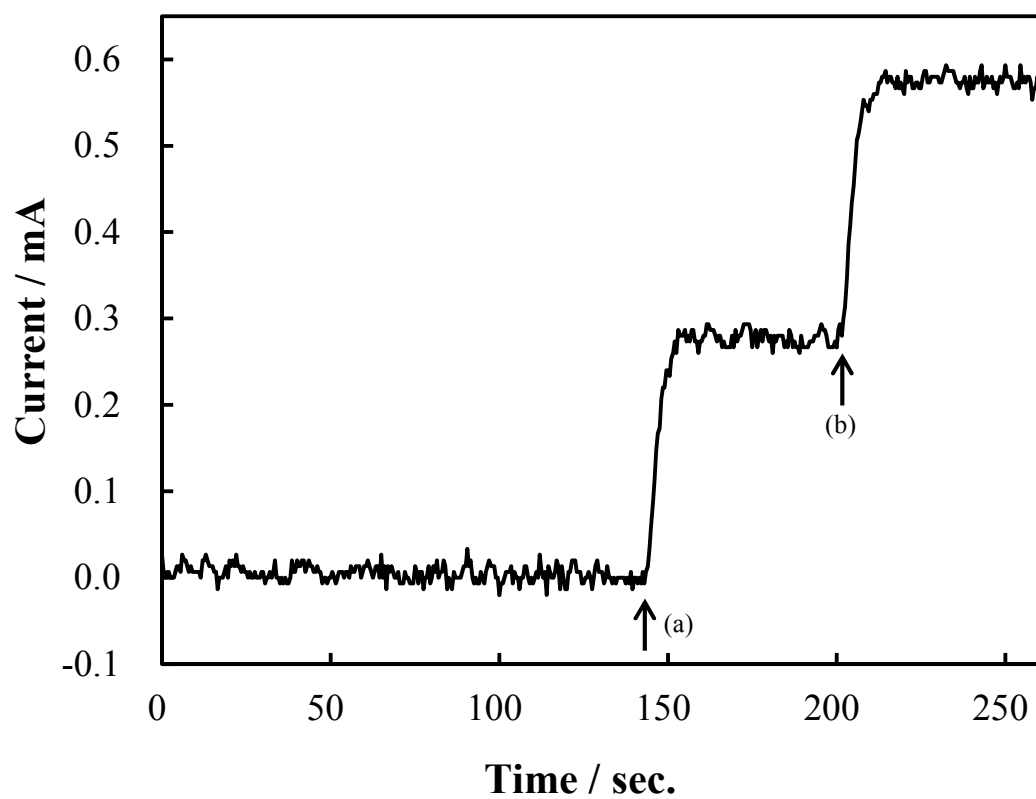
Figure 5.8. Amperometric response of 200 μM sulfite in two different sample solutions such as 0.1 M phosphate buffer (pH 7.0) solution (a) and red wine sample (b).

Table 5.1. Comparison of amperometric sensor for sulfite detection.

Electrodes	Linear range (μM)	LOD (μM)	Sensitivity (μA/mM/cm²)	Working Potential (V)
FeHCF(PB)/GCE [2]	up to 4000	80	2.18	+0.85
AuNPs-rGO/GCE [3]	0.2-2270	0.045	100.60	+0.40
Copper-salen/Pt [34]	4.0-69	1.2	-	+0.45
CNTs-PPDA-AuNPs/GCE [35]	1.2-2500	0.4	0.80	+0.40
CHIT-Fc/MWCNTs/GCE [36]	5.0-1500	2.8	13.08	+0.35
NiO-Nanoplate/GCE [37]	16.2-610	8.8	2.80	+0.55
Pt-NGCE (present work)	up to 5000	3.0	1.40	+0.60

Table 5.2. Recovery test results of sulfite from red wine with the various concentrations added.

Run	added / µM	measured / µM	Recovery / %
1	50	51	102
2	50	51	102
3	50	59	117
4	200	221	110
5	200	187	94.0
6	200	198	99.0